

CHANNEL PHASE AND DATA ESTIMATION IN SLOWLY FADING
FREQUENCY NONSELECTIVE CHANNELS

A THESIS SUBMITTED TO
THE GRADUATE SCHOOL OF NATURAL AND APPLIED SCIENCES
OF
MIDDLE EAST TECHNICAL UNIVERSITY

BY

ENGİN ZEYDAN

IN PARTIAL FULFILLMENT OF THE REQUIREMENTS
FOR
THE DEGREE OF MASTER OF SCIENCE
IN
ELECTRICAL AND ELECTRONICS ENGINEERING

AUGUST 2006

Approval of the Graduate School of Natural and Applied Sciences

Prof. Dr. Canan ÖZGEN
Director

I certify that this thesis satisfies all the requirements as a thesis for the degree of Master of Science.

Prof. Dr. İsmet ERKMEN
Head of Department

This is to certify that we have read this thesis and that in our opinion it is fully adequate, in scope and quality, as a thesis for the degree of Master of Science

Prof. Dr. Kerim DEMİRBAŞ
Supervisor

Examining Committee Members

Prof. Dr. Yalçın TANIK	(METU, EE)	_____
Prof. Dr. Kerim DEMİRBAŞ	(METU, EE)	_____
Asst. Prof. Dr. Ali Özgür YILMAZ	(METU, EE)	_____
Asst. Prof. Dr. Çağatay CANDAN	(METU, EE)	_____
Assoc. Prof. Dr. Fahrettin ARSLAN	(Ankara University, STAT)	_____

I hereby declare that all information in this document has been obtained and presented in accordance with academic rules and ethical conduct. I also declare that, as required by these rules and conduct, I have fully cited and referenced all material and results that are not original to this work.

Name, Last name: Engin ZEYDAN

Signature :

ABSTRACT

CHANNEL PHASE AND DATA ESTIMATION IN SLOWLY FADING FREQUENCY NONSELECTIVE CHANNELS

ZEYDAN, Engin

M.S., Department of Electrical and Electronics Engineering

Supervisor: Prof. Dr. Kerim DEMİRBAŞ

August 2006, 110 pages

In coherent receivers, the effect of the multipath fading channel on the transmitted signal must be estimated to recover the transmitted data. In this thesis, the channel phase and data estimation problems are investigated in a transmitted data sequence when the channel is modeled as slowly fading, frequency non-selective channel. Channel phase estimation in a transmitted data sequence is investigated and data estimation is obtained in a symbol-by-symbol MAP receiver that is designed for minimum symbol error probability criterion.

The channel phase is quantized in an interval of interest, the trellis diagram is constructed and Viterbi decoding algorithm is applied that uses the phase transition and observation models for channel phase estimation. The optimum coherent and noncoherent detectors for binary orthogonal and PSK signals are derived and the modulated signals in a sequence are detected in symbol-by-symbol MAP receivers.

Simulation results have shown that the performance of the receiver with phase estimation is between the performance of the optimum coherent and noncoherent receiver.

Keywords: Channel Phase Estimation, multipath fading, Viterbi Algorithm, Trellis diagram

ÖZ

YAVAŞ SÖNÜMLENEN FREKANS SEÇİCİ OLMAYAN KANALLARDA KANAL FAZI VE DATA TAHMİNİ

ZEYDAN, Engin

Yüksek Lisans, Elektrik ve Elektronik Mühendisliği Bölümü

Tez Yöneticisi: Prof. Dr. Kerim DEMİRBAŞ

Ağustos 2006, 110 sayfa

Evreyumlu alıcılarda, gönderilen bilginin doğru alınabilmesi için gönderilen sinyaldeki çok yollu sönümlü kanalın etkisinin tahmin edilmesi gerekmektedir. Bu tez çalışmasında, yavaş sönümlenen, frekans seçici olmayan kanallarda gönderilen sıralı verilerden kanal fazı ve veri tahmini problemleri incelenmiştir. Gönderilen bir dizi üzerinde kanal fazı tahmini ve minimum sembol hata olasılığı kıstasına göre tasarlanmış en uygun MAP sembol alıcılarda veri tahmini incelenmiştir.

Kanal fazı tahmini için, kanal fazı belli bir aralık içinde nicemlendirildi, kafes diyagramı oluşturuldu ve faz geçişi ve gözlem modelleri kullanılarak Viterbi çözümleme algoritması uygulandı. Çift dik sinyaller ve Çift Fazlı Değişim Anahtarı sinyalleri için en uygun evreyumlu ve evreyumsuz detektörler elde edildi ve gönderilen bir dizideki semboller MAP sembol alıcılarda tespit edildi. Simülasyon

sonuçları faz tahminli alıcının performansının en uygun evreuyumlu ve evreuyumsuz alıcıların performansının arasında olduğunu gösterdi.

Anahtar Kelimeler: Kanal fazı tahmini, çok yollu sönümlleme, Viterbi algoritması, Kafes diyagramı

To my family

ACKNOWLEDGMENTS

I am greatly indebted to my supervisor Prof. Dr. Kerim DEMİRBAŞ, for his guidance, professional advice and valuable supervision during the development of this thesis. This thesis would not be completed without his guidance and support.

I would also like to thank Asst. Prof. Dr. Ali Özgür Yılmaz for his valuable discussions and comments.

I would also like to express my deepest gratitude to my family for their encouragements, support and patience throughout my life in all aspects.

TABLE OF CONTENTS

PLAGIARISM	iii
ABSTRACT	iv
ÖZ	vi
ACKNOWLEDGMENTS	ix
TABLE OF CONTENTS	x
LIST OF FIGURES	xiii
LIST OF ABBREVIATIONS	xv
CHAPTER	
1. INTRODUCTION	1
2. MULTIPATH FADING CHANNEL CHARACTERIZATION.....	6
2.1 Small Scale Fading Characterization of Multipath Fading Channels	6
2.2 Signal time-spreading viewed in time-delay domain- The Multipath Intensity Profile.....	9
2.3 Signal time-spreading viewed in frequency domain- The Spaced Frequency Correlation Coefficient.....	9
2.4 Time variance viewed in time domain - The Spaced Time Correlation Coefficient	10
2.5 Time variance viewed in Doppler shift domain- The Doppler Power Spectrum	10
2.6 Frequency selective and frequency nonselective or flat fading channels viewed in the time-delay domain and in the frequency-delay domain.....	11
2.7 Slow and fast fading channels due to time variance viewed in the time domain and in the Doppler-shift Domain.....	11
2.8 The Concept of Duality	12

3. OPTIMUM DECODING BASED SMOOTHING ALGORITHM (ODSA)	13
3.1 Models and Assumptions	13
3.2 Quantization of Channel Phase	14
3.3 Finite State Model (FSM) for the Phase Transition Model.....	15
3.3.1 Transition Probabilities and Approximate Observation Model	17
3.4 Trellis Diagram for the Phase Transition Model.....	18
3.5 Minimum Error Probability Criterion	20
3.6 Optimum Decision Rule for the Channel Phase Paths.....	21
3.7 Optimum Decoding Based Smoothing Algorithm (ODSA)	24
3.7.1 An Example of the ODSA.....	25
3.8 An example with Interference and Gaussian disturbance and Observation noises	27
3.8.1 The Metric of Branch between the nodes $\phi_q^i(k-1)$ and $\phi_q^i(k)$ of Hypothesis H_i	27
3.9 Slowly Fading Frequency Nonselective Channel (SFFNC) Model and Assumptions	28
4. OPTIMUM RECEIVERS FOR BINARY ORTHOGONAL AND PSK SIGNALS IN SLOWLY FADING FREQUENCY NONSELECTIVE CHANNELS	31
4.1 Optimum Receiver for Binary Signals.....	31
4.1.1 The Optimum Demodulator for Binary Signals.....	32
4.1.2 The Optimum Detector for Binary Signals.....	33
4.2 Optimum Coherent Detector for Binary Orthogonal Signals	34
4.2.1 Application of ODSA to Binary Orthogonal Signals.....	38
4.2.2 The Metric of Branch between the nodes $\phi_q^i(k-1)$ and $\phi_q^i(k)$ of Hypothesis H_i in Binary Orthogonal Signals	40
4.3 Optimum Coherent Detector for BPSK Signals	41
4.3.1 Application of ODSA to BPSK Signals.....	44
4.3.2 The Metric of Branch between the nodes $\phi_q^i(k-1)$ and $\phi_q^i(k)$ of Hypothesis H_i in BPSK signals.....	45
4.4 Optimum Noncoherent Detector for Binary Orthogonal Signals	46
4.5 Phase Estimation with ODSA using Gaussian random walk phase transition model in Gaussian Channels	49

4.5.1 Application of ODSA to Binary Orthogonal Signals.....	49
4.5.2 The Metric of Branch between the nodes $\phi_q^i(k-1)$ and $\phi_q^i(k)$ of Hypothesis H_i in Binary Orthogonal Signals	50
4.5.3 Application of ODSA to BPSK Signals.....	51
4.5.4 The Metric of Branch between the nodes $\phi_q^i(k-1)$ and $\phi_q^i(k)$ of Hypothesis H_i in BPSK signals.....	51
5. SIMULATION RESULTS	52
5.1 Performance comparisons of ODSA with optimum noncoherent and coherent detectors with increasing number of Quantization levels or nodes, M_k	54
5.2 Performance comparisons of ODSA with optimum noncoherent and coherent detectors with increasing size of approximating discrete vector $\alpha_d(k)$, R_k	56
5.3 Performance comparisons of ODSA with optimum noncoherent and coherent detectors with different values of correlation coefficient of the first order Markov fading process, λ	58
5.4 Performance comparisons of ODSA with optimum noncoherent and coherent detectors in different observation noise variances σ^2 or SNR values..	60
5.5 Apriori probability of $u_2(t)$ v.s. BER.....	62
5.6 Computational time of data estimation with ODSA	64
5.7 Performance comparisons of ODSA with optimum noncoherent and coherent detectors using the Gaussian random walk phase transition model in Gaussian Channels	67
6. CONCLUSIONS.....	70
REFERENCES.....	73
APPENDICES	76
A. MODIFIED BESSEL FUNCTION OF ORDER ZERO.....	76
B. APPROXIMATION OF AN ABSOLUTELY CONTINUOUS RANDOM VECTOR BY A DISCRETE RANDOM VECTOR.....	78
C. NUMERICAL CALCULATION OF CHANNEL PHASE TRANSITION PROBABILITIES BY SIMULATING FIRST ORDER MARKOV FADING PROCESS IN MATLAB	103

LIST OF FIGURES

FIGURES

Figure 1: Small Scale fading: degradation categories, effects and	7
Figure 2: Channel correlation and Power density functions [11]	8
Figure 3: Quantization and transition probability	14
Figure 4: The flowchart of finite state model	16
Figure 5: Trellis diagram for phase transition model.....	19
Figure 6: Initial Metric calculation	23
Figure 7: An Example of ODSA.....	25
Figure 8: A Rayleigh fading channel Model.....	28
Figure 9: Optimum receiver for binary signals.....	33
Figure 10: Proposed Receiver for binary orthogonal signals.....	38
Figure 11: Optimum Receiver for BPSK signals.....	42
Figure 12: Proposed Receiver for BPSK signals	44
Figure 13: Optimum Noncoherent Receiver for binary orthogonal signals.....	49
Figure 14: Binary Orthogonal signals (BOS).....	53
Figure 15: Proposed Receiver for half symbol BPSK (HS-BPSK)	53
Figure 16: BER v.s. number of quantization levels M_k for HS-BPSK	54
Figure 17: BER v.s. number of quantization levels M_k for BOS.....	55
Figure 18: BER v.s. number of quantization levels M_k for BOFSK.....	55
Figure 19 : BER v.s. size of $\alpha_d(k)$ for HS-BPSK.....	56
Figure 20 : BER v.s. size of $\alpha_d(k)$ for BOS	57
Figure 21: BER v.s. size of $\alpha_d(k)$ for BOFSK	57
Figure 22: BER v.s. Channel Correlation coefficient λ for HS-BPSK.....	58
Figure 23: BER v.s. Channel Correlation coefficient λ for BOS.....	59
Figure 24: BER v.s. Channel Correlation coefficient λ for BOFSK	59
Figure 25: BER versus SNR for HS-BPSK	60

Figure 26: BER versus SNR for BOS	61
Figure 27: BER versus SNR for BOFSK.....	61
Figure 28: Channel Phase and Estimated Phase at SNR=30dB.....	62
Figure 29: BER v.s. $p(u_2(t))$ for HS-BPSK.....	63
Figure 30: BER v.s. $p(u_2(t))$ for BOS.....	63
Figure 31: BER v.s. $p(u_2(t))$ for BOFSK	64
Figure 32: Computational time v.s. Apriori Probability of $u_2(t)$ for HS-BPSK.....	65
Figure 33: Computational time v.s. Apriori Probability of $u_2(t)$ for BOS	65
Figure 34: Computational time v.s. Apriori Probability of $u_2(t)$ for BOFSK	66
Figure 35: Computational time v.s. Number of quantization levels M_k	66
Figure 36: Computational time v.s. Size of $\alpha_d(k)$, R_k	67
Figure 37: SNR v.s. BER for HS-BPSK signals.....	68
Figure 38: SNR v.s. BER for BOS signals	68
Figure 39: SNR v.s. BER for BOFSK signals	69
Figure 40: Channel Phase and Estimated Phase at SNR=14 dB.....	69

LIST OF ABBREVIATIONS

AWGN	Additive White Gaussian Noise
BER	Bit Error Rate
BOS	Binary Orthogonal Signals
BOFSK	Binary Orthogonal Frequency Shift Keying
CBOFSK	Optimum Coherent Detection of BOFSK
CBOS	Optimum Coherent Detection of BOS
CHS-BPSK	Optimum Coherent Detection of HS-BPSK
EKF	Extended Kalman Filtering
HS-BPSK	Half-symbol BPSK
FSM	Finite State Model
MAP	Maximum A Posteriori
NCBOS	Optimum Noncoherent Detection of BOS
NCBOFSK	Optimum Noncoherent Detection of BOFSK
NCHS-BPSK	Optimum Noncoherent Detection of HS-BPSK
ODSA	Optimum Decoding Based Smoothing Algorithm
PBOS	Proposed Detector for Binary Orthogonal Signals
PBOFSK	Proposed Detector for Binary Orthogonal FSK Signals
PHS-BPSK	Proposed Receiver for Half Symbol BPSK Signals
PDF	Probability Density Function
SFFNC	Slowly Fading Frequency Nonselective Channel
SNR	Signal-to-Noise Ratio
VDA	Viterbi Decoding Algorithm

CHAPTER 1

INTRODUCTION

In mobile and wireless radio channels, the performance of wireless communication systems is severely obstructed and limited by terrain conditions and man-made environments [6], [10]. There are multiple reflective paths from transmitter to receiver and these paths contribute to significant fluctuations in the received signal's amplitude, phase and angle of arrival, resulting in so called *multipath fading* [11] .

In coherent detection, the channel phase must be tracked accurately. In ideal coherent demodulation of any linear or nonlinear modulated signals, the availability of channel phase is assumed. However, in fading channels, amplitude and phase estimation errors can significantly degrade the demodulator performance [4], [12]. Therefore, we need robust and simple receiver designs in order to track the changes in the channel parameters.

In urban and terrestrial mobile communications, the channel is usually modeled as Rayleigh flat-fading channel [6]. Therefore, designing reliable communication systems for this kind of fading channel is significant. Signals transmitted over Rayleigh fading channels are usually demodulated in suboptimal and power efficient ways like non-coherent or differentially coherent techniques. These techniques have irreducible error floors at high fade rates, generate suboptimal soft decisions leading to power inefficiency, or in the case of pilot symbol approaches [3] on fast fading channels, require greater bandwidth [19] .On the other hand, coherent demodulation has superior performance compared to these techniques.

Throughout this thesis, we assume flat (or frequency nonselective) slowly fading channel model. A considerable amount of research has been devoted to channel estimation in frequency-nonselective (flat) Rayleigh fading channels [2], [3], [8], [14], [15], [17], [18], [22], [23], [24],[28],[30].

The optimal solutions to the maximum likelihood sequence estimation (MLSE) in fading channels are studied in [2], [15]. These receivers overcome both the error floor limitation of differential detection and the power/bandwidth limitation of pilot symbol assisted techniques. However, implementation of these optimal solutions requires high dimensional filtering. For example, in [2], for every assumed symbol sequences, we need different Kalman filter structures, where adaptive channel estimation method is proposed by using the Kalman filter.

In [15], MLSE receiver is developed for fading channels to obtain the data sequence which produces the most likely channel samples, however; it produces hard decisions via the Viterbi Algorithm which is unsuitable for applications requiring soft decisions in subsequent stages. In digital communication systems using concatenated processing structures (e.g. modems using forward error-correction codes with interleaving), due to the number of states required, joint demodulation and decoding in a single stage is not practical [19].

In addition to these, channel estimation has been studied in MLSE by employing two stage receiver structures, first, estimating the complex Gaussian channel coefficient and then sequentially detecting the signal. Most of these two stage receivers are suboptimum, but are easily implementable compared to optimal algorithms. In estimating the complex Gaussian channel coefficient, Kalman filters or linear estimators are employed and estimation is simplified by using per-survivor processing [16], [17], pilot symbol assisted modulation [3] or using both pilot symbols and tentative data decisions [18]. An expected maximization algorithm (EM) is proposed in [8] that produce both the data sequence and the Gaussian fading vector estimates as another suboptimal solution to MLSE in fading channel.

In [23], adaptive maximum likelihood sequence detection (MLSD) algorithm for Rayleigh flat-fading environment with complex Gaussian channel coefficient estimation and channel identification is proposed. In this paper, the complex Gaussian channel coefficient is estimated for each path in the trellis diagram by using Kalman filtering, and then the transmitted data is detected for each survivor path by dynamic programming algorithm. The channel is identified by estimating the channel parameters associated with the best previous survivor path.

An algorithm combining decision feedback and adaptive linear prediction (DFALP) to track the phase and amplitude of frequency nonselective fading channels is proposed in [24]. In this algorithm, channel estimation is assisted by periodically inserted pilot symbols.

The advantage of estimating the complex Gaussian channel coefficient or the quadrature components of the fading process of the channel is that it is equivalent to estimating both the Rayleigh amplitude gain and channel phase (or uniform phase shift) due to the fading [30]. However throughout this thesis, we consider the phase distortion in a Rayleigh fading channel as a more severe problem for constant amplitude carrier modulation methods like frequency shift keying (FSK) or Phase Shift Keying (PSK) than amplitude fading distortion induced by the channel similarly to [22], [25]. Therefore, the main channel estimation effort is devoted to tracking channel phase rather than exact estimates for the fading amplitude. In addition, simulation results in [22] have shown that using a simple estimation for fading amplitude and powerful phase estimation technique performs only slightly worse than when having perfect channel amplitude and phase knowledge at the receiver.

In fading channels, carrier phase tracking loops are not the optimum phase estimators [14] and fading causes significant degradation to the phase tracking performance of a carrier loop [13]. Therefore, a Phase-locked loop (PLL), a classical structure for

carrier recovery, does not operate satisfactorily in a fading channel due to the time-variant nature of the fading channel.

Throughout this thesis, Channel phase estimation in a sequence will be obtained by using the Viterbi decoding algorithm on slowly fading frequency nonselective Rayleigh channels. Channel Phase estimates in a sequence will be observed to estimate the transmitted data in a symbol-by- symbol MAP receiver. Fading channels are correlated [24]; therefore sequence estimation is required for optimum detection. However, to ease implementation complexity symbol-symbol detection is usually desirable. Hence, we will deal with the sequential detection of channel phase and symbol-by-symbol detection of the transmitted data at the receiver.

The motivation behind this thesis is robust and reliable estimation of the channel phase in slowly fading frequency nonselective channel. Optimum decoding based smoothing algorithm (ODSA), that is used in this thesis uses Viterbi decoding algorithm as the optimum decoding algorithm [5]. It does not estimate the complex Gaussian channel coefficient by employing linear receiver structures as explained above, instead, it estimates the channel phase that appears nonlinearly in the received signal and track the phase without using nonlinear estimators such as carrier tracking loops. Therefore, linear estimators or Kalman filters can't be used since channel phase estimation needs nonlinear estimator structures. Suboptimal realizable receivers are proposed for nonlinear state estimations such as Extended Kalman Filters (EKF) which is based on linearization of a nonlinear mapping. The basic operation of EKF is the same as the linear Kalman filter. However, the only difference is that EKF is an approximate solution that allows us to extend the Kalman filtering idea to nonlinear state space models [20]. It is shown in [9] that ODSA is far superior to the EKF at estimating nonlinear observation models. The simulation results in [9] show that EKF can not be an appropriate estimator design, which can sometimes cause suboptimal and biased estimates with no reliable accuracy. On the other hand, unlike EKF, ODSA ensured reliable guarantees on performance, accuracy, convergence and optimal estimation.

In this thesis, ODSA estimates the path taken through the trellis of quantized channel phase using the observation and phase transition models. Quantization of unknown phase is commonly utilized in literature as in [1], [22], [25], [26], in an interval of candidate phase estimates.

The organization of the thesis is as follows:

Chapter 2 summarizes the multipath fading channel characterizations.

In Chapter 3, the Optimum Decoding Based Smoothing Algorithm (ODSA) is introduced and the model and assumptions of Slowly Fading Frequency Nonselective Channel (SFFNC) are given.

In Chapter 4, Optimum Receivers for Binary Orthogonal Signals and PSK Signals in frequency nonselective slowly fading channels are derived.

In Chapter 5, the Simulation Results for the performance of proposed receiver with phase estimation are plotted. Performance comparisons with changing the ODSA parameters are investigated. Computational time of data estimation with proposed receiver is also plotted.

In chapter 6, Conclusions are given.

In Appendices Modified Bessel function of zero order is introduced and approximation of an absolutely continuous random vector by a discrete random vector is shown.

CHAPTER 2

MULTIPATH FADING CHANNEL CHARACTERIZATION

There are two types of fading effects that characterize mobile communications: Large scale or long-term and small scale or short-term fading. Large scale fading results from the average signal power attenuation or path loss due to motion over large areas whereas small scale fading has dramatic changes in signal amplitude and phase as a result of propagation path changes between the transmitter and the receiver[11]. For most fading channels, the received waveform structure is mostly affected by small scale fading, and throughout this thesis, we will only assume small scale or short term fading in the channel.

2.1 Small Scale Fading Characterization of Multipath Fading Channels [11]

There are two mechanisms associated with small scale fading channels:

- Time-spreading of the digital pulses within the signal.
- Time-variant behavior of the channel due to motion

Figure 1 summarizes these two small scale mechanisms in two domains: time or delay spread domain and Doppler or frequency spread domain. Time-spreading mechanism is characterized in the time delay domain as a multipath delay spread, and in the frequency domain as a channel coherence bandwidth. Similarly, the time-variant mechanism is characterized in the time domain as a channel coherence time

and in the Doppler-shift or frequency domain as a channel fading rate or Doppler spread.

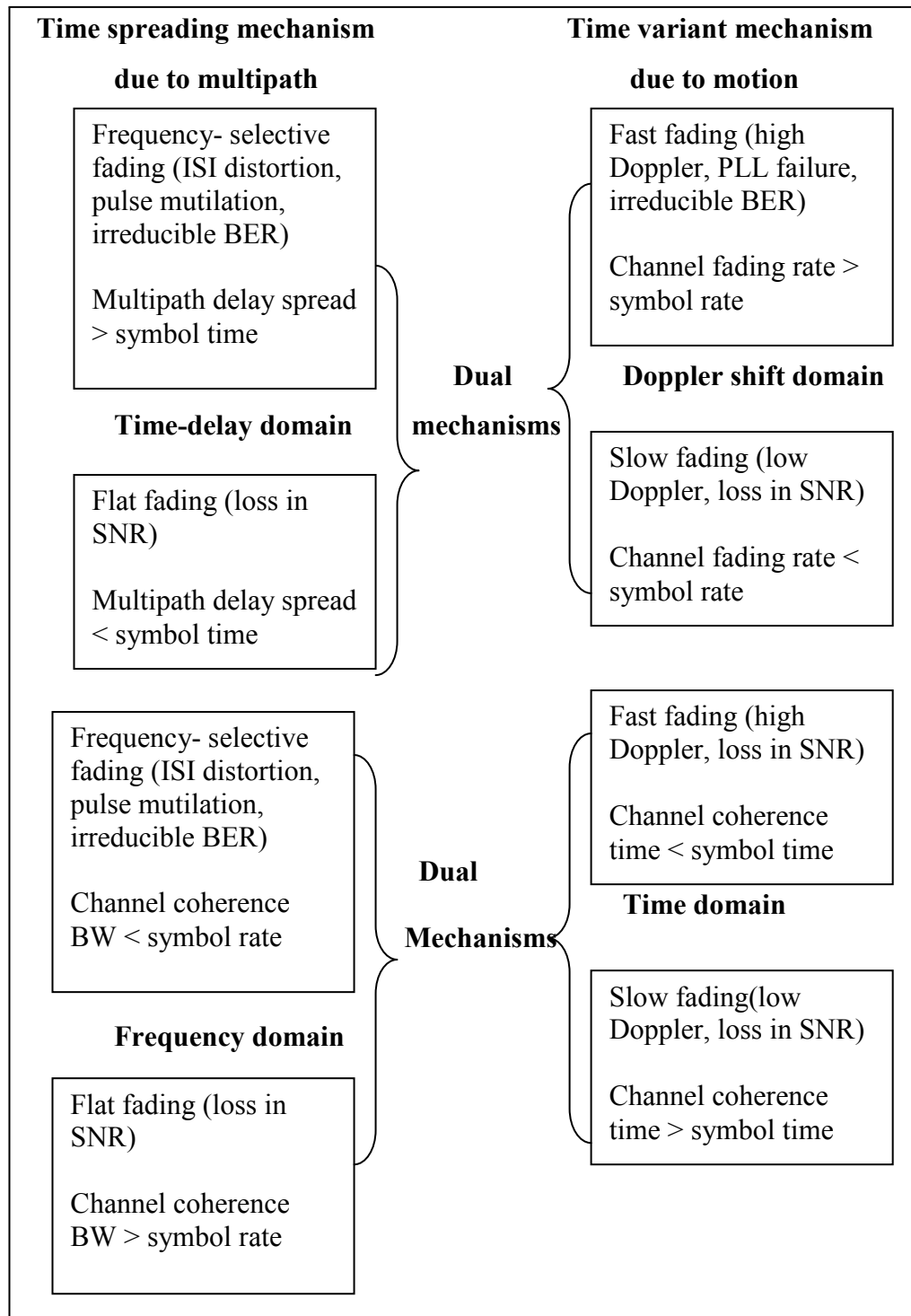


Figure 1: Small Scale fading: degradation categories, effects and Mechanisms [11]

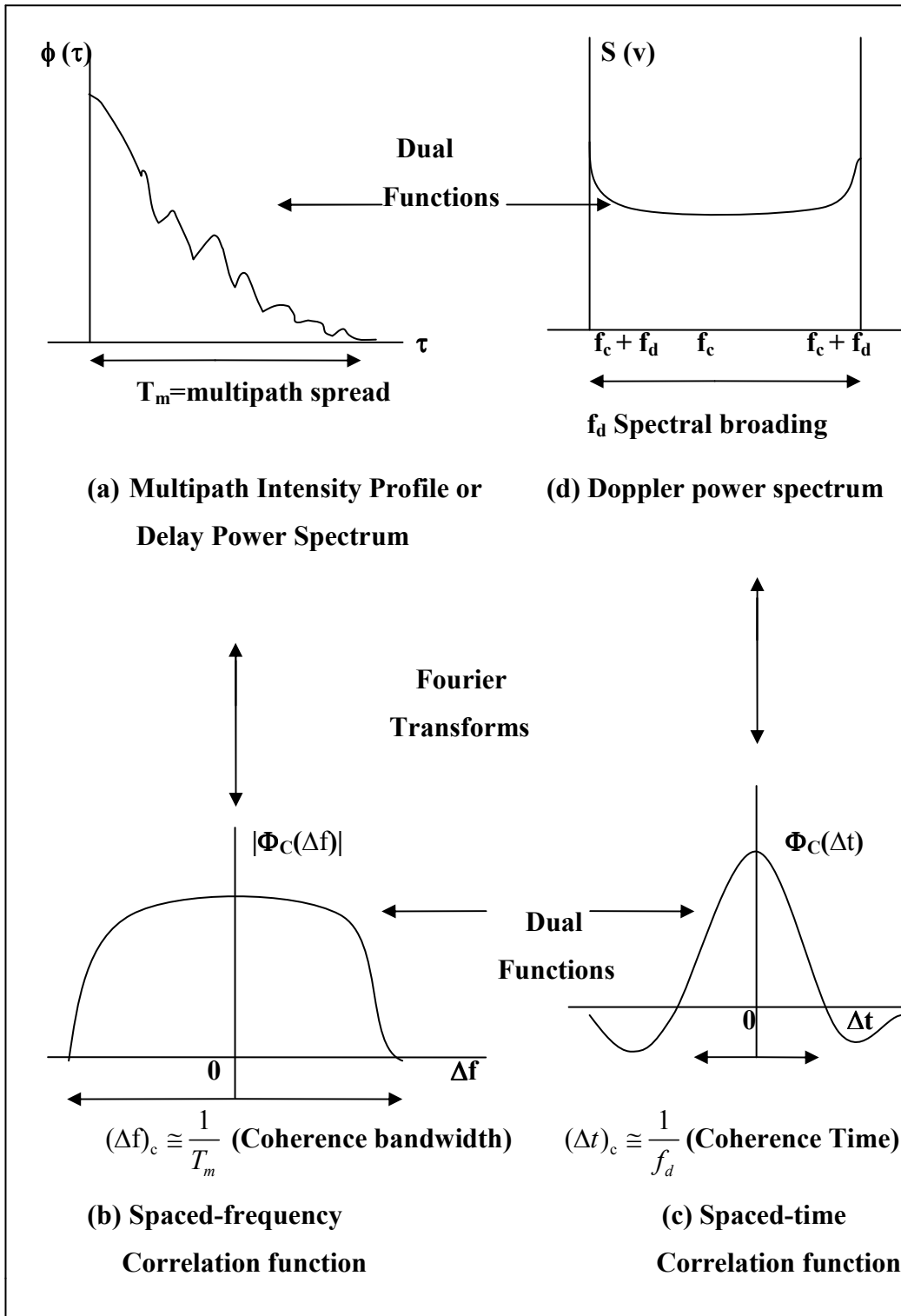


Figure 2: Channel correlation and Power density functions [11]

2.2 Signal time-spreading viewed in time-delay domain- The Multipath Intensity Profile [11]

In Figure 2 (a), the *multipath intensity profile* $\phi(\tau)$ versus delay τ is plotted. $\phi(\tau)$ is the spread of the average received power as a function of the time delay τ where the time delay represents the signal's propagation delay that exceeds the delay of the first signal arrival at the receiver.

The time T_m is the *maximum excess delay* between the first and the last received component, during which the multipath signal power falls to some threshold level below that of the strongest component for a single transmitted impulse. Therefore, for an ideal system of zero excess delay i.e. $T_m=0$, $\phi(\tau)$ is an ideal impulse response with weight equal to the total average received power.

2.3 Signal time-spreading viewed in frequency domain- The Spaced Frequency Correlation Coefficient [11]

In Figure 2 (b), spaced frequency correlation function $|\Phi_C(\Delta f)|$ which can be thought of as the channel's transfer function is plotted. It is the Fourier Transform of $\phi(\tau)$ and represents the correlation between received signals that are spaced in frequency $\Delta f = f_1 - f_2$.

The *coherence bandwidth*, $(\Delta f)_C$, represents the range of frequencies over which the channel passes all spectral components with approximately equal gain and linear phase. In other words, the signal's spectral components in that range are affected by the channel in a similar manner. $(\Delta f)_C$ and $1/T_m$ are approximately equal.

2.4 Time variance viewed in time domain - The Spaced Time

Correlation Coefficient [11]

The information about time-varying nature of the channel caused by relative motion between a transmitter and receiver, or by movement of objects within the channel needs to be known.

In Figure 2 (c), spaced- time correlation function $\Phi_c(\Delta t)$, which is the autocorrelation function of the channel's response to a sinusoid is plotted. $\Phi_c(\Delta t)$ is the correlation between the channel's response to a sinusoid sent at time t_1 and the response to a similar sinusoid sent at time t_2 , where $\Delta t = t_2 - t_1$.

The *coherence time*, $(\Delta t)_C$, is the expected time duration over which the channel's response remains constant. Therefore, the information needed for the rapidity of the fading can be obtained from the function $\Phi_c(\Delta t)$ and coherence time $(\Delta t)_C$. For an ideal time-invariant channel, the function $\Phi_c(\Delta t)$ is a constant function since it is highly correlated for all Δt .

2.5 Time variance viewed in Doppler shift domain- The Doppler Power Spectrum [11]

In Figure 2 (d), *Doppler power spectral density*, $S(\nu)$, which is the Fourier transform of $\Phi_c(\Delta t)$ is plotted as a function of Doppler-frequency shift, ν . The Doppler power spectrum of the channel yields knowledge about the spectral spreading of a transmitted sinusoid (impulse in frequency) in the Doppler shift domain.

$S(\nu)$ gives us the information about the spectral broadening imposed on the signal as a function of the rate of change in the channel state. The width of the Doppler power spectrum f_d is called the *fading bandwidth (Doppler spread or spectral broadening)* of the channel. Doppler spread, f_d , and the coherence time, $1/(\Delta t)_C$, are equal. Hence, the Doppler spread f_d or $1/(\Delta t)_C$ is the *fading rate* of the channel.

2.6 Frequency selective and frequency nonselective or flat fading channels viewed in the time-delay domain and in the frequency-delay domain [11]

There are two different degradation categories in a fading channel due to the relationship between the maximum excess delay time, T_m , and symbol time, T_s which are *frequency selective* and *frequency nonselective or flat fading*.

In time-delay domain, frequency-selective fading occurs whenever the multipath components of the signal extend beyond the symbol's time duration i.e. $T_m > T_s$. In frequency-delay domain, frequency-selective fading distortion occurs whenever a signal's spectral components are not all affected equally by the channel i.e. $(\Delta f)_C < 1 / T_s$. This yields the so called *channel-induced ISI*.

In time-delay domain, frequency-nonselective fading or flat fading occurs whenever $T_m < T_s$. In flat fading channels, there is no *channel-induced ISI* since there is no time spreading or overlap among neighboring received signals, however phasor components can add up destructively to yield a substantial reduction in SNR. In frequency-delay domain, frequency nonselective fading occurs whenever $(\Delta f)_C > 1/T_s$, that is all of the signal's spectral components will be affected by the channel in a similar manner.

2.7 Slow and fast fading channels due to time variance viewed in the time domain and in the Doppler-shift Domain [11]

There are two different degradation categories in describing the time-variant nature of the channel due to the relationship between the channel coherence time, $(\Delta t)_C$, and symbol time, T_s which are *fast fading* and *slow fading*.

In *fast-fading* channels, $(\Delta t)_C < T_s$ in time domain or the symbol rate, $1/T_s$ (approximately equal to the signaling rate or bandwidth W) is less than the fading rate, $1/(\Delta t)_C$ (approximately equal to f_d) in Doppler shift domain; therefore, the fading behaviour of the channel will change several times when a symbol is

transmitted or in a symbol duration, leading to distortion of the baseband pulse shape which results in a loss of SNR that often yields an irreducible error rate. The distorted pulses cause difficulties in defining a matched filter for the receivers.

In *slow-fading* channels, $(\Delta t)_C > T_s$ in time domain or $W > f_d$ in Doppler shift domain, therefore, the channel remains unchanged during the time in which a symbol is transmitted. The degradation in a slow-fading channel, as with flat fading, is loss in SNR.

2.8 The Concept of Duality [11]

If the behaviour of one function with reference to a time-related domain is same as the behaviour of another function corresponding to frequency-related domain, then these two functions are dual. For example, in Figure 2, $|\Phi_C(\Delta f)|$ and $\Phi_C(\Delta t)$ are dual functions, since $|\Phi_C(\Delta f)|$ gives us knowledge about the range of frequencies over which two spectral components of a received signal have a strong correlation. Similarly, $\Phi_C(\Delta t)$ gives us knowledge about the span of time over which two received signals have a strong correlation.

Also as indicated in Figure 2, $S(\nu)$ and $\phi(\tau)$ can be regarded as the dual functions. $S(\nu)$ gives knowledge about the spectral spreading of a transmitted sinusoid (impulse in frequency) in the Doppler shift domain and $\phi(\tau)$ yields knowledge about the time spreading of a transmitted impulse in the time-delay domain.

CHAPTER 3

OPTIMUM DECODING BASED SMOOTHING ALGORITHM (ODSA)

3.1 Models and Assumptions

Throughout this chapter, we deal with the following discrete models:

$$\textit{Phase transition model: } \phi(k+1) = f(k, \phi(k), w(k))$$

$$\textit{Observation model: } z(k) = g(k, \phi(k), \alpha(k), v(k)) \quad (3.1)$$

for channel phase estimation in the presence of interference, where

$k=0,1,\dots,L$ and L is the number of symbols in a transmitted sequence,

$\phi(0)$ is the initial channel phase which is uniformly distributed between $(0, 2\pi)$

$\phi(k)$ is the channel phase at symbol k ,

$\phi(k+1)$ is channel phase at symbol $(k+1)$,

$w(k)$ is a $p \times 1$ Gaussian disturbance-noise vector with zero-mean and covariance matrix $R_w(k)$,

$z(k)$ is the $r \times 1$ observation vector at symbol k ,

$v(k)$ is an $b \times 1$ Gaussian observation noise vector at symbol k with zero mean and covariance matrix $R_v(k)$,

$\alpha(k)$ is an $m \times 1$ interference vector with known statistics.

$f(k, \phi(k), w(k))$ and $g(k, \phi(k), \alpha(k), v(k))$ are linear or nonlinear vectors with appropriate dimensions.

Furthermore, we assume that the random vectors $w(j)$, $w(m)$, $v(j)$, $v(m)$, $\alpha(j)$ and $\alpha(m)$ are assumed to be independent for all j, m .

3.2 Quantization of Channel Phase

The channel phase $\phi(k)$ is in the space \mathbf{R}^1 (1-dimensional Euclidean space between $(0, 2\pi)$). We want to divide this space into non-overlapping subspaces (or gates) \mathbf{R}_i^1 and assign a unique value ϕ_{qi} to each subspace \mathbf{R}_i^1 , where q denotes the quantization. We denote $\phi_q(k)$ the quantized channel phase at symbol k , with its possible values called quantization levels [5].

In this thesis, quantization refers to the case that whenever channel phase $\phi(k)$ at symbol k falls within a given gate (or subspace) \mathbf{R}_i^1 by transmission from the state $\phi(k-1)$ at symbol $k-1$, the channel phase is quantized to the unique value ϕ_{qi} (see Figure 3).

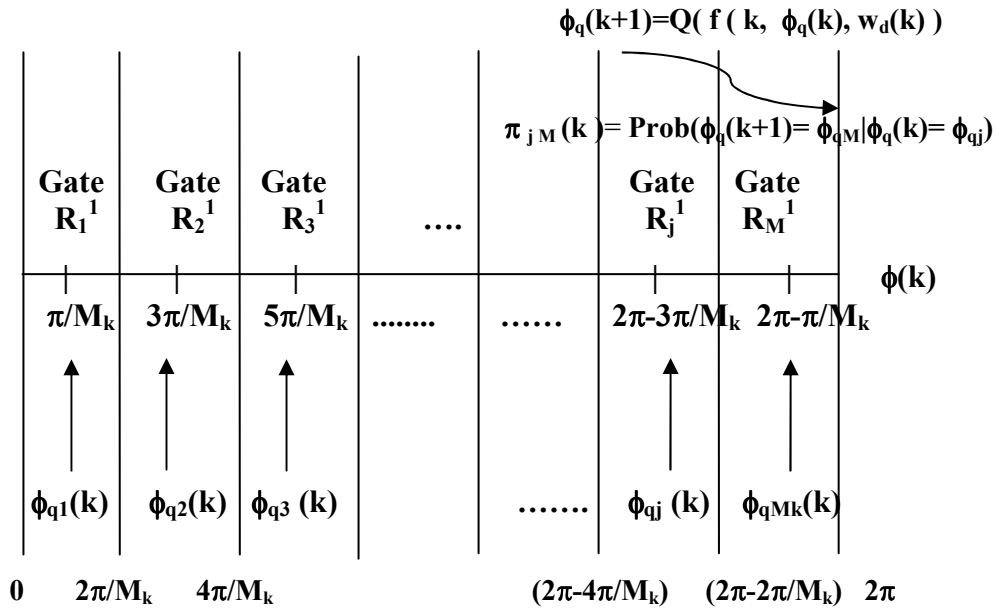


Figure 3: Quantization and transition probability

The transition probability $\pi_{jM}(k)$ is the probability that the phase $\phi(k+1)$ will lie in the gate \mathbf{R}_m^1 when the phase $\phi(k)$ is in the gate \mathbf{R}_j^1 ; i.e.,

$$\pi_{jM}(k) = \text{Pr ob} \{ \phi(k+1) \in \mathbf{R}_m^1 \mid \phi(k) \in \mathbf{R}_j^1 \} \quad (3.2)$$

The transition probability $\pi_{jM}(k)$ is a conditional probability. Hence it can be rewritten as,

$$\begin{aligned}
\pi_{jM}(k) &= \frac{\text{Pr ob}\{\phi(k+1) \in R_m^1, \phi(k) \in R_j^1\}}{\text{Pr ob}\{\phi(k) \in R_j^1\}} \\
&= \left[\int_{R_j^1} p(\phi(k)) d\phi(k) \right]^{-1} \left[\int_{R_j^1} \int_{R_m^1} p(\phi(k+1), \phi(k)) d\phi(k+1) d\phi(k) \right] \\
&= \left[\int_{R_j^1} p(\phi(k)) d\phi(k) \right]^{-1} \left[\int_{R_j^1} \int_{R_m^1} [p(\phi(k+1) | \phi(k)) d\phi(k+1)] p(\phi(k)) d\phi(k) \right]
\end{aligned} \tag{3.3}$$

where $p(\phi(k+1), \phi(k))$ is the joint probability density function of $\phi(k+1)$ and $\phi(k)$; $p(\phi(k))$ is the probability density function of $\phi(k)$; and $p(\phi(k+1) | \phi(k))$ is the conditional probability density function of $\phi(k+1)$ given $\phi(k)$. It is not usually easy to evaluate the transition probability $\pi_{jM}(k)$ analytically. The difficulties are due to the shapes of the R_j^1 and R_m^1 , the statistics of the disturbance noise vectors $w(\cdot)$ and initial channel phase $\phi(0)$. Therefore, due to the evaluation difficulties of the exact transition probabilities between the gates, we discuss an approximate phase transition model which is called finite state model.

3.3 Finite State Model (FSM) for the Phase Transition Model

For numerical calculations of the transition probabilities and channel phase $\phi(k)$, the finite state model can be applied which obtains the phase transition model by quantizing the channel phase and approximating the disturbance noise vector $w(k)$ by discrete random vectors.

The flow chart in Figure 4 describes the finite-state phase transition model used throughout the thesis.

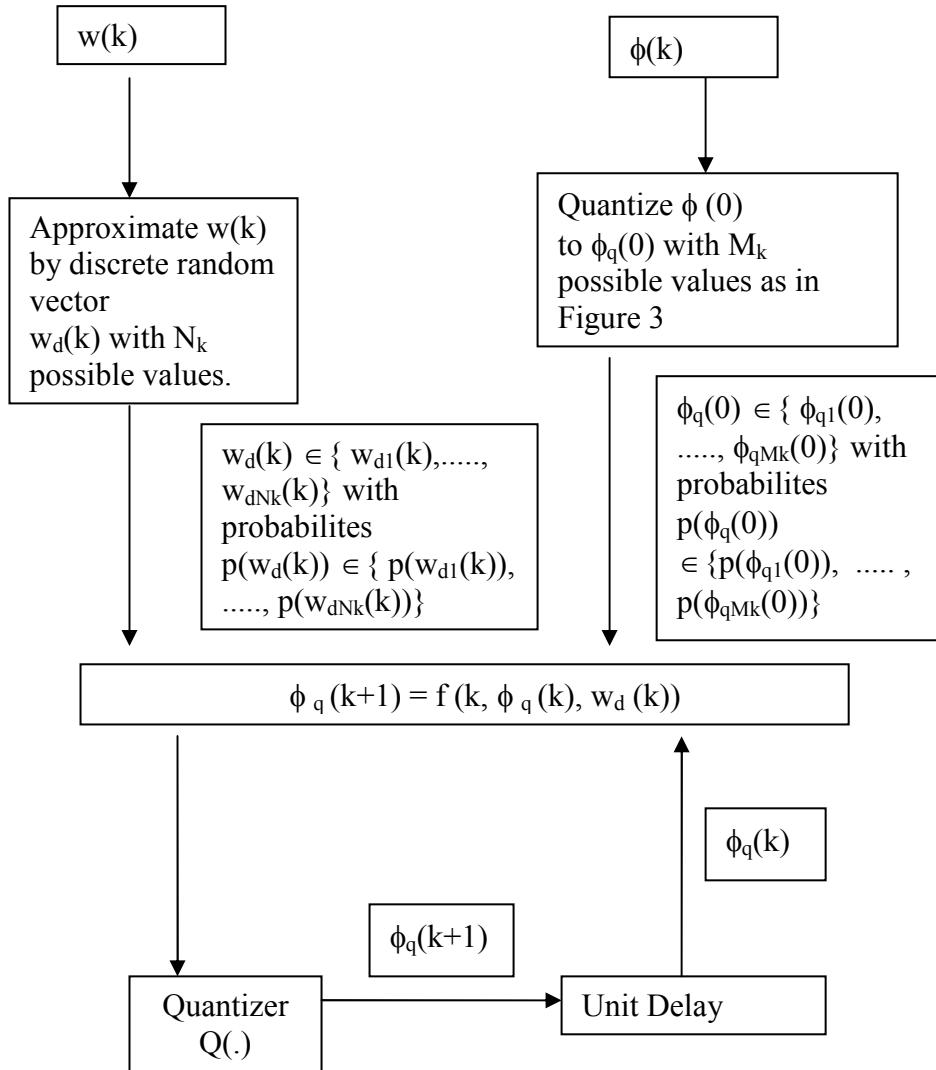


Figure 4: The flowchart of finite state model

For each k , the disturbance noise vector $w(k)$ is approximated by a discrete random vector $w_d(k)$ with possible values of $\{w_{d1}(k), \dots, w_{dNk}(k)\}$; and corresponding probabilities of $\{p(w_{d1}(k)), \dots, p(w_{dNk}(k))\}$ (See Appendix B). Similarly, the initial channel phase $\phi(0)$ is quantized as $\phi_q(0)$ whose possible values are $\phi_{q1}(0), \dots, \phi_{qMk}(0)$; with corresponding probabilities $p(\phi_{q1}(0)), \dots, p(\phi_{qMk}(0))$.

The positive integers N_k and M_k can be selected such that the random vector $w(k)$ and initial channel phase $\phi(0)$ can be satisfactorily approximated by the discrete vector $w_d(k)$ and quantized channel phase $\phi_q(0)$ for the estimation problem.

After, replacing the disturbance noise vector $w(k)$ and initial channel phase $\phi(0)$ with their discrete random vector $w_d(k)$ and quantized channel phase $\phi_q(0)$ respectively, we quantize the channel phase $\phi(k)$ by a Quantizer which has the following formula [5]:

$$\text{Quantizer: } \phi_q(\cdot) = \mathbf{Q}\{\phi(\cdot)\} = \phi_{qi}(\cdot) \quad \text{if } \phi(\cdot) \in \mathbf{R}_i^1 \quad (3.4)$$

where ϕ_{qi} is the center of the gate \mathbf{R}_i^1 .

Therefore, the phase transition model reduces to finite-state model,

$$\phi_q(k+1) = \mathbf{Q}\{f(k, \phi_q(k), w_d(k))\} \quad (3.5)$$

where $\mathbf{Q}\{\cdot\}$ is the Quantizer, $\phi_q(k)$ is the quantized channel phase at symbol k and its values are $\{\phi_{q1}(k), \phi_{q2}(k), \dots, \phi_{qM}(k)\}$ where M_k is the number of possible quantization levels of the channel phase $\phi_q(k)$.

3.3.1 Transition Probabilities and Approximate Observation Model

The transition probability $\pi_{jM}(k)$ is defined as the conditional probability that the quantized channel phase $\phi_q(k+1)$ will be equal to the quantization level ϕ_{qM} for gate \mathbf{R}_M^1 , given that the quantized channel phase $\phi_q(k)$ is equal to the quantization level ϕ_{qj} for gate \mathbf{R}_j^1 , namely;

$$\pi_{jM}(k) = \text{Pr ob}\{\phi_q(k+1) = \phi_{qM} \mid \phi_q(k) = \phi_{qj}\} \quad (3.6)$$

We assume that the quantized channel phase $\phi_q(k)$ is equal to the quantization level ϕ_{qj} for gate \mathbf{R}_j^1 . (i.e. the channel phase value is in \mathbf{R}_j^1 at symbol k)

The transitions from the quantized channel phase ϕ_{qj} for gate \mathbf{R}_j^1 to the others are determined by the discrete random vector $w_d(k)$ and the function $\mathbf{Q}\{f(k, \phi_q(k) = \phi_{qj}, w_d(k))\}$. The discrete random vector $w_d(k)$ can take any value in the set $\{w_{d1}(k), w_{d2}(k), \dots, w_{dNk}(k)\}$ with corresponding probabilities $\{p(w_{d1}(k)), p(w_{d2}(k)), \dots, p(w_{dNk}(k))\}$. Therefore, the quantized channel phase $\phi_q(k+1)$ may at most be equal to M_k various quantization levels.

If the function $f(k, \phi_q(k) = \phi_{qj}, w_d(k))$ maps ϕ_{qj} into another gate, say \mathbf{R}_h^1 for only one possible value, say $w_{dh}(k)$, of the discrete random vector $w_d(k)$, then the transition probability $\pi_{jh}(k)$ from gate \mathbf{R}_j^1 to gate \mathbf{R}_h^1 is the probability that the possible value $w_{dh}(k)$ of $w_d(k)$ occurs, i.e., $\pi_{jh}(k) = p(w_{dh}(k))$.

On the other hand, if the function $f(k, \phi_q(k) = \phi_{qj}, w_d(k))$ maps ϕ_{qj} into another gate, say \mathbf{R}_m^1 for more than one possible value, say $w_{d1}(k)$ and $w_{d2}(k)$, of the discrete random vector $w_d(k)$, the transition probability $\pi_{jm}(k)$ from gate \mathbf{R}_j^1 to gate \mathbf{R}_m^1 is the probability that the discrete random vector $w_d(k)$ is equal to either of the possible values $w_{d1}(k)$ or $w_{d2}(k)$, i.e. $\pi_{jm}(k) = \sum_n p(w_{dn}(k)) = p(w_{d1}(k)) + p(w_{d2}(k))$,

where the summation is over all n such that $\mathbf{Q}\{f(k, \phi_q(k) = \phi_{qj}, w_{dn}(k))\} = \phi_{qm}$.

We have reduced the phase-transition model to a FSM that uses the quantized channel phase $\phi_q(k)$ in Eq. (3.5). However, in the observation model of Eq. (3.1), we use the channel phase $\phi(k)$. Therefore, we need to use the approximate observation model in Eq. (3.1) by replacing the channel phase $\phi(k)$ with the quantized channel phase $\phi_q(k)$.

$$\text{Observation model} \quad : \quad z(k) = g(k, \phi_q(k), \alpha(k), v(k)) \quad (3.7)$$

3.4 Trellis Diagram for the Phase Transition Model

Quantized channel phase $\phi_q(k)$ has M_k possible values, $\phi_{q1}(k), \phi_{q2}(k), \dots, \phi_{qM_k}(k)$. We want to represent the phase transition model in a trellis diagram.

- We want to represent every possible value of the quantized channel phase $\phi_q(k)$ on the k 'th column by points called nodes, with the corresponding possible quantization levels of $\phi_q(k)$ where $k=0,1,\dots,L$.
- We want to represent the phase transition from one node in the k 'th column to another node at the $(k+1)$ 'th column by a line in the direction that indicates the direction of phase transition.

Therefore, the phase transition in phase transition model of Eq. (3.5) can be represented from symbol zero to symbol L by a directed graph which can be called the trellis diagram of phase transition model as shown in Figure 5.

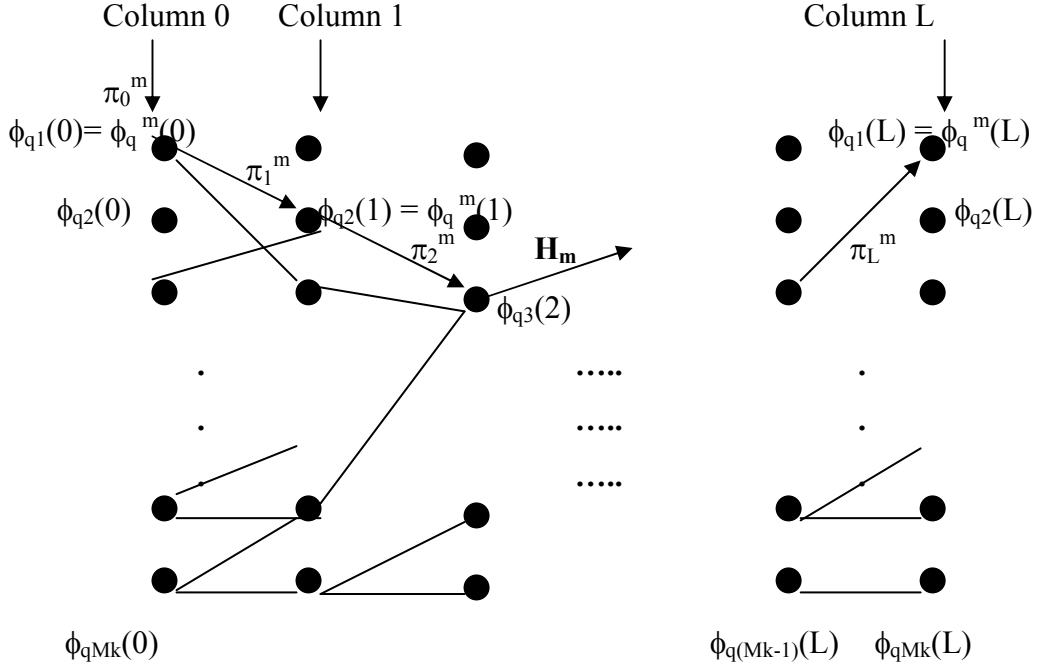


Figure 5: Trellis diagram for phase transition model

The following notations in Figure 5 are explained as follows:

\mathbf{M}_k : The number of quantization levels of quantized channel phase $\phi_q(k)$ at symbol $k=0, 1, \dots, L$.

\mathbf{H}_m : The m 'th path through the trellis diagram, indicated by arrowed lines.

$\phi_q^m(\mathbf{k})$: The quantization level (or node) for the gate in which the phase can take value at symbol k when it follows path \mathbf{H}_m . It is the possible value of the quantized channel phase $\phi_q(k)$ at which m 'th path passes. For example, in the trellis diagram of Figure 5, $\phi_q^m(0) = \phi_{q1}(0)$, $\phi_q^m(1) = \phi_{q2}(1)$,, $\phi_q^m(L) = \phi_{q1}(L)$

π_0^m : Probability that the possible value of the initial channel phase $\phi_q(0)$ from which the m 'th path passes occurs, $\pi_0^m = \text{Prob}\{\phi_q(0) = \phi_q^m(0)\}$. In Figure 5, $\pi_0^m = \text{Prob}\{\phi_q(0) = \phi_{q1}(0)\}$

π_i^m : The transition probability from the $(i-1)$ 'th gate to the i 'th gate for the m 'th path.
 $\pi_i^m = \text{Prob}\{\phi_q(i) = \phi_q^m(i) | \phi_q(i-1) = \phi_q^m(i-1)\}$.

In Figure 5,

$$\pi_1^m = \text{Prob}\{\phi_q(1) = \phi_q^m(1) | \phi_q(0) = \phi_q^m(0)\} = \text{Prob}\{\phi_q(1) = \phi_{q2}(1) | \phi_q(0) = \phi_{q1}(0)\},$$

$$\pi_2^m = \text{Prob}\{\phi_q(2) = \phi_q^m(2) | \phi_q(1) = \phi_q^m(1)\} = \text{Prob}\{\phi_q(2) = \phi_{q3}(2) | \phi_q(1) = \phi_{q2}(1)\}$$

$\Phi_L^m = \{\phi_q^m(0), \phi_q^m(1), \dots, \phi_q^m(L)\}$: Sequence of the quantization levels (nodes) on which the m'th path passes through.

Np: the number of possible paths through the trellis, this number is equal to or less than M_k^{L+1}

$Z^L = \{z(1), \dots, z(L)\}$: Observation sequences from symbol 1 to L.

$\alpha^L = \{\alpha(1), \dots, \alpha(L)\}$: Interference sequence from symbol 1 to L.

The channel phase moves randomly along one of the possible Np paths along the trellis diagram. We want to estimate the most likely path H_i followed by channel phase by using the observation sequence Z^L . Based on the observation sequence, we need to solve a statistical optimization problem with minimum error probability criterion, which is a special case of Bayes' criterion [5]. Therefore, the problem of finding the most likely path H_i reduces to the multiple-(composite) hypothesis-testing problem.

3.5 Minimum Error Probability Criterion [5]

There are Np paths through the trellis diagram of Figure 5. We can represent each of them as H_1, H_2, \dots, H_{Np} or hypothesis. We want to decide the true hypothesis H_i (i.e. the most likely path followed by channel phase) by using the minimum error probability criterion and the observation sequence. The observation space D is divided into Np subspaces D_1, D_2, \dots, D_{Np} . If the observations fall in the decision subspace D_i , which can be called the decision subspace for hypothesis H_i , we decide the most likely path as the hypothesis H_i .

Hence, we want to minimize the overall probability of error, R, (sometimes called Risk) by choosing the true decision region D_i , over all the decision regions namely,

$$R = \sum_{j=1}^{Np} \sum_{\substack{i=1 \\ i \neq j}}^{Np} \left\{ \int_{z^L \in D_i} p(H_j) p(Z^L | H_j) dz^L \right\} \quad (3.8)$$

where

$$p(Z^L | H_j) = \int_{\alpha^L} p(Z^L | H_j, \alpha^L) p(\alpha^L) d\alpha^L$$

$p(Z^L | H_j, \alpha^L)$: Conditional probability of the observation sequence Z^L given the hypothesis H_j and interference sequence α^L .

$p(\alpha^L)$: Joint density function of interference sequence.

$p(H_j)$: A-priori probability for hypothesis H_j .

Therefore, the optimum decision rule is,

$$\text{Choose } H_i \text{ if } p(H_i)p(Z^L | H_i) > p(H_j)p(Z^L | H_j) \text{ for all } i \neq j \quad (3.9)$$

If the inequality in Eq. (3.9) becomes equality for more than one hypothesis, the decision is made randomly among the hypothesis satisfying the equality.

3.6 Optimum Decision Rule for the Channel Phase Paths [5]

We consider the approximate phase transition model in Eq. (3.5). Since the disturbance noise vector $w(k)$ is assumed to be independent of $w(m)$ and $\phi(0)$, and the interference vector $\alpha(k)$ is independent of $\alpha(m)$, for $k \neq m$, the a-priori probability for hypothesis H_i and joint density function of interference sequence α^L can be written as,

$$p(H_i) = \prod_{k=0}^L \pi_k^i \quad (3.10)$$

$$p(\alpha^L) = \prod_{k=1}^L p(\alpha(k)) \quad (3.11)$$

where $p(\alpha(k))$ is the probability density function of the interference vector $\alpha(k)$.

The sequence ϕ_L^i defined before describes the hypothesis H_i completely. Hence, using Eq. (3.11) and under the assumptions of independent observation noise from sample to sample, the function $p(Z^L | H_i)$ in Eq. (3.9) is (see [5] for proof),

$$p(Z^L | H_i) = p(Z^L | \phi_L^i) = \prod_{k=1}^L p(z(k) | \phi_q^i(k)) \quad (3.12)$$

where

$$p(z(k) | \phi_q^i(k)) = \int_{\alpha(k)} p(z(k) | \phi_q^i(k), \alpha(k)) p(\alpha(k)) d\alpha(k) \quad (3.13)$$

Evaluating the integral might be difficult in some cases. Therefore, we can approximate the interference vector $\alpha(k)$ by a discrete random vector $\alpha_d(k)$ whose

possible values are $\{\alpha_{d1}(k), \alpha_{d2}(k), \dots, \alpha_{dR_k}(k)\}$ with corresponding probabilities $\{p(\alpha_{d1}(k)), p(\alpha_{d2}(k)), \dots, p(\alpha_{dR_k}(k))\}$ (see Appendix B) to get an approximate solution of,

$$\int_{\alpha(k)} p(z(k) | \phi_q^i(k), \alpha(k)) p(\alpha(k)) d\alpha(k) \cong \sum_{l=1}^{R_k} p(z(k) | \phi_q^i(k), \alpha_{dl}(k)) p(\alpha_{dl}(k)) \quad (3.14)$$

where R_k is the number of possible values of the approximating discrete vector $\alpha_d(k)$. In other words, by changing the interference $\alpha(k)$ to $\alpha_d(k)$, we make another approximation for the observation model in Eq. (3.7). The observation model becomes,

$$\begin{aligned} z(k) &= g(k, \phi_q(k), \alpha(k) = \alpha_d(k), v(k)) \\ &= g(k, \phi_q(k), \alpha_d(k), v(k)) \end{aligned} \quad (3.15)$$

Substituting Eq. (3.10) and (3.12) into optimum decision rule of Eq. (3.9), we obtain,

Choose H_i if

$$\pi_0^i \prod_{k=1}^L \pi_k^i p(z(k) | \phi_q^i(k)) > \pi_0^j \prod_{k=1}^L \pi_k^j p(z(k) | \phi_q^j(k)) \quad \text{for all } j \neq i.$$

Or equivalently,

Choose H_i if

$$\begin{aligned} \ln(\pi_0^i) + \sum_{k=1}^L \left\{ \ln(\pi_k^i) + \ln(p(z(k) | \phi_q^i(k))) \right\} \\ > \ln(\pi_0^j) + \sum_{k=1}^L \left\{ \ln(\pi_k^j) + \ln(p(z(k) | \phi_q^j(k))) \right\} \end{aligned} \quad (3.16)$$

for all $j \neq i$

where $p(z(k) | \phi_q^i(k)) = \sum_{l=1}^{R_k} p(z(k) | \phi_q^i(k), \alpha_{dl}(k)) p(\alpha_{dl}(k))$ by Eq. (3.14)

$$\text{and } p(z(k) | \phi_q^i(k), \alpha_{dl}(k)) = p(z(k) | \phi_q(k) = \phi_q^i(k), \alpha_d(k) = \alpha_{dl}(k)) \quad (3.17)$$

Therefore, we can use Eq. (3.16) as the optimum decision rule for deciding the most probably followed path by channel phase.

Definition 1: The metric, MN $\{\phi_{qi}(0)\}$, of the initial node $\phi_{qi}(0)$ (a quantization level or node at symbol zero), is

$$\text{MN } \{ \phi_{qi}(0) \} = \ln \{ \text{Prob}(\phi_q(0) = \phi_{qi}(0)) \}$$

Therefore,

$$MN \{ \phi_q^m(0) \} = \ln \{ \pi_0^m \} = \ln (1/M_k) \quad (\text{see Figure 6}) \quad (3.18)$$

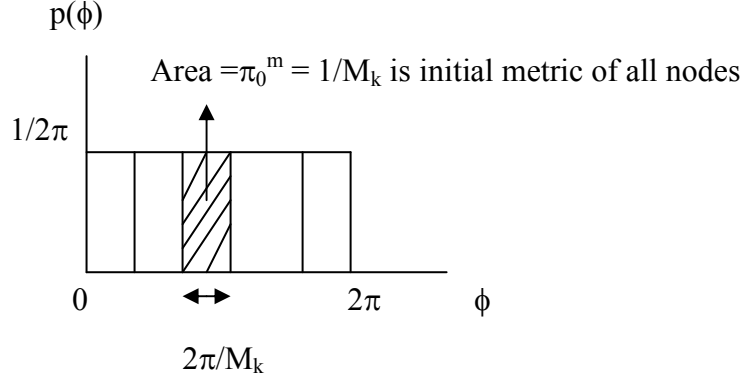


Figure 6: Initial Metric calculation

In Figure 6, $p(\phi)$ is the PDF of the channel phase $\phi(0)$. We partition $p(\phi)$ into M_k equal sections and compute area of each section for initial metric calculations.

Definition 2: The metric of the branch that connects the quantization level (node) $\phi_{qi}(k-1)$ to the quantization level $\phi_{qi}(k)$ which is denoted by $M(\phi_{qi}(k-1) \rightarrow \phi_{qi}(k))$ is,

$$M \{ \phi_{qi}(k-1) \rightarrow \phi_{qi}(k) \} = \ln \{ \text{Prob}(\phi_q(k) = \phi_{qi}(k) | \phi_q(k-1) = \phi_{qi}(k-1)) \} + \ln \{ p(z(k) | \phi_{qi}(k)) \} \quad (3.19)$$

Definition 3: The metric $M(\phi_q^m(p))$ of a path H_m from $\phi_q^m(0)$ at symbol zero, to $\phi_q^m(p)$ at symbol p is the summation of the metric of the initial node from which the path starts i.e. $\ln \{ \pi_0^m \}$ and the metrics of the branches of which the path consists i.e.

$\sum_{k=1}^p [\ln \{ \pi_k^m \} + \ln \{ p(z(k) | \phi_q^m(k)) \}]$, Hence;

$$M(\phi_q^m(p)) = \ln \{ \pi_0^m \} + \sum_{k=1}^p [\ln \{ \pi_k^m \} + \ln \{ p(z(k) | \phi_q^m(k)) \}] \quad (3.20)$$

The optimum decision rule in Eq. (3.16) for deciding the most likely followed path by channel phase from symbol 0 to symbol L is to choose the path with the largest metric as defined in Definition 3 through the trellis diagram as the decision. In this thesis, the optimum decoding algorithm that is used for selecting the Maximum A-Posteriori (MAP) path is Viterbi Decoding Algorithm (VDA) [5]. We call the whole algorithm as Optimum decoding based smoothing algorithm (ODSA).

Therefore, in ODSA, we first construct a trellis diagram for the phase transition model of Eq. (3.5), and then we apply the VDA to obtain the MAP estimate of the channel phase from symbol 0 to L.

3.7 Optimum Decoding Based Smoothing Algorithm (ODSA)

First Step: Construct a trellis diagram for the phase transition model from symbol zero to symbol L by reducing the model to a finite state model as in Eq. (3.5). Then assign its initial metric $M_N \{\phi_{qi}(0)\}$, to each initial node $\phi_{qi}(0)$.

Second Step: By using the observation $z(1)$, calculate the metrics of each node (or quantization level) at symbol 1 (i.e. calculate metrics of M_k quantized nodes). Also, calculate the transition probabilities $\ln \{\text{Prob}(\phi_q(1) = \phi_{qi}(1)) | \phi_q(0) = \phi_{qi}(0)\}$ that connect the initial nodes at symbol zero to the next nodes at symbol 1. Add these metrics to the metrics of the initial nodes from which the branches start, find the metrics of the paths merging at the each node at symbol 1, label the paths with the largest metric, (which are called the best paths for each node at symbol 1), and then discard the other paths. Finally, assign the largest metrics to the nodes at symbol 1, (which are called the metric of the nodes at symbol 1).

k'th Step : By using the observation $z(k)$, calculate the metrics of each node (or quantization level) at symbol k (i.e. calculate metrics of M_k quantized nodes). Also, calculate the transition probabilities $\ln \{\text{Prob}(\phi_q(k) = \phi_{qi}(k)) | \phi_q(k-1) = \phi_{qi}(k-1)\}$ that connect the initial nodes at symbol k-1 to the next nodes at symbol k. Add these metrics to the metrics of the previous nodes, find the metrics of the paths merging at the each node at symbol k, label the paths with the largest metric, (which are called the best paths for each node at symbol k), and then discard the other paths. Finally, assign the largest metrics to the nodes at symbol k, (which are called the metric of the nodes at symbol k).

At the end of symbol L, choose from the nodes at symbol L the largest metric and decide the best path for this node as the most likely path followed by channel phase from symbol 1 to L.

3.7.1 An Example of the ODSA

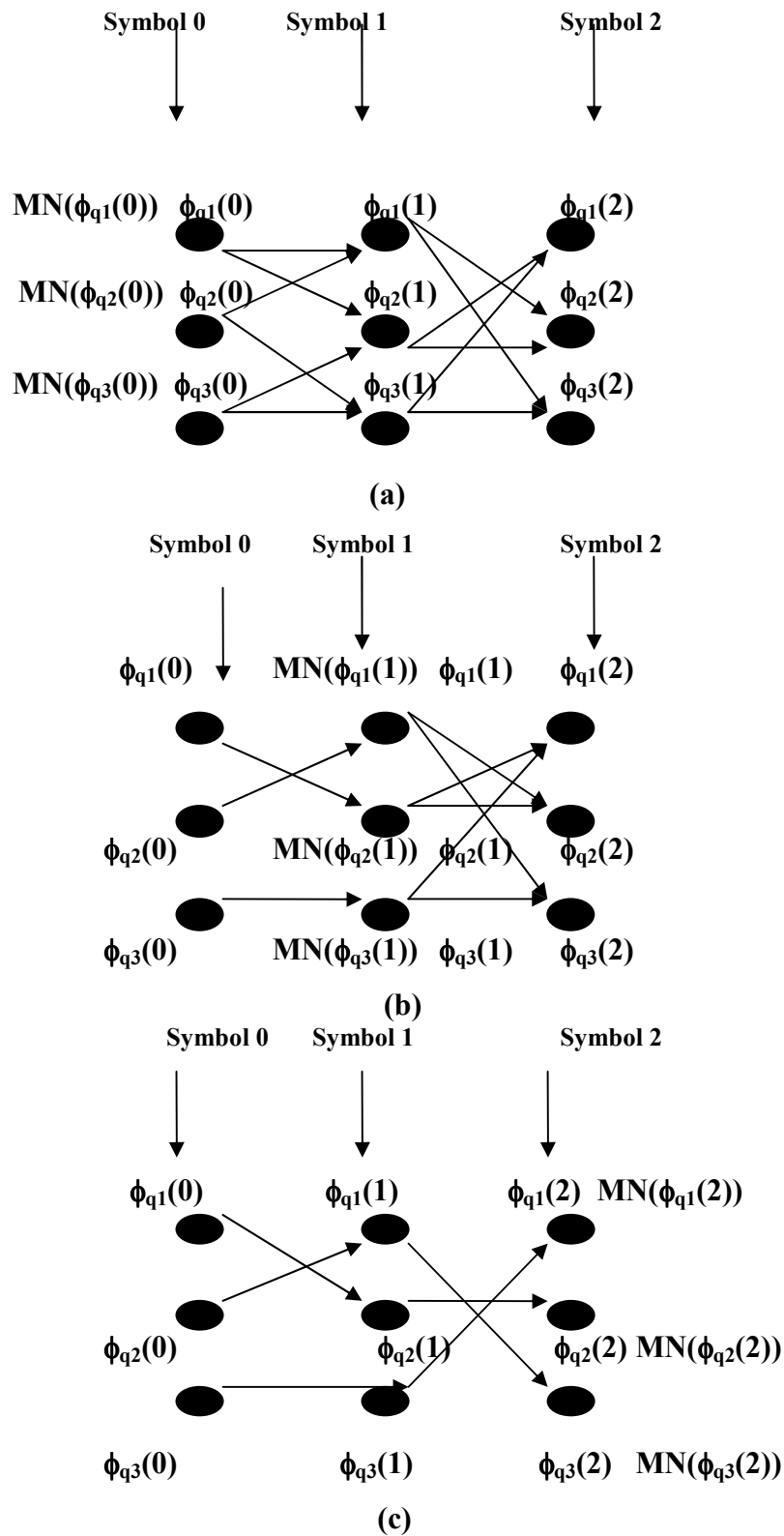


Figure 7: An Example of ODSA

Consider a phase transition model from symbol zero to symbol 2 with $M_k=3$ nodes (or quantization levels) at each symbol. Using ODSA, we would like to find the most likely followed path by the channel phase in the trellis diagram.

First Step: Assign its initial metric to each initial node,

$$MN(\phi_{qi}(0)) = \ln \{ \text{Prob} \{ \phi_q(0) = \phi_{qi}(0) \} \} = \ln \{ 1/M_k \} = \ln \{ 1/3 \}$$

where $M_k=3$ is the number of nodes at symbol 0.

Second Step: Consider the node $\phi_{q1}(1)$. The branches $\phi_{q2}(0) \rightarrow \phi_{q1}(1)$ and $\phi_{q1}(0) \rightarrow \phi_{q1}(1)$ are connecting the nodes at symbol zero to the node $\phi_{q1}(1)$. Hence, we calculate the metrics of these branches and add these metrics to the metrics of nodes $\phi_{q2}(0)$ and $\phi_{q1}(0)$ and obtain the following:

$$ME_{11} = M(\phi_{q1}(0) \rightarrow \phi_{q1}(1)) + MN(\phi_{q1}(0))$$

$$ME_{12} = M(\phi_{q2}(0) \rightarrow \phi_{q1}(1)) + MN(\phi_{q2}(0))$$

Assuming $ME_{12} > ME_{11}$, the path $\phi_{q2}(0) \rightarrow \phi_{q1}(1)$ is chosen as the best path for the node $\phi_{q1}(1)$, and ME_{12} is assigned to the node $\phi_{q1}(1)$ as its metric, $MN(\phi_{q1}(1)) = ME_{12}$. The path $\phi_{q1}(0) \rightarrow \phi_{q1}(1)$ is then discarded.

Similarly, for the node $\phi_{q2}(1)$ and $\phi_{q3}(1)$, $\phi_{q1}(0) \rightarrow \phi_{q2}(1)$ and $\phi_{q3}(0) \rightarrow \phi_{q3}(1)$ are correspondingly chosen as the best path and

$$MN(\phi_{q2}(1)) = M(\phi_{q1}(0) \rightarrow \phi_{q2}(1)) + MN(\phi_{q1}(0))$$

$$MN(\phi_{q3}(1)) = M(\phi_{q3}(0) \rightarrow \phi_{q3}(1)) + MN(\phi_{q3}(0))$$

Therefore, we have Figure 7 (b) at second step.

Third Step: Consider the node $\phi_{q1}(2)$. The branches $\phi_{q2}(1) \rightarrow \phi_{q1}(2)$ and $\phi_{q3}(1) \rightarrow \phi_{q1}(2)$ are connecting the nodes at symbol one to the node $\phi_{q1}(2)$. Hence, we calculate the metrics of these branches and add these metrics to the metrics of nodes $\phi_{q2}(1)$ and $\phi_{q3}(1)$ and obtain the following:

$$ME_{21} = M(\phi_{q2}(1) \rightarrow \phi_{q1}(2)) + MN(\phi_{q2}(1))$$

$$ME_{22} = M(\phi_{q3}(1) \rightarrow \phi_{q1}(2)) + MN(\phi_{q3}(1))$$

Assuming $ME_{22} > ME_{21}$, the path $\phi_{q3}(1) \rightarrow \phi_{q1}(2)$ is chosen as the best path for the node $\phi_{q1}(2)$, and ME_{22} is assigned to the node $\phi_{q1}(2)$ as its metric, $MN(\phi_{q1}(2)) = ME_{22}$. The path $\phi_{q2}(1) \rightarrow \phi_{q1}(2)$ is then discarded.

Similarly, for the node $\phi_{q2}(2)$ and $\phi_{q3}(2)$, $\phi_{q2}(1) \rightarrow \phi_{q2}(2)$ and $\phi_{q1}(1) \rightarrow \phi_{q3}(2)$ are correspondingly chosen as the best path and

$$MN(\phi_{q2}(2)) = M(\phi_{q2}(1) \rightarrow \phi_{q2}(2)) + MN(\phi_{q2}(1))$$

$$MN(\phi_{q3}(2)) = M(\phi_{q1}(1) \rightarrow \phi_{q3}(2)) + MN(\phi_{q1}(1))$$

Therefore, we have Figure 7 (c) at third step.

3.8 An example with Interference and Gaussian disturbance and Observation noises

We consider the following Phase Transition and Observation Models.

$$\text{Phase transition model: } \phi(k+1) = f(k, \phi(k), w(k))$$

$$\text{Observation model: } z(k) = g(k, \phi(k), \alpha(k)) + v(k) \quad (3.21)$$

where $\phi(0)$, $\phi(k)$, $w(k)$, $z(k)$ and $f(k, \phi(k), w(k))$ are defined in Section 3.1, $g(k, \phi(k), \alpha(k))$ is $r \times 1$ vector, $v(k)$ is an $b \times 1$ Gaussian observation noise vector with zero mean and covariance matrix $R_v(k)$, $\alpha(k)$ is an $m \times 1$ interference vector with known statistics. Furthermore, we assume the random vectors $w(j)$, $w(k)$, $v(b)$, $v(m)$, $\alpha(n)$ and $\alpha(p)$ are independent for all j, k, b, m, n, p .

3.8.1 The Metric of Branch between the nodes $\phi_q^i(k-1)$ and $\phi_q^i(k)$ of Hypothesis H_i

Consider the observation model in Eq. (3.21). The observation $z(k)$ is a linear function of the Gaussian observation noise vector $v(k)$. Therefore, the conditional probability density function of $z(k)$ given that $\phi(k) = \phi_q^i(k)$ and $\alpha(k)$, is a multivariate gaussian density function, namely,

$$\begin{aligned} p(z(k) | \phi_q^i(k), \alpha(k)) &= p(z(k) | \phi(k) = \phi_q^i(k), \alpha(k)) \\ &= A \exp -(B/2) \end{aligned} \quad (3.22)$$

where

$$\begin{aligned} A &= (2\pi)^{-r/2} \det \{ R_v(k) \}^{-1/2} \\ B &= [z(k) - g(k, \phi_q^i(k), \alpha(k))]^T [R_v(k)]^{-1} [z(k) - g(k, \phi_q^i(k), \alpha(k))] \end{aligned} \quad (3.23)$$

From Eq. (3.17), we have,

$$p(z(k)|\phi_q^i(k)) = \sum_{l=1}^{R_k} p(z(k)|\phi_q^i(k), \alpha_{dl}(k)) p(\alpha_{dl}(k)) \quad (3.24)$$

where $p(z(k)|\phi_q^i(k), \alpha_{dl}(k)) = p(z(k)|\phi_q^i(k), \alpha(k)=\alpha_{dl}(k))$, which is given by Eq. (3.22).

Substituting Eq. (3.24) into Eq. (3.19) yields the metric of the branch between the nodes $\phi_q^i(k-1)$ and $\phi_q^i(k)$,

$$M(\phi_q^i(k-1) \rightarrow \phi_q^i(k)) = \ln(\pi_k^i) + \ln p(z(k)|\phi_q^i(k)) \quad (3.25)$$

3.9 Slowly Fading Frequency Nonselective Channel (SFFNC) Model and Assumptions

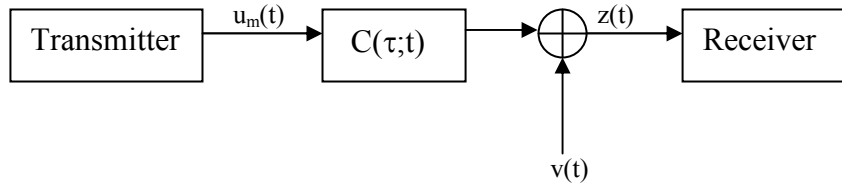


Figure 8: A Rayleigh fading channel Model

The low pass equivalent of the received signal in Figure 8 in Rayleigh fading channel can be expressed as

$$\begin{aligned} z(t) &= C(\tau; t) * u_m(t) + v(t) \\ &= \int_{-\infty}^{\infty} C(\tau; t) u_m(t - \tau) d\tau + v(t) \\ &= \int_{-\infty}^{\infty} C(f; t) U_m(f) \exp(j2\pi ft) df + v(t) \quad m=1,2 \end{aligned} \quad (3.26)$$

where $u_m(t)$ is the transmitted low pass equivalent of the bandpass signal $s_m(t)$ over a Rayleigh fading channel.

$v(t) = v_1(t) + j v_2(t)$ is the complex envelope of the bandpass Additive White Gaussian Noise (AWGN) $N(t)$ with $E\{v(t)\} = 0$ and $E\{v(t)v^*(t+\tau)\} = 2\sigma^2\delta(\tau)$ (* denotes

conjugation). $v_1(t)$ and $v_2(t)$ are the in-phase and quadrature components of noise $N(t)$ respectively. The power spectrum of $N(t)$ is assumed to be symmetric around the carrier so that $v_1(t)$ and $v_2(t)$ are uncorrelated white Gaussian noise processes [21], with zero mean and variances σ^2 .

$C(t;\tau)$ represents the response of the channel at time t due to an impulse applied at time $t-\tau$. In Rayleigh fading channels, $C(t;\tau)$ is a zero mean, complex Gaussian process.

$$C(f;t) = F\{C(\tau;t)\} = \int_{-\infty}^{\infty} C(\tau;t) \exp(-j2\pi f\tau) d\tau \quad (3.27)$$

where $F\{\}$ is the Fourier Transform and $C(f;t)$ is called the time-varying transfer function of multipath fading channel.

In frequency nonselective channels, Eq. (3.26) becomes,

$$\begin{aligned} z(t) &= C(0;t) \int_{-\infty}^{\infty} U_m(f) \exp(j2\pi ft) df + v(t) \\ &= C(0;t) u_m(t) + v(t) \\ &= \alpha(t) \exp(-j\phi(t)) u_m(t) + v(t) \end{aligned} \quad (3.28)$$

where $C(0;t) = C(t)$ represents the complex Gaussian channel coefficient. $C(t)$ can be expressed as $C(t) = X(t) + j Y(t)$ where $X(t)$ and $Y(t)$ are zero-mean stationary independent Gaussian random processes with autocorrelation functions $R_{XX}(\tau) = R_{YY}(\tau)$.

$\alpha(t) = \sqrt{(X(t))^2 + (Y(t))^2}$ is a Rayleigh distributed random process.

$\phi(t) = \tan^{-1}\left(\frac{Y(t)}{X(t)}\right)$ is the uniformly distributed channel phase process.

We assume slowly fading channel i.e. the fading bandwidth is small but non-zero. Hence, the complex Gaussian channel coefficient remains approximately constant over symbol duration of T . Therefore, both Rayleigh distributed random process $\alpha(t)$ and uniformly distributed channel phase $\phi(t)$ can be assumed to be constant or independent of time during a symbol interval, i.e. $\alpha(t) = \alpha$, $\phi(t) = \phi$. Therefore, Eq. (3.28) simplifies into,

$$z(t) = \alpha \exp(-j\phi) u_m(t) + v(t) \quad (3.29)$$

where α is a Rayleigh random variable and ϕ is a random variable that is uniformly distributed between $(0, 2\pi)$.

The continuous-time Gaussian Channel coefficient process $C(t)$ is slowly varying and assumed to be constant during a signaling interval. Therefore, it can be approximated by the piecewise-constant process $\{C(k) = X(k) + j Y(k)\}$. Throughout this thesis, we assume the first order Markov fading process for a slowly fading, frequency nonselective channel where $X(k)$ and $Y(k)$ are mutually uncorrelated, zero mean Gaussian random processes each with autocorrelation functions $R_{XX}(\tau) = R_{YY}(\tau) = \gamma \lambda^{|\tau|}$ similarly to [14], [28], [29] and [30]. Therefore, complex Gaussian channel coefficient's inphase and quadrature components are,

$$\begin{aligned} \text{Inphase component} & : & X(k+1) &= \lambda X(k) + n_1(k) \\ \text{Quadarature component} & : & Y(k+1) &= \lambda Y(k) + n_2(k) \end{aligned} \quad (3.30)$$

where $k=1, \dots, L$ and L is the number of transmitted symbols, $n_1(k)$ and $n_2(k)$ are sets of independent identically distributed (i.i.d) zero mean, Gaussian random variables with variance $\gamma(1-\lambda^2)$, λ is the correlation coefficient of the channel and γ is the variance of inphase and quadrature components. In Eq. (3.30), the Channel Coefficient is assumed to change from symbol-to-symbol i.e. the Channel Coefficient is constant at k 'th symbol interval and changes from one symbol interval to another.

In addition, we assume that the random variables $\phi(0)$, $n_1(j)$, $n_1(m)$, $n_2(j)$, $n_2(m)$, $v(j)$ and $v(m)$ are assumed to be independent for all j, m .

CHAPTER 4

OPTIMUM RECEIVERS FOR BINARY ORTHOGONAL AND PSK SIGNALS IN SLOWLY FADING FREQUENCY NONSELECTIVE CHANNELS

In this chapter, we obtain the optimum receivers for the carrier modulated binary signals (BPSK and binary orthogonal signals) both in coherent (i.e. channel phase is known or estimated in receiver) and noncoherent (i.e. channel phase is unknown and no attempt is made to estimate its value at the receiver) detection in slowly fading, frequency nonselective channels.

4.1 Optimum Receiver for Binary Signals

We want to transmit the information by using two carrier modulated signals $s_1(t)$ and $s_2(t)$ in a binary communication system where

$$s_m(t) = \text{Re}\{u_m(t)\exp(j2\pi f_c t)\}, \quad m=1,2 \quad 0 \leq t \leq T \quad (4.1)$$

and $u_m(t)$, $m=1,2$ are the equivalent low-pass signals. In addition we assume that the two signals are assumed to have equal energy,

$$\int_0^T |u_m(t)|^2 dt = 2E_m = 2E \quad m=1,2 \quad (4.2)$$

and are characterized by the complex-valued correlation coefficient

$$\rho = \frac{\int_0^T u_1(t)u_2^*(t)dt}{2E} \quad (4.3)$$

The equivalent low-pass received signal $z(t)$ in frequency-nonselctive slowly fading channel may be expressed as,

$$z(t) = \alpha \exp(-j\phi)u_m(t) + v(t), \quad m=1,2 \quad 0 \leq t \leq T \quad (4.4)$$

The received signal $z(t)$ is passed through a demodulator whose sampled output at $t=T$ is passed to the detector to obtain the output decision.

4.1.1 The Optimum Demodulator for Binary Signals

In [6], it is shown that if the received signal was correlated with a set of orthonormal functions $\{f_n(t)\}$ that spanned the signal space, the outputs from the bank of correlators provide a set of sufficient statistics for the detector to make a decision that minimizes the probability of error. It is also demonstrated that a bank of matched filters could be substituted for the bank of correlators.

Similar orthonormal decomposition can also be employed for a received signal in slowly fading frequency nonselective Rayleigh channel with channel phase ϕ and Rayleigh amplitude gain α [6], [10].

In this chapter, we deal with the equivalent low-pass signals and specify the signal correlators or matched filters in terms of the equivalent low-pass signal waveforms.

Hence, the impulse response $h_m(t)$ of a filter that is matched to the complex-valued equivalent low-pass signal $u_m(t)$, $0 \leq t \leq T$ is given as

$$h_m(t) = u_m^*(T-t) \quad m=1,2 \quad (4.5)$$

and the output of such a filter at $t=T$ is simply,

$$\int_0^T |u_m(t)|^2 dt = 2E \quad m=1,2 \quad (4.6)$$

where E is the signal energy. A similar result can also be obtained if the signal $u_m(t)$ is correlated with $u_m^*(t)$ and the correlator is sampled at $t=T$. Therefore the optimum demodulator for the equivalent low-pass received signal $z(t)$ in Eq. (4.4) may be realized by two matched filter receivers in parallel, one matched to $u_1(t)$ and the other to $u_2(t)$ as shown in Figure 9. The output of the matched filters or correlators at the sampling instant are the two complex numbers $Z_1 = Z_{1r} + j Z_{1m}$, $Z_2 = Z_{2r} + j Z_{2m}$.

If we suppose that the transmitted signal is $u_1(t)$. Then,

$$Z_1 = 2 \alpha E \cos(\phi) + V_{1r} + j (-2E \sin(\phi) + V_{1m})$$

$$Z_2 = 2 \alpha E \rho \cos(\phi) + V_{2r} + j (-2E \rho \sin(\phi) + V_{2m}) \quad (4.7)$$

And if we suppose that the transmitted signal is $u_2(t)$. Then,

$$Z_1 = 2 \alpha E \rho \cos(\phi) + V_{1r} + j (-2E \rho \sin(\phi) + V_{1m})$$

$$Z_2 = 2 \alpha E \cos(\phi) + V_{2r} + j (-2E \sin(\phi) + V_{2m}) \quad (4.8)$$

Where ρ is the complex-valued correlation coefficient of the two signals $u_1(t)$ and $u_2(t)$ which is defined in Eq. (4.3). The random variables V_{1r} , V_{1m} , V_{2r} and V_{2m} are jointly Gaussian, with zero mean and equal variance.

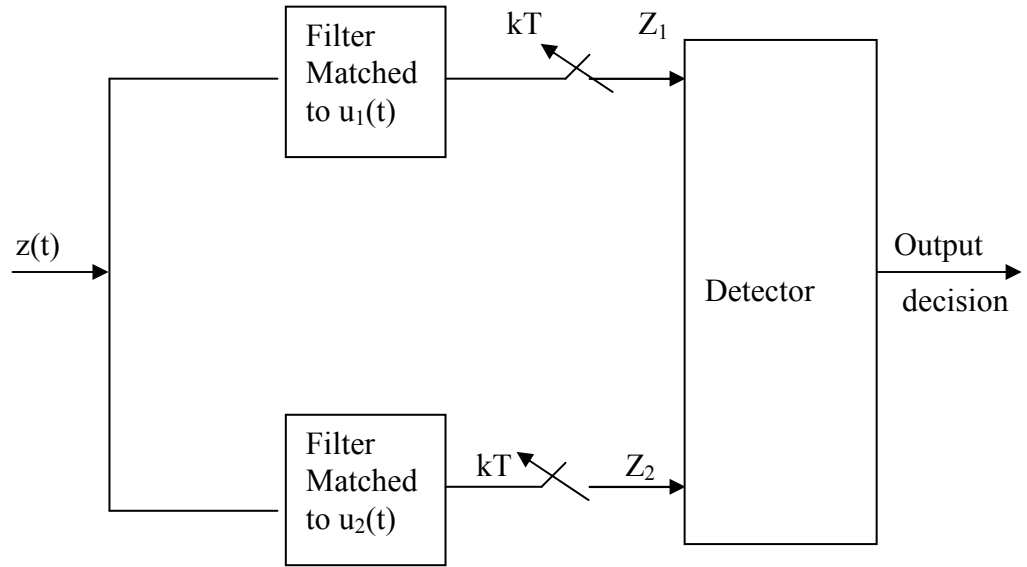


Figure 9: Optimum receiver for binary signals

4.1.2 The Optimum Detector for Binary Signals

The optimum detector or decision rule observes the random variables

$\vec{Z} = [Z_{1r} \ Z_{1m} \ Z_{2r} \ Z_{2m}]$ where $Z_1 = Z_{1r} + j \ Z_{1m}$ and $Z_2 = Z_{2r} + j \ Z_{2m}$ and outputs its decision on the posterior probabilities $p(u_m / \vec{Z})$ $m=1,2$. These probabilities may be expressed as,

$$p(u_m / \vec{Z}) = \frac{p(\vec{Z} / u_m) p(u_m)}{p(\vec{Z})} \quad m=1,2 \quad (4.9)$$

And hence the optimum decision rule may be expressed as,

$$p(u_1 | \bar{Z}) \underset{u_2}{\overset{u_1}{>}} p(u_2 | \bar{Z}) \quad (4.10)$$

Or equivalently,

$$\frac{p(\bar{Z}/u_1)}{p(\bar{Z}/u_2)} \underset{u_2}{\overset{u_1}{\geq}} \frac{p(u_2)}{p(u_1)} \quad (4.11)$$

The ratio of PDFs on the left hand side of Eq. (4.11) is the *likelihood ratio*, which is denoted as,

$$\Omega(\bar{Z}) = \frac{p(\bar{Z}/u_1)}{p(\bar{Z}/u_2)} \quad (4.12)$$

The right hand side of the Eq. (4.11) is the ratio of the two prior probabilities, which is unity when the two signals are equally probable.

4.2 Optimum Coherent Detector for Binary Orthogonal Signals

In coherent demodulation, the channel phase $\{\phi\}$ is assumed to be known or estimated at the receiver. On the other hand, in deriving the optimum detector or decision variable, we assume that the Rayleigh amplitude gain α is assumed to be unknown at the receiver.

The probability density functions $p(\bar{Z}/u_1)$ and $p(\bar{Z}/u_2)$ can be obtained by averaging the PDFs $p(\bar{Z}/u_m, \alpha)$ over the PDF of the Rayleigh amplitude gain α , i.e.

$$p(\bar{Z}/u_m) = \int_{-\infty}^{\infty} p(\bar{Z}/u_m, \alpha) p(\alpha) d\alpha \quad (4.13)$$

We want to perform the integration indicated in Eq. (4.13) for the binary orthogonal signals, i.e, $\rho=0$. In this case, the outputs of the demodulator Z_1 and Z_2 are;

If we assume $u_1(t)$ is transmitted;

$$Z_1 = Z_{1r} + j Z_{1m}$$

$$\begin{aligned}
&= 2 \alpha E \cos(\phi) + V_{1r} + j (-2 \alpha E \sin(\phi) + V_{1m}) \\
Z_2 &= Z_{2r} + j Z_{2m} \\
&= V_{2r} + j V_{2m}
\end{aligned} \tag{4.14}$$

And if we assume $u_2(t)$ is transmitted;

$$\begin{aligned}
Z_1 &= Z_{1r} + j Z_{1m} \\
&= V_{1r} + j V_{1m} \\
Z_2 &= Z_{2r} + j Z_{2m} \\
&= 2 \alpha E \cos(\phi) + V_{2r} + j (-2 \alpha E \sin(\phi) + V_{2m})
\end{aligned} \tag{4.15}$$

where $(V_{1r}, V_{1m}, V_{2r}, V_{2m})$ are mutually uncorrelated and hence statistically independent, zero-mean Gaussian random variables [6]. Hence, the joint PDF of $\vec{Z} = [Z_{1r}, Z_{1m}, Z_{2r}, Z_{2m}]$ may be expressed as a product of the marginal PDFs. Consequently,

If we assume $u_1(t)$ is transmitted,

$$\begin{aligned}
p(Z_{1r}, Z_{1m} / u_1, \alpha) &= \frac{1}{2\pi\sigma^2} \exp \left[-\frac{(Z_{1r} - 2\alpha E \cos(\phi))^2 + (Z_{1m} + 2\alpha E \sin(\phi))^2}{2\sigma^2} \right] \\
p(Z_{2r}, Z_{2m} / u_1) &= \frac{1}{2\pi\sigma^2} \exp \left[-\frac{Z_{2r}^2 + Z_{2m}^2}{2\sigma^2} \right]
\end{aligned} \tag{4.16}$$

where

$$\begin{aligned}
\sigma^2 &= \int_{-\infty}^{\infty} S_v(f) df = \int_{-\infty}^{\infty} S_w(f) |H(f)|^2 df \\
&= N_0 \int_{-\infty}^{\infty} |H(f)|^2 df = N_0 \int_0^T |h(t)|^2 dt \quad (\text{By Parseval's Theorem}) \\
&= N_0 \int_0^T |u_m(T-t)|^2 dt = 2N_0 E
\end{aligned} \tag{4.17}$$

In Eq. (4.17), $H(f)$ is the frequency response of the matched filter $h(t)$ or $u_m(T-t)$, $S_w(f)$ is the Power spectral density of white Gaussian noise i.e. $S_w(f) = N_0$ for all f , and $S_v(f)$ is the power spectral density of noise at matched filter output.

The PDF of the envelope α is Rayleigh distributed. Hence,

$$p(\alpha) = \begin{cases} \frac{\alpha}{\sigma_1^2} \exp \left[-\frac{\alpha^2}{2\sigma_1^2} \right] & \text{for } \alpha \geq 0 \\ 0 & \text{otherwise} \end{cases} \tag{4.18}$$

where σ_1^2 is the parameter of the Rayleigh PDF. With $p(\alpha)$ substituted into the integral in Eq. (4.13), we obtain,

$$\begin{aligned}
p(Z_{1r}, Z_{1m} / u_1) &= \int_0^{\infty} p(Z_{1r}, Z_{1m} / u_1, \alpha) p(\alpha) d\alpha \\
&= \frac{1}{2\pi\sigma_1^2\sigma^2} \int_0^{\infty} \alpha \exp\left[-\frac{(Z_{1r} - 2E\alpha \cos(\phi))^2 + (Z_{1m} + 2E\alpha \sin(\phi))^2}{2\sigma^2} - \frac{\alpha^2}{2\sigma_1^2}\right] d\alpha \\
&= \frac{1}{2\pi\sigma_1^2\sigma^2} \exp\left[-\frac{Z_{1r}^2 + Z_{1m}^2}{2\sigma^2}\right] \\
&\quad \int_0^{\infty} \alpha \exp\left[\alpha^2\left(-\frac{1}{2\sigma_1^2} - \frac{4E^2}{\sigma^2}\right) + \left(\frac{2E\alpha}{\sigma^2}(Z_{1r} \cos(\phi) - Z_{1m} \sin(\phi))\right)\right] d\alpha
\end{aligned} \tag{4.19}$$

By performing a similar integration as in Eq. (4.19) under the assumption that the signal $u_2(t)$ is transmitted, we obtain the results,

$$p(Z_{1r}, Z_{1m} / u_2) = \frac{1}{2\pi\sigma^2} \exp\left[-\frac{Z_{1r}^2 + Z_{1m}^2}{2\sigma^2}\right] \tag{4.20}$$

and

$$\begin{aligned}
p(Z_{2r}, Z_{2m} / u_2) &= \int_0^{\infty} p(Z_{2r}, Z_{2m} / u_2, \alpha) p(\alpha) d\alpha \\
&= \frac{1}{2\pi\sigma_1^2\sigma^2} \int_0^{\infty} \alpha \exp\left[-\frac{(Z_{2r} - 2E\alpha \cos(\phi))^2 + (Z_{2m} + 2E\alpha \sin(\phi))^2}{2\sigma^2} - \frac{\alpha^2}{2\sigma_1^2}\right] d\alpha \\
&= \frac{1}{2\pi\sigma_1^2\sigma^2} \exp\left[-\frac{Z_{2r}^2 + Z_{2m}^2}{2\sigma^2}\right] \\
&\quad \int_0^{\infty} \alpha \exp\left[\alpha^2\left(-\frac{1}{2\sigma_1^2} - \frac{4E^2}{\sigma^2}\right) + \left(\frac{2E\alpha}{\sigma^2}(Z_{2r} \cos(\phi) - Z_{2m} \sin(\phi))\right)\right] d\alpha
\end{aligned} \tag{4.21}$$

When we substitute these results into the likelihood ratio given by Eq. (4.11), we obtain the result,

$$\Omega(\bar{Z}) = \frac{\left(\int_0^\infty \alpha \exp \left[\alpha^2 \left(-\frac{1}{2\sigma_1^2} - \frac{4E^2}{\sigma^2} \right) + \alpha \left(\frac{2E}{\sigma^2} (Z_{1r} \cos(\phi) - Z_{1m} \sin(\phi)) \right) \right] d\alpha \right)^{u_1}}{\left(\int_0^\infty \alpha \exp \left[\alpha^2 \left(-\frac{1}{2\sigma_1^2} - \frac{4E^2}{\sigma^2} \right) + \alpha \left(\frac{2E}{\sigma^2} (Z_{2r} \cos(\phi) - Z_{2m} \sin(\phi)) \right) \right] d\alpha \right)^{u_2}} \underset{u_2}{>} \underset{u_1}{\frac{p(u_2)}{p(u_1)}} \quad (4.22)$$

A significant simplification in the implementation of the optimum detector occurs when the two signals are equally probable. In such a case the threshold becomes unity, and the optimum detection rule simplifies into,

$$\underset{u_2}{\left[Z_{1r} \cos(\phi) - Z_{1m} \sin(\phi) \right]} \underset{u_1}{>} \underset{u_2}{\left[Z_{2r} \cos(\phi) - Z_{2m} \sin(\phi) \right]} \quad (4.23)$$

Or equivalently,

$$\underset{u_2}{\operatorname{Re} \{ \exp(j\phi)(Z_1) \}} \underset{u_1}{>} \underset{u_2}{\operatorname{Re} \{ \exp(j\phi)(Z_2) \}} \quad (4.24)$$

The proposed receiver is shown in Figure 10. The channel phase is estimated by the ODSA and the optimum decision (or detection rule) in Eq. (4.23) or Eq. (4.24) decides on the transmitted signal.

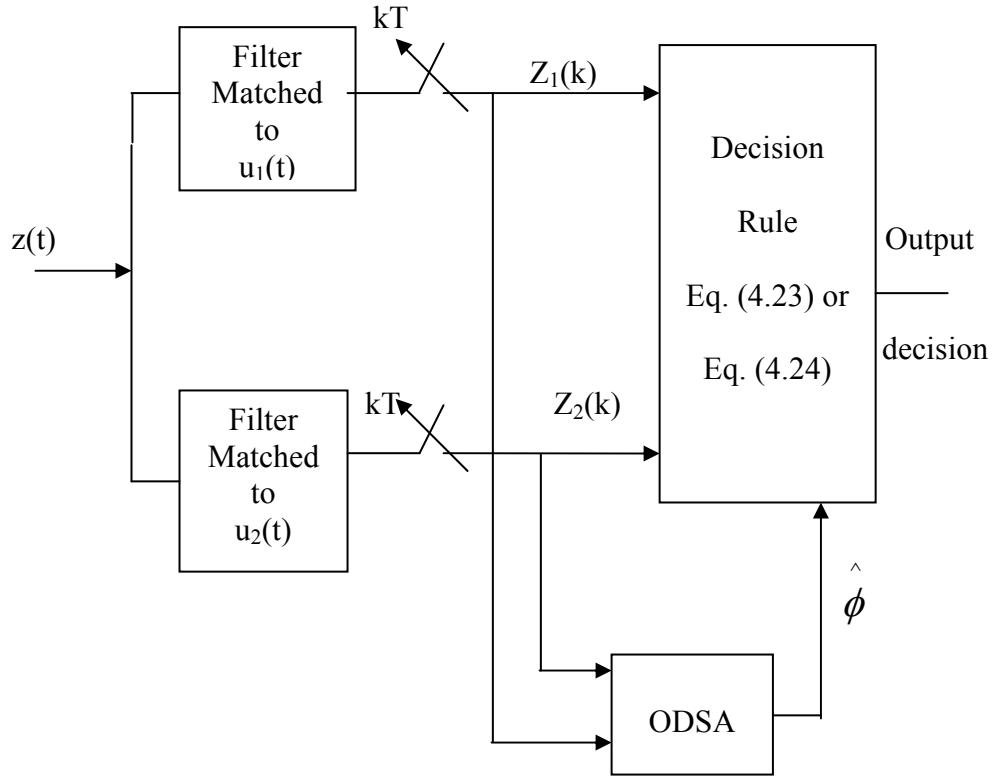


Figure 10: Proposed Receiver for binary orthogonal signals

4.2.1 Application of ODSA to Binary Orthogonal Signals

We use the following Phase Transition and Observation Models for Binary Orthogonal Signals in SFFNC.

Phase transition model:

$$\begin{aligned} \phi(k+1) &= \tan^{-1} \left(\frac{Y(k+1)}{X(k+1)} \right) = \tan^{-1} \left(\frac{\lambda Y(k) + n_2(k)}{\lambda X(k) + n_1(k)} \right) \\ &= \tan^{-1} \left(\frac{-\lambda \alpha(k) \sin(\phi(k)) + n_2(k)}{\lambda \alpha(k) \cos(\phi(k)) + n_1(k)} \right) \end{aligned}$$

Observation models:

$$Z_1(k) = \int_{(k-1)T}^{kT} z(t)u_1^*(t)dt, \quad Z_2(k) = \int_{(k-1)T}^{kT} z(t)u_2^*(t)dt$$

where $z(t) = \alpha(t) \exp(-j\phi(t)) [\beta u_1(t) + (1-\beta) u_2(t)] + v_1(t) + j v_2(t)$.

The outputs of the demodulator $Z_1(k)$ and $Z_2(k)$ at the $\{(k-1)T, kT\}$ symbol interval are;

$$\begin{aligned} Z_1(k) &= \alpha(k) \exp(-j\phi(k)) [\beta 2E] + v_{1,1}(k) + jv_{1,2}(k) \\ Z_2(k) &= \alpha(k) \exp(-j\phi(k)) [(1-\beta) 2E] + v_{2,1}(k) + jv_{2,2}(k) \end{aligned} \quad (4.25)$$

where $k=1, \dots, L$ and L is the number of transmitted bits, $X(k+1) = \lambda X(k) + n_1(k)$ and $Y(k+1) = \lambda Y(k) + n_2(k)$ are the Inphase and Quadrature components of the Complex Gaussian Channel Coefficient $C(k+1)$, λ is the correlation coefficient of the first order Markov fading process, $n_1(k)$ and $n_2(k)$ are uncorrelated zero mean Gaussian random variables with variances $\sigma_n^2 = \gamma(1-\lambda^2)$, $\alpha(k) = \alpha$ is a random variable with Rayleigh PDF at the k 'th symbol (i.e. it is constant during a symbol interval $\{(k-1)T, kT\}$) with parameter σ_1^2 for $k=1, \dots, L$,

$$\begin{aligned} \sigma_1^2 &= \sigma_{1,k}^2 = \lambda^2 \sigma_{1,k-1}^2 + \sigma_n^2 = \lambda^{2k-2} \sigma_{1,1}^2 + \sigma_n^2 (\lambda^{2k-4} + \lambda^{2k-6} + \dots + \lambda^2 + \lambda^0) \\ &= \lambda^{2k-2} \sigma_{1,1}^2 + \gamma (1-\lambda^{2k-2}) = \gamma \end{aligned} \quad (4.26)$$

where $\sigma_{1,k}^2$ is the parameter of the Rayleigh PDF at symbol k , $\sigma_{1,1}^2 = \gamma$ and $\alpha(k)$ is correlated with $\alpha(m)$ for $k \neq m$, $\phi(k)$ is the channel phase at k 'th transmitted symbol, $v_{1,1}(k)$, $v_{1,2}(k)$, $v_{2,1}(k)$ and $v_{2,2}(k)$ are mutually uncorrelated Gaussian random variables with $N(0, 2EN_0)$ at the k 'th symbol and are mutually independent of $v_{1,1}(m)$, $v_{1,2}(m)$, $v_{2,1}(m)$ and $v_{2,2}(m)$ at the m 'th symbol[6].

$$\beta = \begin{cases} 1 & \text{with probability 0.5 if signals are equally likely} \\ 0 & \text{with probability 0.5 if signals are equally likely} \end{cases}$$

In ODSA, we reduce the phase transition model into,

Phase transition model:

$$\begin{aligned}\phi_q(k+1) &= Q \left\{ \tan^{-1} \left(\frac{Y(k+1)}{X(k+1)} \right) \right\} = Q \left\{ \tan^{-1} \left(\frac{\lambda Y(k) + n_2(k)}{\lambda X(k) + n_1(k)} \right) \right\} \\ &= Q \left\{ \tan^{-1} \left(\frac{-\lambda \alpha(k) \sin(\phi_q(k)) + n_2(k)}{\lambda \alpha(k) \cos(\phi_q(k)) + n_1(k)} \right) \right\}\end{aligned}\quad (4.27)$$

4.2.2 The Metric of Branch between the nodes $\phi_q^i(k-1)$ and $\phi_q^i(k)$ of Hypothesis H_1 in Binary Orthogonal Signals

The observations $Z_1(k)$ and $Z_2(k)$ given in Eq. (4.25) are linear functions of the Gaussian observation noises $v_{1,1}(k) + jv_{1,2}(k)$ and $v_{2,1}(k) + jv_{2,2}(k)$ respectively. Therefore, the conditional probability density function of $Z_1(k)$ and $Z_2(k)$ given that $\phi(k) = \phi_q^i(k)$ and $\alpha(k)$, is a Gaussian density function,

$$\begin{aligned}p(Z_1(k), Z_2(k) | \phi_q^i(k), \alpha(k), \beta) &= \\ p(Z_1(k) | \phi(k) = \phi_q^i(k), \alpha(k), \beta) &p(Z_2(k) | \phi(k) = \phi_q^i(k), \alpha(k), \beta)\end{aligned}\quad (4.28)$$

and

$$\begin{aligned}p(Z_1(k), Z_2(k) | \phi_q^i(k), \alpha(k)) &= \\ \left[\sum_{\beta=0,1} p(Z_1(k) | \phi_q^i(k), \alpha(k), \beta) &p(Z_2(k) | \phi_q^i(k), \alpha(k), \beta) p(\beta) \right]\end{aligned}\quad (4.29)$$

where

$$p(Z_1(k) | \phi_q^i(k), \alpha(k), \beta) = \frac{1}{\sqrt{2\pi\sigma^2}} \exp \left(-\frac{|Z_1(k) - 2\alpha(k) \exp(-j\phi_q^i(k)) \beta E|^2}{2\sigma^2} \right)$$

and

$$p(Z_2(k) | \phi_q^i(k), \alpha(k), \beta) = \frac{1}{\sqrt{2\pi\sigma^2}} \exp \left(-\frac{|Z_2(k) - 2\alpha(k) \exp(-j\phi_q^i(k)) (1-\beta) E|^2}{2\sigma^2} \right)\quad (4.30)$$

and $\sigma^2 = 2EN_0$.

After approximating $\alpha(k)$ by a discrete random vector $\alpha_d(k)$ whose possible values are $\{\alpha_{d1}(k), \alpha_{d2}(k), \dots, \alpha_{dR_k}(k)\}$ with corresponding probabilities $\{p(\alpha_{d1}(k)), p(\alpha_{d2}(k)), \dots, p(\alpha_{dR_k}(k))\}$ where R_k is the size of the vector $\alpha_d(k)$,

$$\begin{aligned} p(Z_1(k)|\phi_q^i(k)) &= \sum_{\beta=0,1} \sum_{l=1}^{R_k} p(Z_1(k)|\phi_q^i(k), \beta, \alpha_{dl}(k)) p(\alpha_{dl}(k)) p(\beta) \\ p(Z_2(k)|\phi_q^i(k)) &= \sum_{\beta=0,1} \sum_{l=1}^{R_k} p(Z_2(k)|\phi_q^i(k), \beta, \alpha_{dl}(k)) p(\alpha_{dl}(k)) p(\beta) \end{aligned} \quad (4.31)$$

where $p(Z_1(k)|\phi_q^i(k), \beta, \alpha_{dl}(k)) = p(Z_1(k)|\phi_q^i(k), \beta, \alpha(k) = \alpha_{dl}(k))$, and

$$p(Z_2(k)|\phi_q^i(k), \beta, \alpha_{dl}(k)) = p(Z_2(k)|\phi_q^i(k), \beta, \alpha(k) = \alpha_{dl}(k))$$

Therefore, the metric of the branch between the nodes $\phi_q^i(k-1)$ and $\phi_q^i(k)$ is,

$$M(\phi_q^i(k-1) \rightarrow \phi_q^i(k)) = \ln(\pi_k^i) + \ln(p(Z_1(k), Z_2(k)|\phi_q^i(k))) \quad (4.32)$$

Channel phase transition probability π_k^i which is defined in Eq. (3.3) between the nodes $\phi_q^i(k-1)$ and $\phi_q^i(k)$ depends on the conditional PDF $p(\phi_q^i(k)|\phi_q^i(k-1))$ which is difficult to obtain analytically and approximate with FSM as can be seen in Eq. (4.27). Hence, Channel phase transition probabilities are obtained numerically from simulation results by running the Rayleigh fading channel model in MATLAB. The numeric values of approximated transition probabilities for different values of quantization levels M_k and channel's correlation coefficient λ that are commonly used in simulations are tabulated in Appendix C.

4.3 Optimum Coherent Detector for BPSK Signals

The probability density function $p(\bar{Z}/u_1)$ and $p(\bar{Z}/u_2)$ can be obtained by averaging the PDFs $p(\bar{Z}/u_m, \alpha)$ over the PDF of the Rayleigh amplitude gain α , i.e.

$$p(\bar{Z}/u_m) = \int_{-\infty}^{\infty} p(\bar{Z}/u_m, \alpha) p(\alpha) d\alpha \quad (4.33)$$

We want to perform the integration indicated in Eq. (4.33) for the BPSK signals. In this case, the optimum demodulator can be shown to be as in Figure 11 [6],

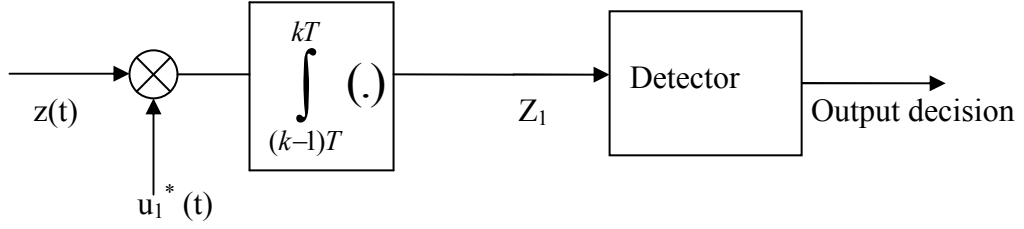


Figure 11: Optimum Receiver for BPSK signals

The output of the demodulator Z_1 is:

a-) If we assume $u_1(t)$ is transmitted;

$$\begin{aligned} Z_1 &= Z_{1r} + j Z_{1m} \\ &= 2 \alpha E \cos(\phi) + V_{1r} + j (-2 \alpha E \sin(\phi) + V_{1m}) \end{aligned} \quad (4.34)$$

b-) If we assume $u_2(t)$ is transmitted;

$$\begin{aligned} Z_1 &= Z_{1r} + j Z_{1m} \\ &= -2 \alpha E \cos(\phi) + V_{2r} + j (2 \alpha E \sin(\phi) + V_{2m}) \end{aligned} \quad (4.35)$$

Where V_{1r} and V_{1m} , V_{2r} and V_{2m} are uncorrelated and hence statistically independent, zero-mean Gaussian random variables. Hence, the joint PDF of $\vec{Z} = [Z_{1r} \ Z_{1m}]$ may be expressed as a product of the marginal PDFs. Consequently,

If we assume $u_1(t)$ is transmitted,

$$p(Z_{1r}, Z_{1m} / u_1, \alpha) = \frac{1}{2\pi\sigma^2} \exp \left[-\frac{(Z_{1r} - 2\alpha E \cos(\phi))^2 + (Z_{1m} + 2\alpha E \sin(\phi))^2}{2\sigma^2} \right] \quad (4.36)$$

With $p(\alpha)$ substituted into the integral in Eq. (4.33), we obtain,

$$\begin{aligned} p(Z_{1r}, Z_{1m} / u_1) &= \int_0^\infty p(Z_{1r}, Z_{1m} / u_1, \alpha) p(\alpha) d\alpha \\ &= \frac{1}{2\pi\sigma_1^2 \sigma^2} \int_0^\infty \alpha \exp \left[-\frac{(Z_{1r} - 2E\alpha \cos(\phi))^2 + (Z_{1m} + 2E\alpha \sin(\phi))^2}{2\sigma^2} - \frac{\alpha^2}{2\sigma_1^2} \right] d\alpha \end{aligned}$$

$$\begin{aligned}
&= \frac{1}{2\pi\sigma_1^2\sigma^2} \exp\left[-\frac{Z_{1r}^2 + Z_{1m}^2}{2\sigma^2}\right] \\
&\quad \int_0^\infty \alpha \exp\left[\alpha^2\left(-\frac{1}{2\sigma_1^2} - \frac{4E^2}{\sigma^2}\right) + \left(\frac{2E\alpha}{\sigma^2}(Z_{1r}\cos(\phi) - Z_{1m}\sin(\phi))\right)\right] d\alpha
\end{aligned} \tag{4.37}$$

By performing a similar integration as in Eq. (4.37) under the assumption that the signal $u_2(t)$ is transmitted, we obtain the result,

$$\begin{aligned}
p(Z_{1r}, Z_{1m} / u_2) &= \int_0^\infty p(Z_{1r}, Z_{1m} / u_2, \alpha) p(\alpha) d\alpha \\
&= \frac{1}{2\pi\sigma_1^2\sigma^2} \int_0^\infty \alpha \exp\left[-\frac{(Z_{1r} + 2E\alpha\cos(\phi))^2 + (Z_{1m} - 2E\alpha\sin(\phi))^2}{2\sigma^2} - \frac{\alpha^2}{2\sigma_1^2}\right] d\alpha \\
&= \frac{1}{2\pi\sigma_1^2\sigma^2} \exp\left[-\frac{Z_{1r}^2 + Z_{1m}^2}{2\sigma^2}\right] \\
&\quad \int_0^\infty \alpha \exp\left[\alpha^2\left(-\frac{1}{2\sigma_1^2} - \frac{4E^2}{\sigma^2}\right) + -\frac{2E\alpha}{\sigma^2}(Z_{1r}\cos(\phi) - Z_{1m}\sin(\phi))\right] d\alpha
\end{aligned} \tag{4.38}$$

When we substitute these results into the likelihood ratio given by Eq. (4.11), we obtain the result,

$$\Omega(\bar{Z}) = \frac{\left(\int_0^\infty \alpha \exp\left[\alpha^2\left(-\frac{1}{2\sigma_1^2} - \frac{4E^2}{\sigma^2}\right) + \alpha\left(\frac{2E}{\sigma^2}(Z_{1r}\cos(\phi) - Z_{1m}\sin(\phi))\right)\right] d\alpha\right)^{u_1}}{\left(\int_0^\infty \alpha \exp\left[\alpha^2\left(-\frac{1}{2\sigma_1^2} - \frac{4E^2}{\sigma^2}\right) + \alpha\left(-\frac{2E}{\sigma^2}(Z_{1r}\cos(\phi) - Z_{1m}\sin(\phi))\right)\right] d\alpha\right)^{u_2}} > \frac{p(u_2)}{p(u_1)} \tag{4.39}$$

A significant simplification in the implementation of the optimum detector occurs when the two signals are equally probable. In such a case, the threshold becomes unity, and the optimum detection rule simplifies into,

$$\begin{aligned}
& \begin{matrix} u_1 \\ [Z_{1r}\cos(\phi) - Z_{1m}\sin(\phi)] > 0 \\ u_2 \end{matrix} \tag{4.40}
\end{aligned}$$

Or equivalently,

$$\begin{array}{c} u_1 \\ \text{Re}\{\exp(j\phi)(Z_1)\} \begin{array}{l} > \\ < \end{array} 0 \\ u_2 \end{array} \quad (4.41)$$

The proposed receiver is shown in Figure 12. The channel phase is estimated by the ODSA and the optimum decision or detection rule in Eq. (4.40) or Eq. (4.41) decides on the transmitted signal.

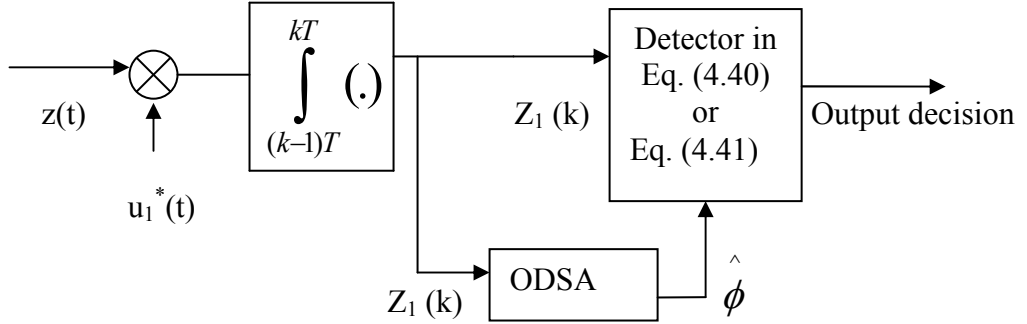


Figure 12: Proposed Receiver for BPSK signals

4.3.1 Application of ODSA to BPSK Signals

We use the following Phase Transition and Observation Models in SFFNC for BPSK signals.

Phase transition model:

$$\begin{aligned} \phi(k+1) &= \tan^{-1}\left(\frac{Y(k+1)}{X(k+1)}\right) = \tan^{-1}\left(\frac{\lambda Y(k) + n_2(k)}{\lambda X(k) + n_1(k)}\right) \\ &= \tan^{-1}\left(\frac{-\lambda\alpha(k)\sin(\phi(k)) + n_2(k)}{\lambda\alpha(k)\cos(\phi(k)) + n_1(k)}\right) \end{aligned}$$

$$\text{Observation model: } Z_1(k) = \int_{(k-1)T}^{kT} z(t)u_1^*(t)dt$$

where $z(t) = \alpha(t) \exp(-j\phi(t)) [\beta u_1(t) + (1-\beta) u_2(t)] + v_1(t) + j v_2(t)$

The output of the demodulator $Z_1(k)$ at the $\{(k-1)T, kT\}$ symbol interval is,

$$Z_1(k) = \alpha(k) \exp(-j\phi(k)) [(2\beta - 1)2E] + v_{1,1}(k) + jv_{1,2}(k) \quad (4.42)$$

where $k = 1, \dots, L$ and L is the number of transmitted bits, $X(k)$, $Y(k)$, $n_1(k)$, $n_2(k)$, λ , $\alpha(k)$, $\phi(k)$, $v_{1,1}(k)$, $v_{1,2}(k)$ and β are defined in Section 4.2.1

In ODSA, we reduce the phase transition model into,

Phase transition model:

$$\begin{aligned} \phi_q(k+1) &= Q \left\{ \tan^{-1} \left(\frac{Y(k+1)}{X(k+1)} \right) \right\} = Q \left\{ \tan^{-1} \left(\frac{\lambda Y(k) + n_2(k)}{\lambda X(k) + n_1(k)} \right) \right\} \\ &= Q \left\{ \tan^{-1} \left(\frac{-\lambda \alpha(k) \sin(\phi_q(k)) + n_2(k)}{\lambda \alpha(k) \cos(\phi_q(k)) + n_1(k)} \right) \right\} \end{aligned} \quad (4.43)$$

4.3.2 The Metric of Branch between the nodes $\phi_q^i(k-1)$ and $\phi_q^i(k)$ of Hypothesis H_i in BPSK signals

The observation $Z_1(k)$ given in Eq. (4.42) is a linear function of the Gaussian observation noise $v_{1,1}(k) + jv_{1,2}(k)$. Therefore, the conditional probability density function of $Z_1(k)$ given that $\phi(k) = \phi_q^i(k)$ and $\alpha(k)$, is a Gaussian density function,

$$p(Z_1(k) | \phi_q^i(k), \alpha(k)) = p(Z_1(k) | \phi(k) = \phi_q^i(k), \alpha(k)) \quad (4.44)$$

and

$$p(Z_1(k) | \phi_q^i(k), \alpha(k)) = \left[\sum_{\beta=0,1} p(Z_1(k) | \phi_q^i(k), \alpha(k), \beta) p(\beta) \right] \quad (4.45)$$

where

$$p(Z_1(k) | \phi_q^i(k), \alpha(k), \beta) = \frac{1}{\sqrt{2\pi\sigma^2}} \exp \left(-\frac{|Z_1(k) - \alpha(k) \exp(-j\phi_q^i(k)) (2\beta - 1) 2E|^2}{2\sigma^2} \right) \quad (4.46)$$

After approximating $\alpha(k)$ by a discrete random vector $\alpha_d(k)$ whose possible values are $\{\alpha_{d1}(k), \alpha_{d2}(k), \dots, \alpha_{dR_k}(k)\}$ with corresponding probabilities $\{p(\alpha_{d1}(k)), p(\alpha_{d2}(k)), \dots, p(\alpha_{dR_k}(k))\}$ where R_k is the size of the vector $\alpha_d(k)$,

$$p(Z_1(k) | \phi_q^i(k)) = \sum_{\beta=0,1} \sum_{l=1}^{R_k} p(Z_1(k) | \phi_q^i(k), \beta, \alpha_{dl}(k)) p(\alpha_{dl}(k)) p(\beta) \quad (4.47)$$

where $p(Z_1(k) | \phi_q^i(k), \beta, \alpha_{dl}(k)) = p(Z_1(k) | \phi_q^i(k), \beta, \alpha(k) = \alpha_{dl}(k))$.

Therefore, the metric of the branch between the nodes $\phi_q^i(k-1)$ and $\phi_q^i(k)$ is,

$$M(\phi_q^i(k-1) \rightarrow \phi_q^i(k)) = \ln(\pi_k^i) + \ln(p(Z_1(k) | \phi_q^i(k))) \quad (4.48)$$

Again, the Channel Phase Transition probabilities π_k^i between the nodes $\phi_q^i(k-1)$ and $\phi_q^i(k)$ are obtained from simulation results by running the Rayleigh fading channel model in MATLAB. (See Appendix C)

4.4 Optimum Noncoherent Detector for Binary Orthogonal Signals

In noncoherent detector, both the channel phase $\{\phi\}$ and Rayleigh amplitude gain α are assumed to be unknown.

Therefore, the probability density functions $p(\bar{Z}/u_1)$ and $p(\bar{Z}/u_2)$ can be obtained by averaging the PDFs $p(\bar{Z}/u_m, \phi, \alpha)$ over the PDF of the Rayleigh amplitude gain α , and uniformly distributed channel phase ϕ i.e.,

$$p(\bar{Z}/u_m) = \int_0^\infty \int_{-\infty}^{2\pi} p(\bar{Z}/u_m, \phi, \alpha) p(\alpha) p(\phi) d\alpha d\phi \quad (4.49)$$

We shall perform the integration indicated in Eq. (4.49) for binary orthogonal signals, i.e, $\rho=0$. In this case, the outputs of the demodulator are already given in Eq. (4.14) and Eq. (4.15),

The joint PDF of $\bar{Z} = [Z_{1r} \ Z_{1m} \ Z_{2r} \ Z_{2m}]$ may be expressed as a product of the marginal PDFs. Consequently,

If we assume $u_1(t)$ is transmitted,

$$p(Z_{1r}, Z_{1m} / u_1, \alpha, \phi) = \frac{1}{2\pi\sigma^2} \exp\left[-\frac{(Z_{1r} - 2\alpha E \cos(\phi))^2 + (Z_{1m} + 2\alpha E \sin(\phi))^2}{2\sigma^2}\right]$$

$$p(Z_{2r}, Z_{2m} / u_1) = \frac{1}{2\pi\sigma^2} \exp\left[-\frac{Z_{2r}^2 + Z_{2m}^2}{2\sigma^2}\right] \quad (4.50)$$

where $\sigma^2 = 2EN_0$.

The PDF of the Rayleigh amplitude gain, $p(\alpha)$ is already given in Eq. (4.18). The PDF of ϕ is uniformly distributed between $(0, 2\pi)$. Hence,

$$p(\phi) = \frac{1}{2\pi} \quad 0 \leq \phi \leq 2\pi \quad (4.51)$$

With $p(\alpha)$ and $p(\phi)$ substituted into the integral in Eq. (4.49), we obtain,

$$p(Z_{1r}, Z_{1m} / u_1) = \int_0^\infty \int_0^{2\pi} p(Z_{1r}, Z_{1m} / u_1, \phi, \alpha) p(\phi) p(\alpha) d\alpha$$

$$\begin{aligned}
&= \frac{1}{4\pi^2\sigma_1^2\sigma^2} \int_0^{2\pi} \int_0^\infty \alpha \exp \left[-\frac{(Z_{1r} - 2E\alpha \cos(\phi))^2 + (Z_{1m} + 2E\alpha \sin(\phi))^2}{2\sigma^2} - \frac{\alpha^2}{2\sigma_1^2} \right] d\alpha d\phi \\
&= \frac{1}{2\pi\sigma_1^2\sigma^2} \exp \left\{ -\frac{Z_{1r}^2 + Z_{1m}^2}{2\sigma^2} \right\} \\
&\quad \int_0^\infty \alpha \exp \left[\alpha^2 \left(-\frac{1}{2\sigma_1^2} - \frac{4E^2}{\sigma^2} \right) \right] \left[\frac{1}{2\pi} \int_0^{2\pi} \exp \left[\frac{2E\alpha}{\sigma^2} (Z_{1r} \cos(\phi) - Z_{1m} \sin(\phi)) \right] d\phi d\alpha \right]
\end{aligned} \tag{4.52}$$

But,

$$\frac{1}{2\pi} \int_0^{2\pi} \exp \left(\frac{2\alpha E}{\sigma^2} (Z_{1r} \cos(\phi) - Z_{1m} \sin(\phi)) \right) d\phi = I_0 \left(\frac{2E\alpha}{\sigma^2} \sqrt{(Z_{1r})^2 + (Z_{1m})^2} \right)$$

(see Appendix A)

Then,

$$\begin{aligned}
p(Z_{1r}, Z_{1m} / u_1) &= \frac{1}{2\pi\sigma_1^2\sigma^2} \exp \left\{ -\frac{Z_{1r}^2 + Z_{1m}^2}{2\sigma^2} \right\} \\
&\quad \int_0^\infty \alpha \exp \left[\alpha^2 \left(-\frac{1}{2\sigma_1^2} - \frac{4E^2}{\sigma^2} \right) \right] I_0 \left(\frac{2E\alpha}{\sigma^2} \sqrt{(Z_{1r})^2 + (Z_{1m})^2} \right) d\alpha
\end{aligned} \tag{4.53}$$

and

$$p(Z_{2r}, Z_{2m} / u_1) = \frac{1}{2\pi\sigma^2} \exp \left\{ -\frac{Z_{2r}^2 + Z_{2m}^2}{2\sigma^2} \right\} \tag{4.54}$$

By performing a similar integration as in Eq. (4.52) under the assumption that the signal $u_2(t)$ is transmitted, we obtain the result,

$$p(Z_{1r}, Z_{1m} / u_2) = \frac{1}{2\pi\sigma^2} \exp \left[-\frac{Z_{1r}^2 + Z_{1m}^2}{2\sigma^2} \right] \tag{4.55}$$

and

$$\begin{aligned}
p(Z_{2r}, Z_{2m} / u_2) &= \frac{1}{2\pi\sigma_1^2\sigma^2} \exp \left\{ -\frac{Z_{2r}^2 + Z_{2m}^2}{2\sigma^2} \right\} \\
&\quad \int_0^\infty \alpha \exp \left[\alpha^2 \left(-\frac{1}{2\sigma_1^2} - \frac{4E^2}{\sigma^2} \right) \right] I_0 \left(\frac{2E\alpha}{\sigma^2} \sqrt{(Z_{2r})^2 + (Z_{2m})^2} \right) d\alpha
\end{aligned} \tag{4.56}$$

When we substitute these results into the likelihood ratio given by Eq. (4.11), we obtain the result,

$$\Omega(\bar{Z}) = \frac{\left(\int_0^\infty \alpha \exp \left[\alpha^2 \left(-\frac{1}{2\sigma_1^2} - \frac{4E^2}{\sigma^2} \right) \right] I_0 \left(\frac{2E\alpha}{\sigma^2} \sqrt{(Z_{1r})^2 + (Z_{1m})^2} \right) d\alpha \right)_{u_1} > \frac{p(u_2)}{p(u_1)}}{\left(\int_0^\infty \alpha \exp \left[\alpha^2 \left(-\frac{1}{2\sigma_1^2} - \frac{4E^2}{\sigma^2} \right) \right] I_0 \left(\frac{2E\alpha}{\sigma^2} \sqrt{(Z_{2r})^2 + (Z_{2m})^2} \right) d\alpha \right)_{u_2} < \frac{p(u_1)}{p(u_2)}} \quad (4.57)$$

When the two signals are *equally probable*, the threshold becomes unity and due to the monotonicity of the Bessel function $I_0(\cdot)$ [6], the optimum decision rule simplifies into,

$$\begin{array}{c} u_1 \\ \sqrt{(Z_{1r})^2 + (Z_{1m})^2} > \sqrt{(Z_{2r})^2 + (Z_{2m})^2} \\ < \\ u_2 \end{array} \quad (4.58)$$

Or equivalently,

$$\begin{array}{c} u_1 \\ \left| \int_0^T z(t)u_1^*(t)dt \right| > \left| \int_0^T z(t)u_2^*(t)dt \right| \\ < \\ u_2 \end{array} \quad (4.59)$$

Thus, the optimum detector bases its decision on the two envelopes $\sqrt{(Z_{1r})^2 + (Z_{1m})^2}$ and $\sqrt{(Z_{2r})^2 + (Z_{2m})^2}$, hence it is called an *envelope detector*. Equivalently, the decision may be based on the computation of the square envelopes $Z_{1r}^2 + Z_{1m}^2$ and $Z_{2r}^2 + Z_{2m}^2$, in which case the detector is called a *square-law detector* [6]. The optimum noncoherent receiver for binary orthogonal signals is shown in Figure 13.

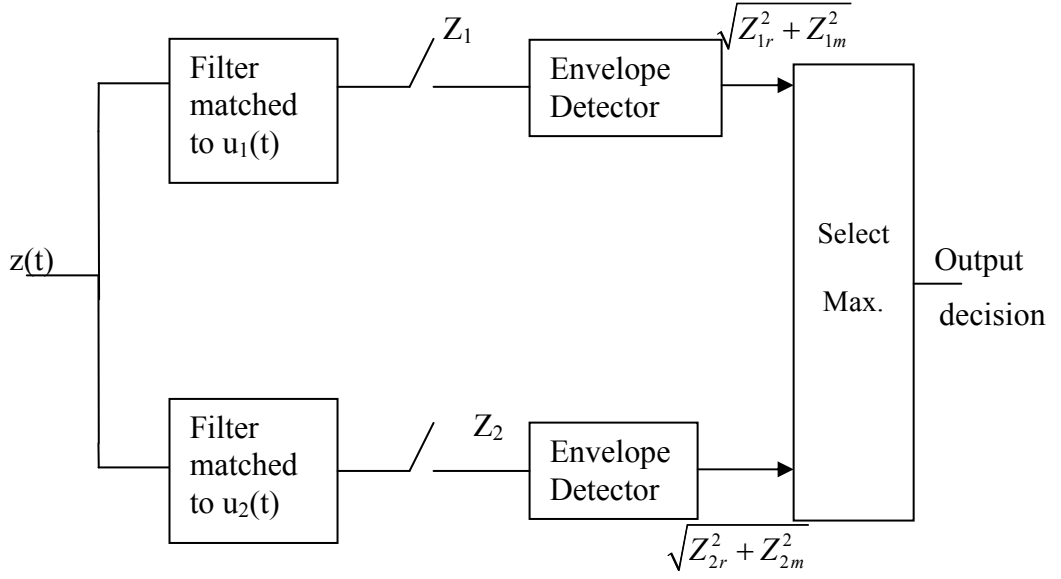


Figure 13: Optimum Noncoherent Receiver for binary orthogonal signals

4.5 Phase Estimation with ODSA using Gaussian random walk phase transition model in Gaussian Channels

4.5.1 Application of ODSA to Binary Orthogonal Signals

We use the following Phase Transition and Observation Models for Binary Orthogonal Signals for estimating the Gaussian random walk phase with ODSA.

$$\text{Phase transition model: } \phi(k+1) = \phi(k) + w(k)$$

Observation models:

$$Z_1(k) = \int_{(k-1)T}^{kT} z(t)u_1^*(t)dt, \quad Z_2(k) = \int_{(k-1)T}^{kT} z(t)u_2^*(t)dt$$

where $z(t) = A \exp(-j\phi(t)) [\beta u_1(t) + (1-\beta) u_2(t)] + v_1(t) + j v_2(t)$

In phase transition model, phase is assumed to change from symbol-to-symbol according to Gaussian random walk phase model similarly to [1] and [27], i.e. phase is constant at k'th symbol interval and changes from one symbol interval to another.

The outputs of the demodulators $Z_1(k)$ and $Z_2(k)$ in Figure 10 are;

$$Z_1(k) = A \exp(-j\phi(k)) [\beta 2E] + v_{1,1}(k) + jv_{1,2}(k)$$

$$Z_2(k) = A \exp(-j\phi(k))[(1-\beta)2E] + v_{2,1}(k) + jv_{2,2}(k) \quad (4.60)$$

where $k = 1, \dots, L$ and L is the number of transmitted bits, $\phi(0)$ is the channel phase at symbol 0 that is uniformly distributed between $(0, 2\pi)$, A is a constant value, $\phi(k)$, $v_{1,1}(k)$, $v_{1,2}(k)$, $v_{2,1}(k)$, $v_{2,2}(k)$ and β are defined in Section 4.2.1

In ODSA, we reduce the phase transition model into,

$$\text{Phase transition model: } \phi_q(k+1) = Q \{ \phi_q(k) + w_d(k) \} \quad (4.61)$$

4.5.2 The Metric of Branch between the nodes $\phi_q^i(k-1)$ and $\phi_q^i(k)$ of Hypothesis H_i in Binary Orthogonal Signals

The observations $Z_1(k)$ and $Z_2(k)$ given in Eq. (4.60) are linear functions of the Gaussian observation noises $v_{1,1}(k) + jv_{1,2}(k)$ and $v_{2,1}(k) + jv_{2,2}(k)$ respectively. Therefore, the conditional probability density function of $Z_1(k)$ and $Z_2(k)$ given that $\phi(k) = \phi_q^i(k)$ is a Gaussian density function,

$$\begin{aligned} p(Z_1(k), Z_2(k) | \phi_q^i(k), \beta) = \\ p(Z_1(k) | \phi(k) = \phi_q^i(k), \beta) p(Z_2(k) | \phi(k) = \phi_q^i(k), \beta) \end{aligned} \quad (4.62)$$

and

$$\begin{aligned} p(Z_1(k), Z_2(k) | \phi_q^i(k)) = \\ \left[\sum_{\beta=0,1} p(Z_1(k) | \phi_q^i(k), \beta) p(Z_2(k) | \phi_q^i(k), \beta) p(\beta) \right] \end{aligned} \quad (4.63)$$

where

$$p(Z_1(k) | \phi_q^i(k), \beta) = \frac{1}{\sqrt{2\pi\sigma^2}} \exp\left(-\frac{|Z_1(k) - A \exp(-j\phi_q^i(k)) \beta 2E|^2}{2\sigma^2}\right)$$

and

$$p(Z_2(k) | \phi_q^i(k), \beta) = \frac{1}{\sqrt{2\pi\sigma^2}} \exp\left(-\frac{|Z_2(k) - A \exp(-j\phi_q^i(k)) (1-\beta) 2E|^2}{2\sigma^2}\right) \quad (4.64)$$

Therefore, the metric of the branch between the nodes $\phi_q^i(k-1)$ and $\phi_q^i(k)$ is,

$$M(\phi_q^i(k-1) \rightarrow \phi_q^i(k)) = \ln(\pi_k^i) + \ln(p(Z_1(k), Z_2(k) | \phi_q^i(k))) \quad (4.65)$$

4.5.3 Application of ODSA to BPSK Signals

We use the following Phase Transition and Observation Models for BPSK signals.

$$\text{Phase transition model: } \phi(k+1) = \phi(k) + w(k)$$

$$\text{Observation model: } Z_1(k) = \int_{(k-1)T}^{kT} z(t)u_1^*(t)dt$$

where $z(t) = A \exp(-j\phi(t)) [\beta u_1(t) + (1-\beta) u_2(t)] + v_1(t) + j v_2(t)$

The output of the demodulator $Z_1(k)$ in Figure 12 is,

$$Z_1(k) = A \exp(-j\phi(k)) [(2\beta - 1)2E] + v_{1,1}(k) + jv_{1,2}(k) \quad (4.66)$$

where $k = 1, \dots, L$ and L is the number of transmitted bits, A is a constant value, $\phi(k)$, $v_{1,1}(k)$, $v_{1,2}(k)$ and β are defined in Section 4.2.1

In ODSA, we reduce the phase transition model into,

$$\text{Phase transition model: } \phi_q(k+1) = Q \{ \phi_q(k) + w_d(k) \} \quad (4.67)$$

4.5.4 The Metric of Branch between the nodes $\phi_q^i(k-1)$ and $\phi_q^i(k)$ of Hypothesis H_i in BPSK signals

The observation $Z_1(k)$ given in Eq. (4.66) is a linear function of the Gaussian observation noise $v_{1,1}(k) + jv_{1,2}(k)$. Therefore, the conditional probability density function of $Z_1(k)$ given that $\phi(k) = \phi_q^i(k)$ is a Gaussian density function,

$$p(Z_1(k) | \phi_q^i(k)) = p(Z_1(k) | \phi(k) = \phi_q^i(k)) \quad (4.68)$$

and

$$p(Z_1(k) | \phi_q^i(k)) = \left[\sum_{\beta=0,1} p(Z_1(k) | \phi_q^i(k), \beta) p(\beta) \right] \quad (4.69)$$

where

$$p(Z_1(k) | \phi_q^i(k), \beta) = \frac{1}{\sqrt{2\pi\sigma^2}} \exp \left(-\frac{|Z_1(k) - A \exp(-j\phi_q^i(k)) (2\beta - 1)2E|^2}{2\sigma^2} \right) \quad (4.70)$$

Therefore, the metric of the branch between the nodes $\phi_q^i(k-1)$ and $\phi_q^i(k)$ is,

$$M(\phi_q^i(k-1) \rightarrow \phi_q^i(k)) = \ln(\pi_k^i) + \ln(p(Z_1(k) | \phi_q^i(k))) \quad (4.71)$$

CHAPTER 5

SIMULATION RESULTS

In this chapter, ODSA discussed in Chapter 3 has been simulated in MATLAB for channel phase estimation and the receivers that are derived in Chapter 4 are used for data detection. The channel phase estimation algorithm (or ODSA) is suboptimum in SFFNC because Rayleigh amplitude gains of the channel at every symbol are correlated.

For simulation results, we have used the following two low-pass equivalent signals.

- For binary orthogonal frequency shift keying (BOFSK), it is shown in [6] that the minimum frequency separation required for orthogonality of signals for envelope or square-law detection of FSK signals is $\Delta f = 1/T$. This separation is twice as large as phase-coherent FSK detection. Hence in simulations, we used two orthogonal BOFSK signals which are $\Delta f = 1/T$ frequency separated, namely,

$$\begin{aligned} s_1(t) &= \cos(2\pi (f_c + 1/2T) t); & s_2(t) &= \cos(2\pi (f_c - 1/2T) t) \\ s_1(t) &= \text{Re}\{u_1(t) \exp(j2\pi f_c t)\}; & s_2(t) &= \text{Re}\{u_2(t) \exp(j2\pi f_c t)\} \end{aligned} \quad (5.1)$$

where $u_1(t) = \exp(-j\pi t/T)$; $u_2(t) = \exp(j\pi t/T)$ are the low-pass equivalents of bandpass signals $s_1(t)$ and $s_2(t)$ for BOFSK.

- Consider the equivalent low-pass signals in Figure 14. These signals are orthogonal. Therefore, we can call them Binary Orthogonal Signals (BOS). However, when we use the receiver structure in Figure 15 for these orthogonal signals, we will call these signals as half-symbol BPSK (HS-BPSK). In HS-BPSK, we use the interval $\{(k-1)T, (k-1/2)T\}$ in ODSA to estimate the channel phase in a symbol interval and use the interval $\{(k-1/2)T, kT\}$ in the BPSK detector to estimate

the transmitted data where $k=1,2,\dots,L$. We can not estimate the channel phase directly by ODSA for BPSK signals, since there is a phase ambiguity by π [6].



Figure 14: Binary Orthogonal signals (BOS) or Half symbol BPSK signals (HS-BPSK)

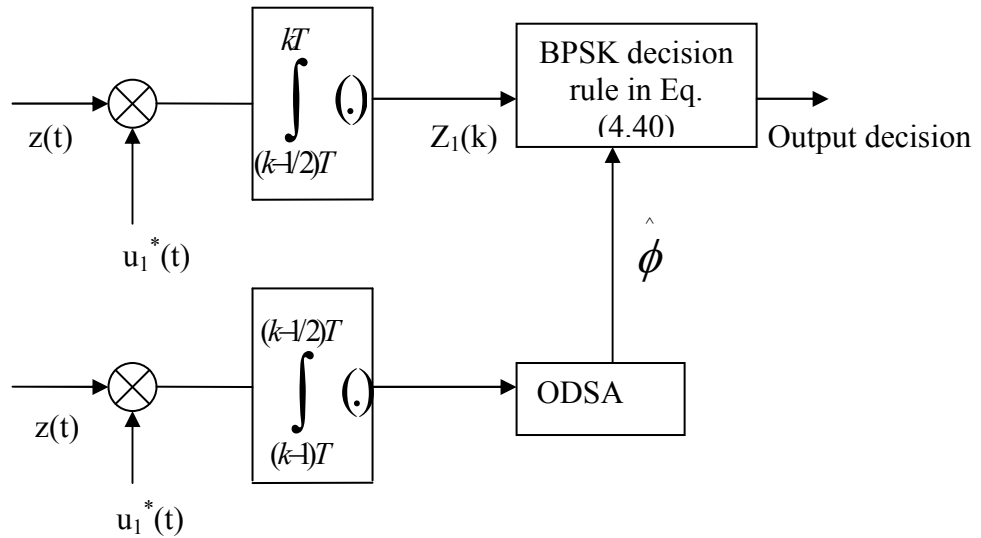


Figure 15: Proposed Receiver for half symbol BPSK (HS-BPSK) Signals

The notations used in simulations can be summarized as below:

σ_w^2 is the variance of the Gaussian disturbance noise $w(k)$, σ_1^2 is the parameter of the Rayleigh PDF in Eq. (4.18) which is defined in Eq. (4.26), E is the energy of the signals, N_0 is the power spectral density of AWGN, T is the symbol duration, M_k is

the number of quantization levels, N_k is the size of vector $w_d(k)$, R_k is the size of vector $\alpha_d(k)$, σ^2 is the variance of observation noise where $\sigma^2 = 2EN_0$ for orthogonal signal receiver and $\sigma^2 = EN_0$ for Half symbol BPSK receiver, Signal to noise ratio is defined as $SNR = 2 \gamma E/N_0$ as in [8] [14], [28], [29], [30] where γ is the variance of inphase and quadrature components $X(k)$ and $Y(k)$, λ is the channel's correlation coefficient, $\gamma(1-\lambda^2)$ is the variance of $n_1(k)$ and $n_2(k)$. In all simulations, we used the following values:

$\gamma = \sigma_{1,1}^2 = 0.25$, $T=10^{-5}$, $E = T/2 = 5 \times 10^{-6}$, $\sigma_w^2 = 0.01 \text{ rad}^2$ with simulation of 1000 bits with 2000 runs.

5.1 Performance comparisons of ODSA with optimum noncoherent and coherent detectors with increasing number of Quantization levels or nodes, M_k

The effect of number of Quantization levels M_k on the performances of PHS-BPSK, PBOS and PBOFSK are compared in Figure 16, Figure 17 and Figure 18.

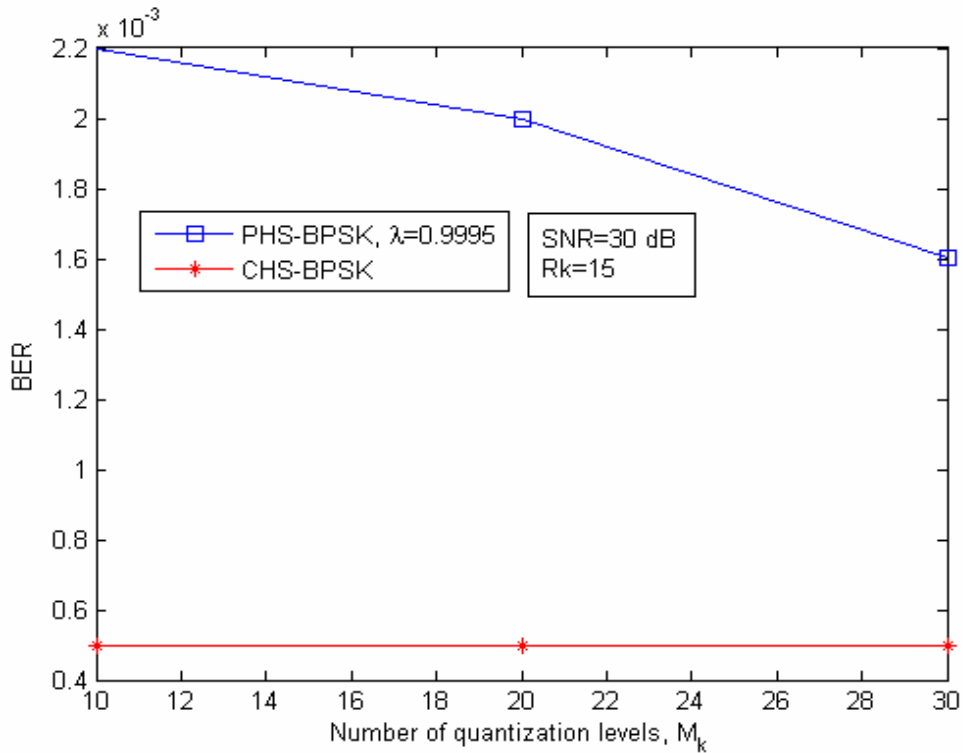


Figure 16: BER v.s. number of quantization levels M_k for HS-BPSK

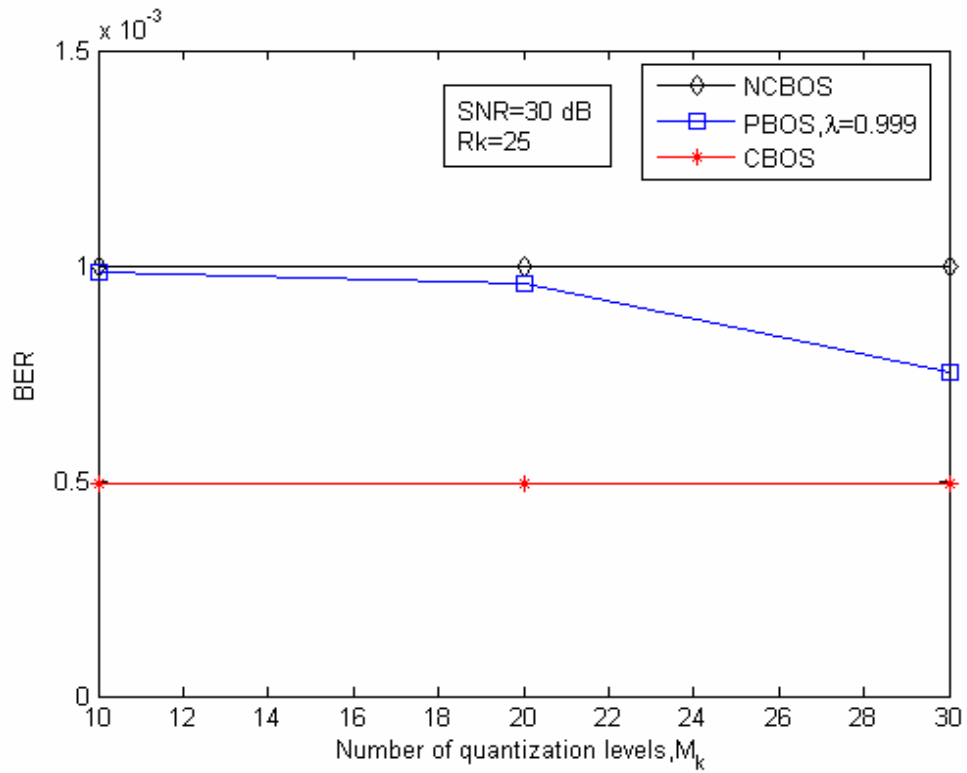


Figure 17: BER v.s. number of quantization levels M_k for BOS

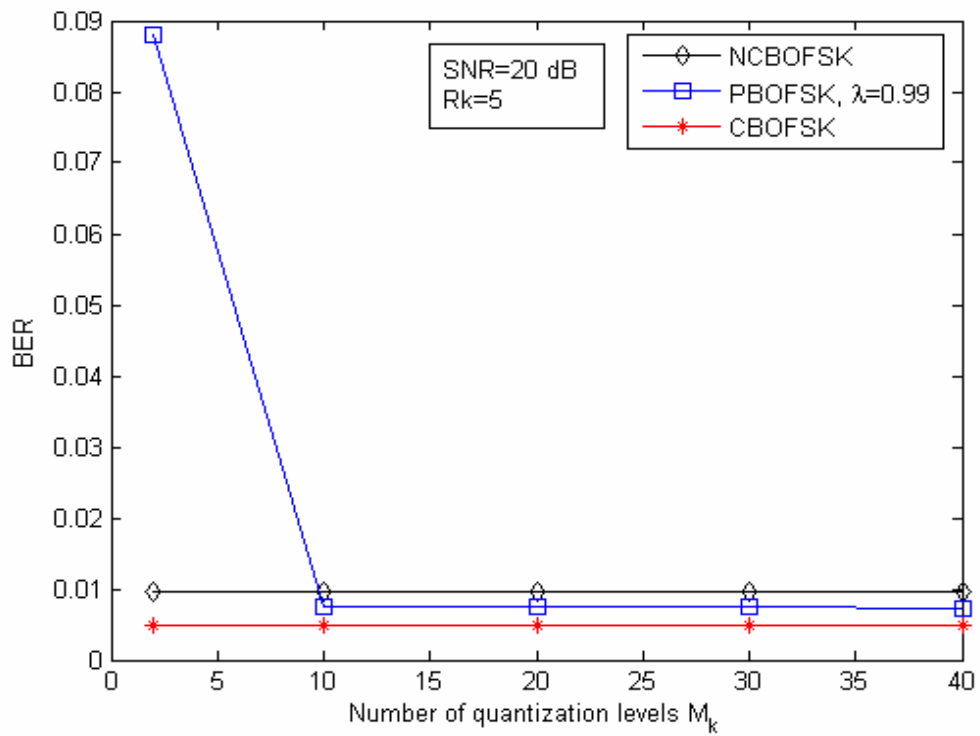


Figure 18: BER v.s. number of quantization levels M_k for BOFSK

Comment: Increasing the quantization level or number of nodes M_k increases the performance of proposed receiver since the estimates of channel phase in ODSA are more accurate.

5.2 Performance comparisons of ODSA with optimum noncoherent and coherent detectors with increasing size of approximating discrete vector $\alpha_d(\mathbf{k})$, R_k

The effect of R_k on the performances of PHS-BPSK, PBOS and PBOFSK are compared in Figure 19, Figure 20 and Figure 21.

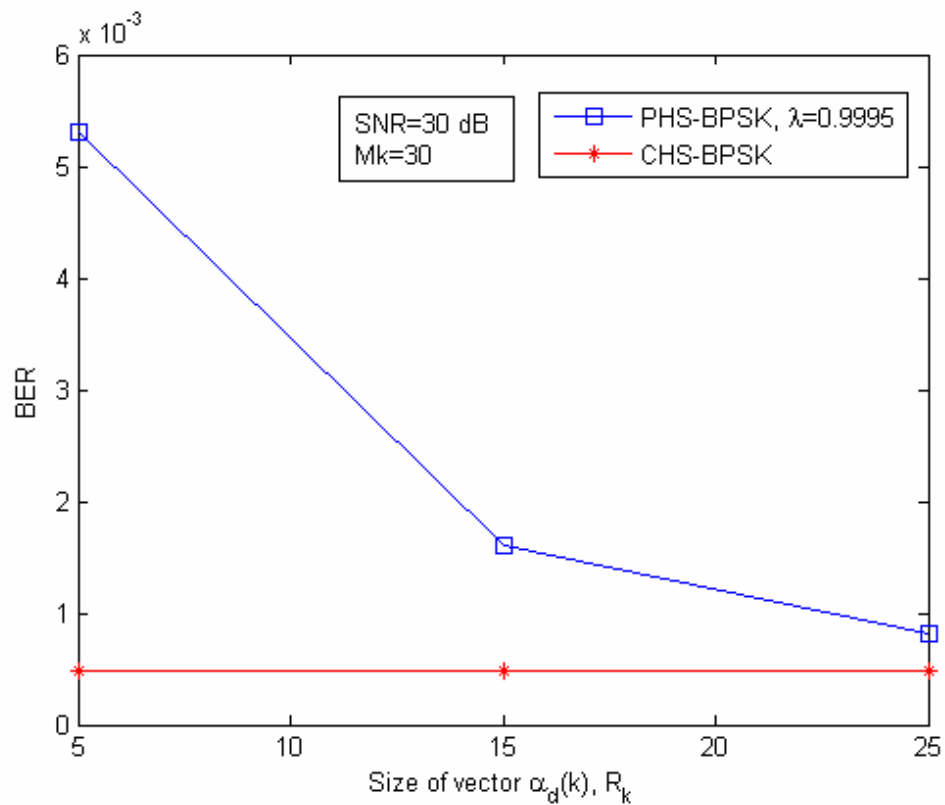


Figure 19 : BER v.s. size of $\alpha_d(\mathbf{k})$ for HS-BPSK

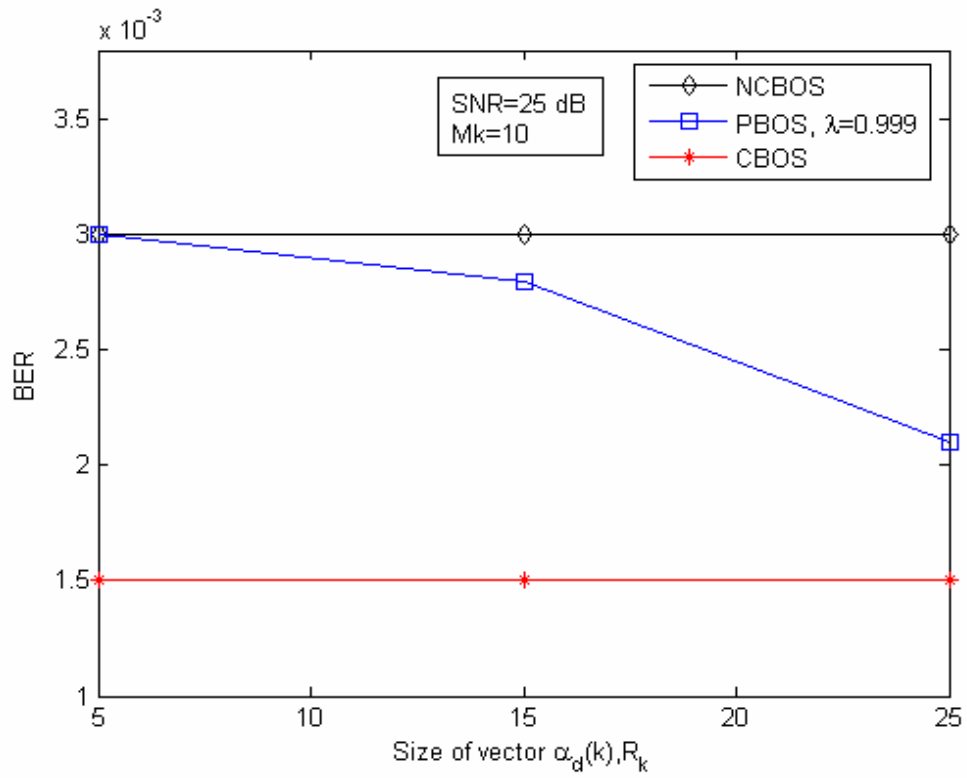


Figure 20 : BER v.s. size of $\alpha_d(k)$ for BOS

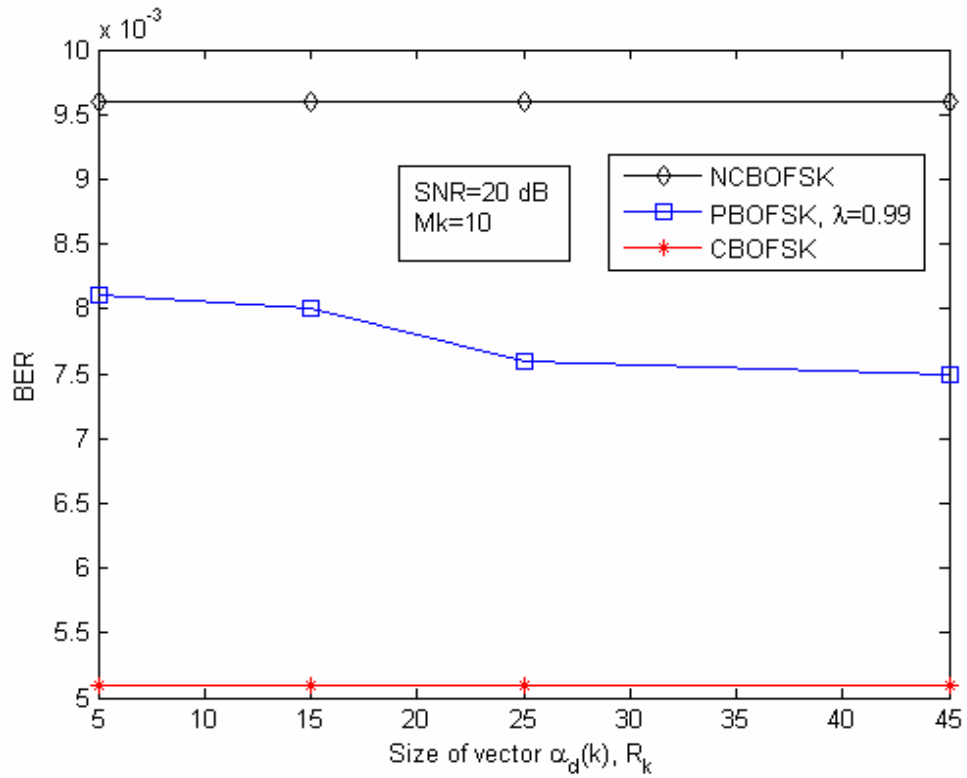


Figure 21: BER v.s. size of $\alpha_d(k)$ for BOFSK

Comment: Increasing the size of the approximating discrete vector $\alpha_d(k)$ decreases the BER of the proposed receiver (especially useful at high SNRs), because the conditional PDF $p(z(k)|\phi_q^i(k))$ in Eq. (3.24) is more precisely calculated. However, the computational complexity of the receiver increases.

5.3 Performance comparisons of ODSA with optimum noncoherent and coherent detectors with different values of correlation coefficient of the first order Markov fading process, λ

The effect of the λ on the performances of the optimum noncoherent, coherent detectors and PHS-BPSK, PBOS PBOFSK are compared in Figure 22, Figure 23 and Figure 24

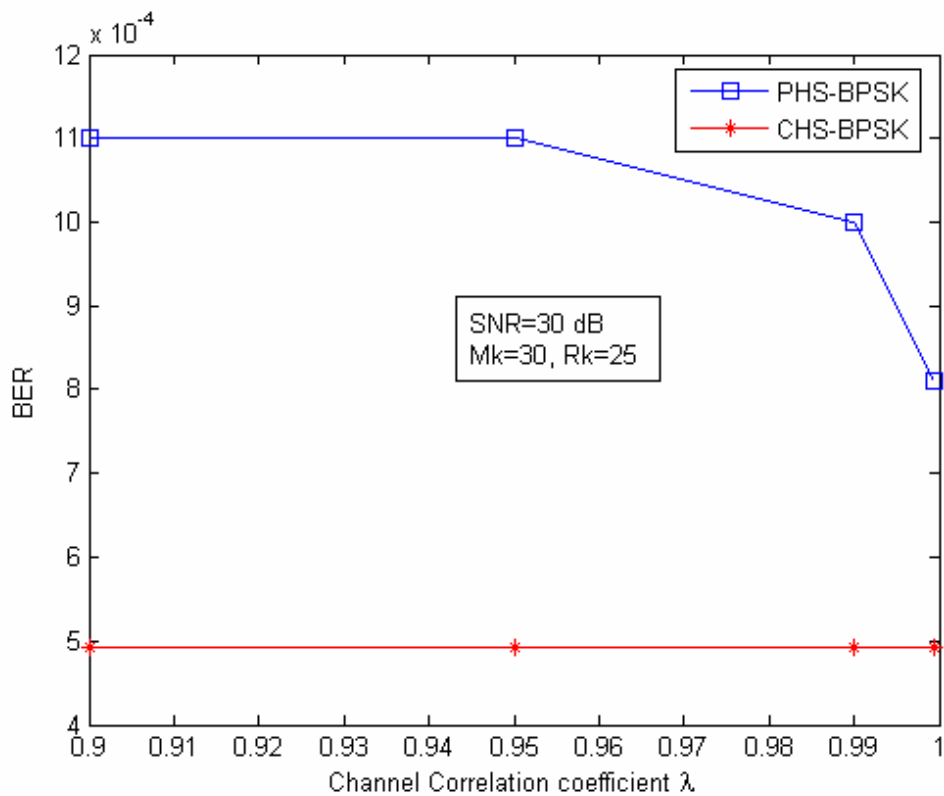


Figure 22: BER v.s. Channel Correlation coefficient λ for HS-BPSK

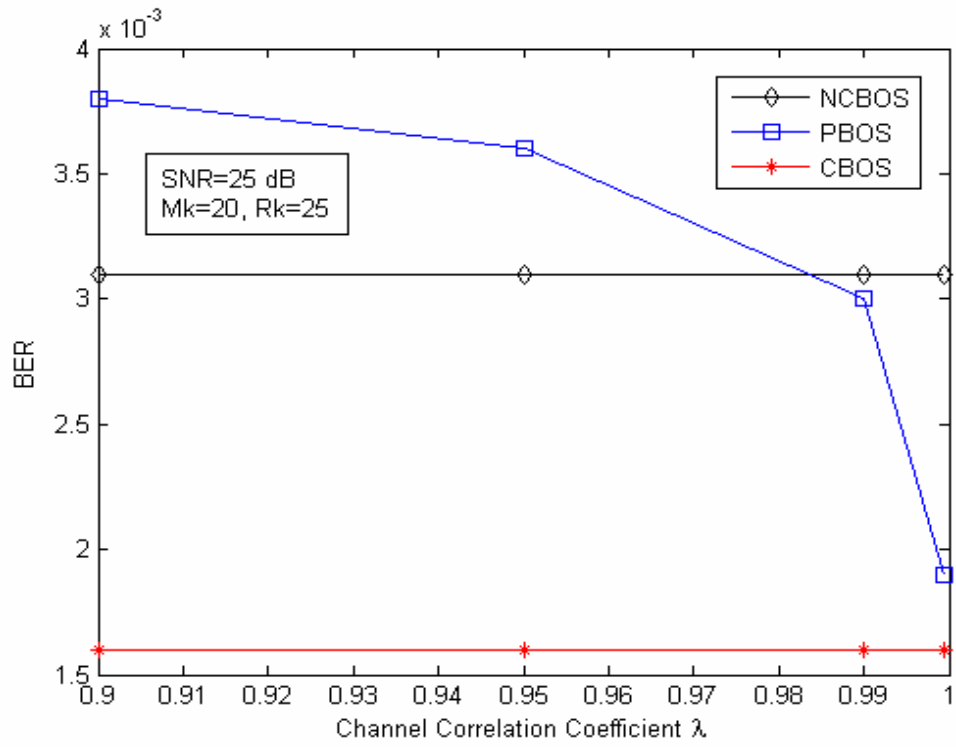


Figure 23: BER v.s. Channel Correlation coefficient λ for BOS

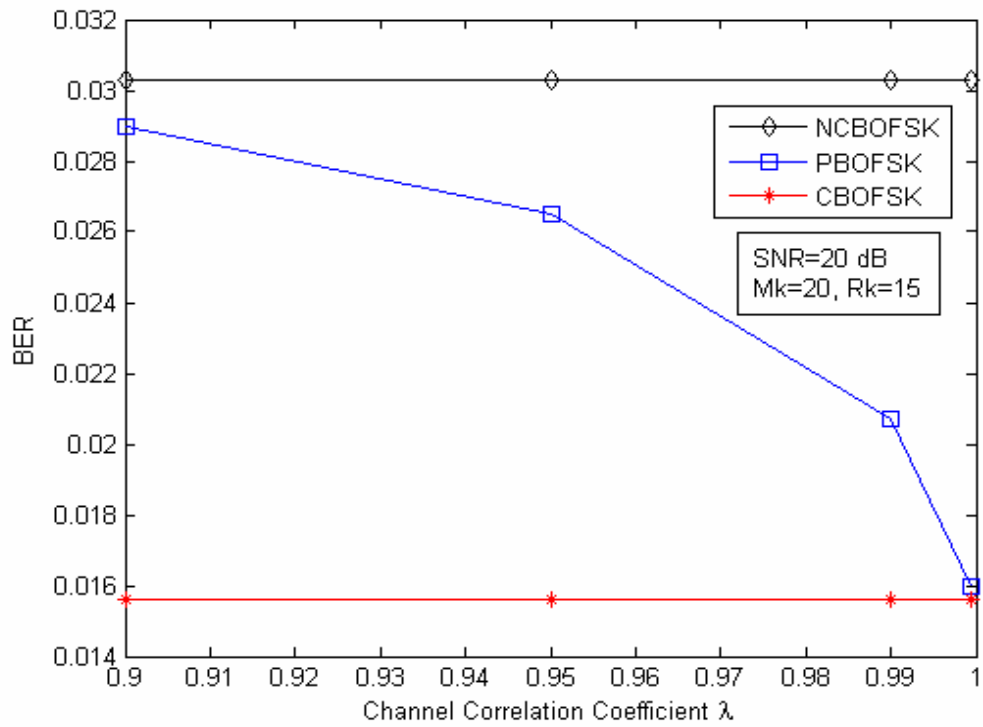


Figure 24: BER v.s. Channel Correlation coefficient λ for BOFSK

Comment: Increasing the Channel Correlation coefficient of the first order Markov process λ , which is a measure of rate of fluctuation of the channel fading process [28], decreases the BER of the proposed receiver because increasing the correlation between the received signals increases the performance of Viterbi algorithm in ODSA. Gaussian channel coefficient $C(k)$ changes slowly as λ increases. However, when λ increases, samples of the Rayleigh distributed amplitude gains $\alpha(k)$ and $\alpha(m)$ for $k \neq m$ are more correlated and which causes an increase in suboptimality of the channel phase estimation algorithm compared to low channel correlation coefficient.

5.4 Performance comparisons of ODSA with optimum noncoherent and coherent detectors in different observation noise variances σ^2 or SNR values

The SNR versus the BER performances of the optimum noncoherent, coherent detectors and PHS-BPSK, PBOS, PBOFSK are compared in Figure 25, Figure 26 and Figure 27.

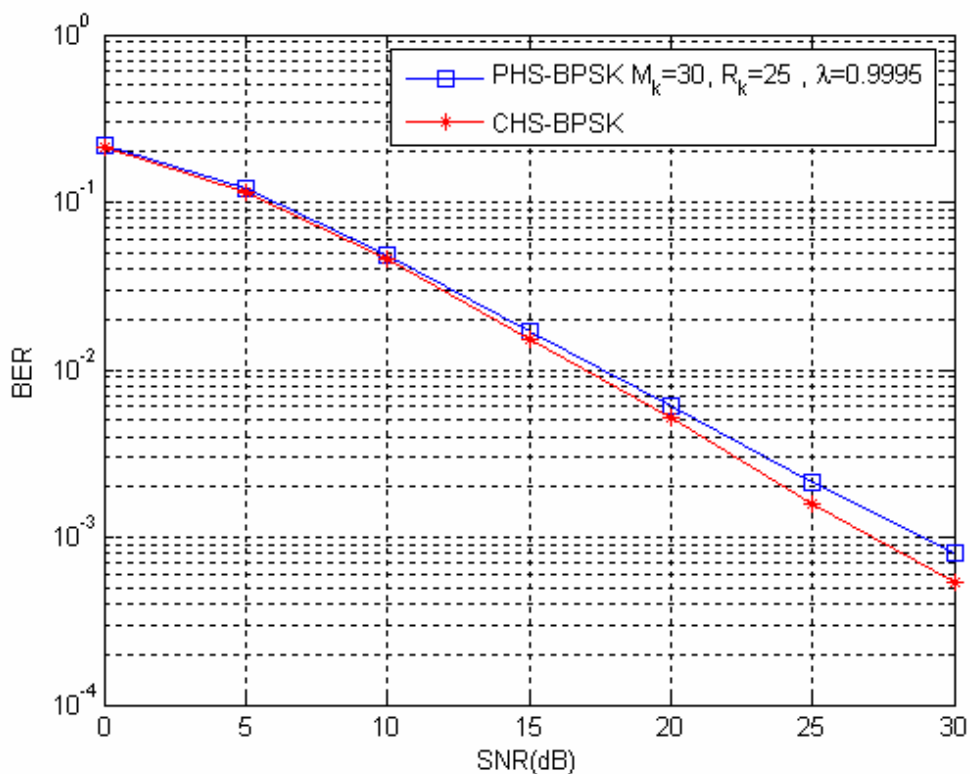


Figure 25: BER versus SNR for HS-BPSK

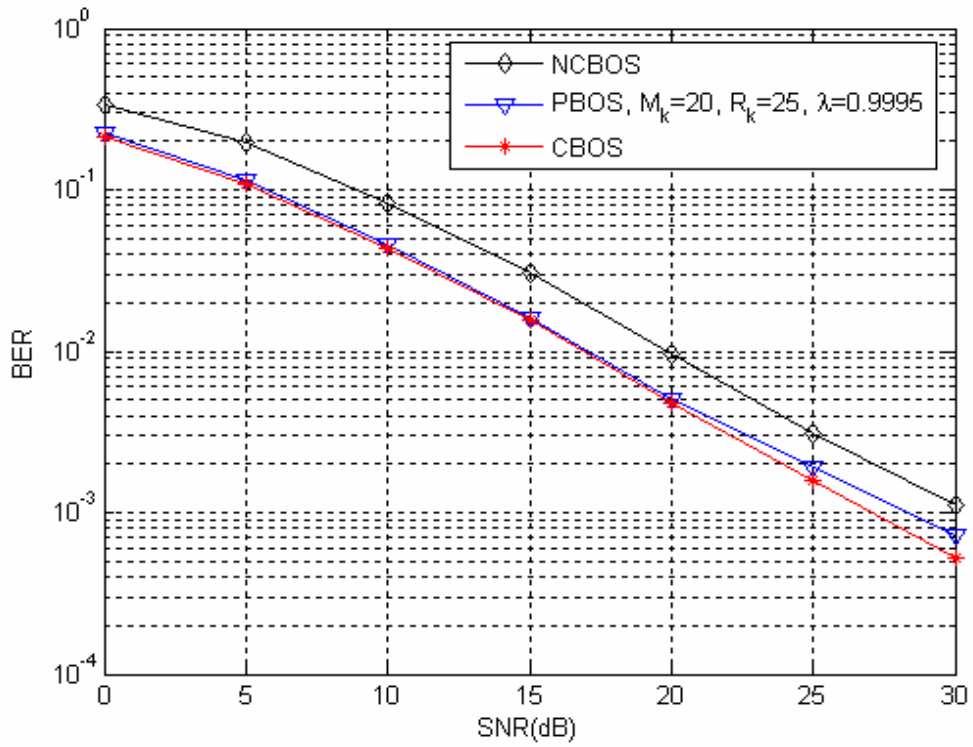


Figure 26: BER versus SNR for BOS

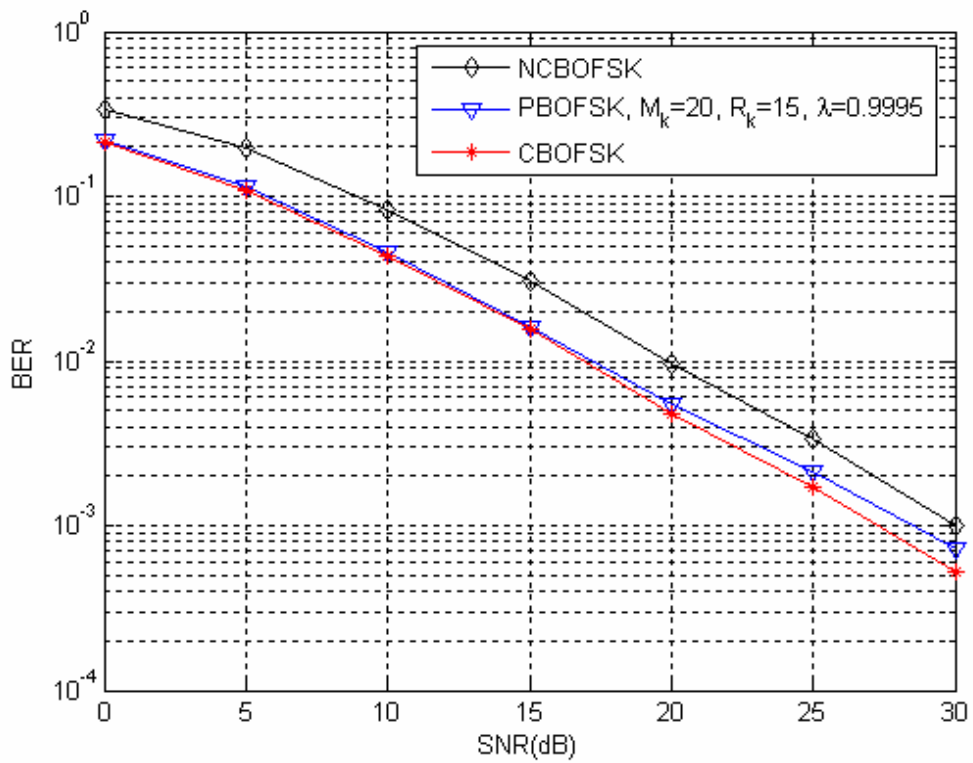


Figure 27: BER versus SNR for BOFSK

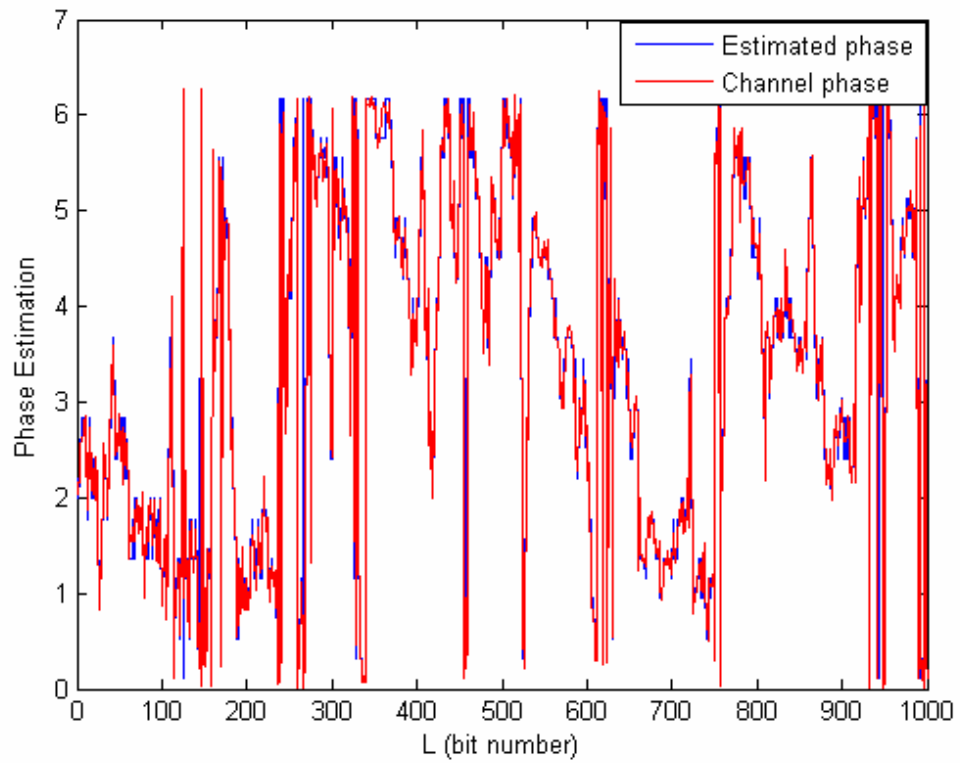


Figure 28: Channel Phase and Estimated Phase at SNR=30dB

Comment: By selecting the ODSA parameters conveniently, we can obtain the BER performance of proposed receiver between the performances of noncoherent and coherent detectors at different SNR values.

5.5 Apriori probability of $u_2(t)$ v.s. BER

If the apriori probabilities of the binary signals are not equal, then the decision rules are the integral equations in Eq. (4.22) and Eq. (4.39) for binary orthogonal and PSK signals respectively in coherent detection, and Eq. (4.57) for binary orthogonal signals for noncoherent detection. Probability of $u_2(t)$ is transmitted, $p(u_2(t))$, versus BER plot is shown in Figure 29, Figure 30 and Figure 31 with 1000 bits and 10 runs.

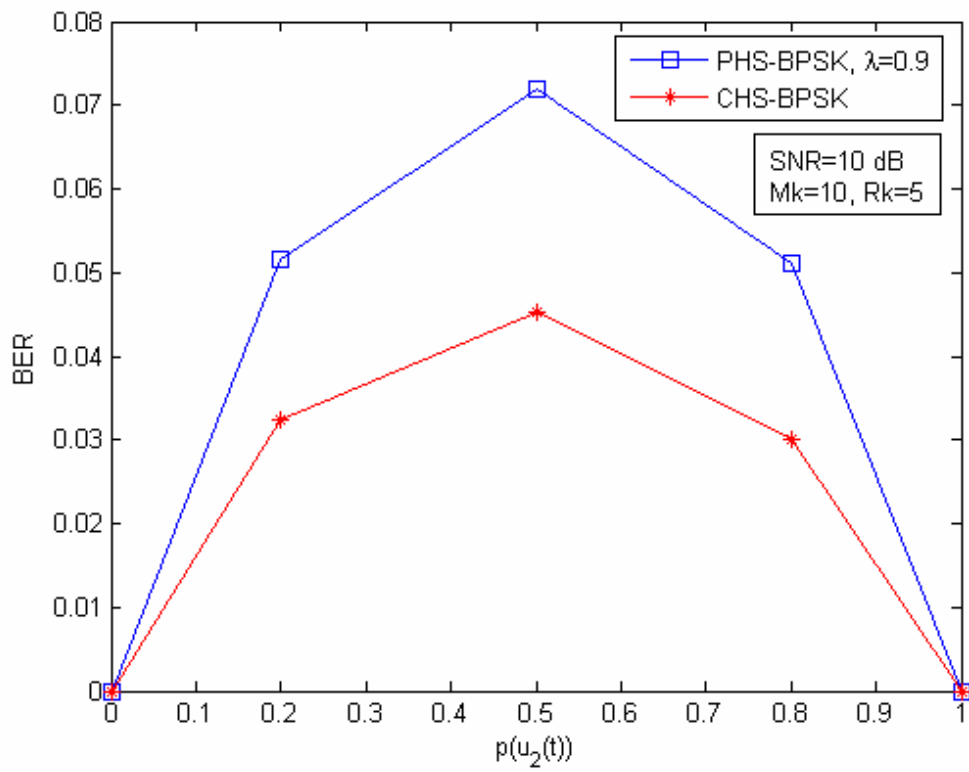


Figure 29: BER v.s. $p(u_2(t))$ for HS-BPSK

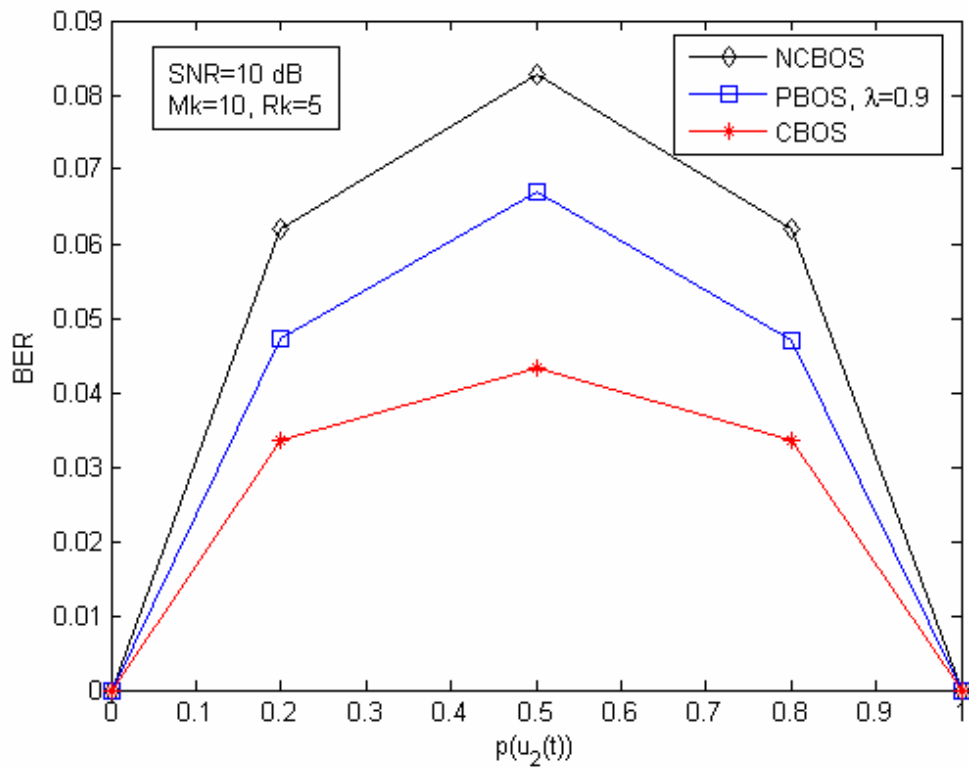


Figure 30: BER v.s. $p(u_2(t))$ for BOS

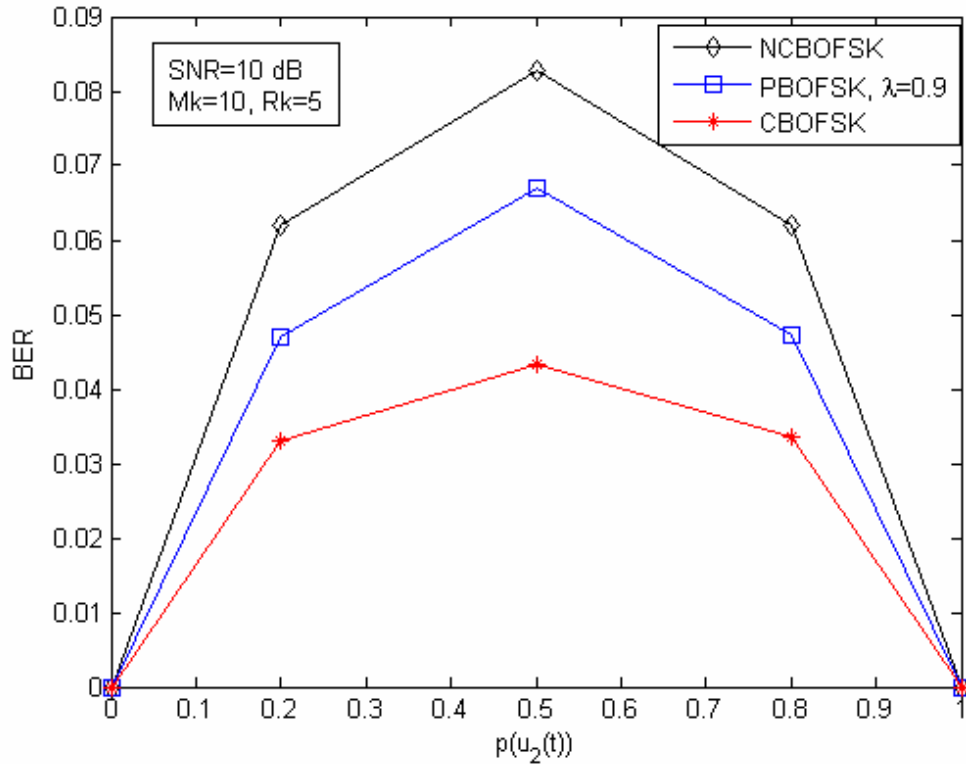


Figure 31: BER v.s. $p(u_2(t))$ for BOFSK

Comment: If the transmitted signals are not equally likely, the detectors are more complex. Therefore, the proposed receiver's computational complexity increases.

5.6 Computational time of data estimation with ODSA

The computational time of the ODSA is determined by the number of quantization levels M_k , size of the vector $\alpha_d(k)$, R_k at a fixed number of transmitted data sequences, L .

If the apriori probabilities of the transmitted signals are not equally likely, the computational time of the detector increases. The computational time of the one bit data estimation versus different apriori probabilities is simulated in Figure 32, Figure 33 and Figure 34 for $L=500$.

The computational time of the one bit data estimation versus M_k , and R_k is also simulated in Figure 35, and Figure 36 for PHS-BPSK, PBOS and PBOFSK for $L=500$.

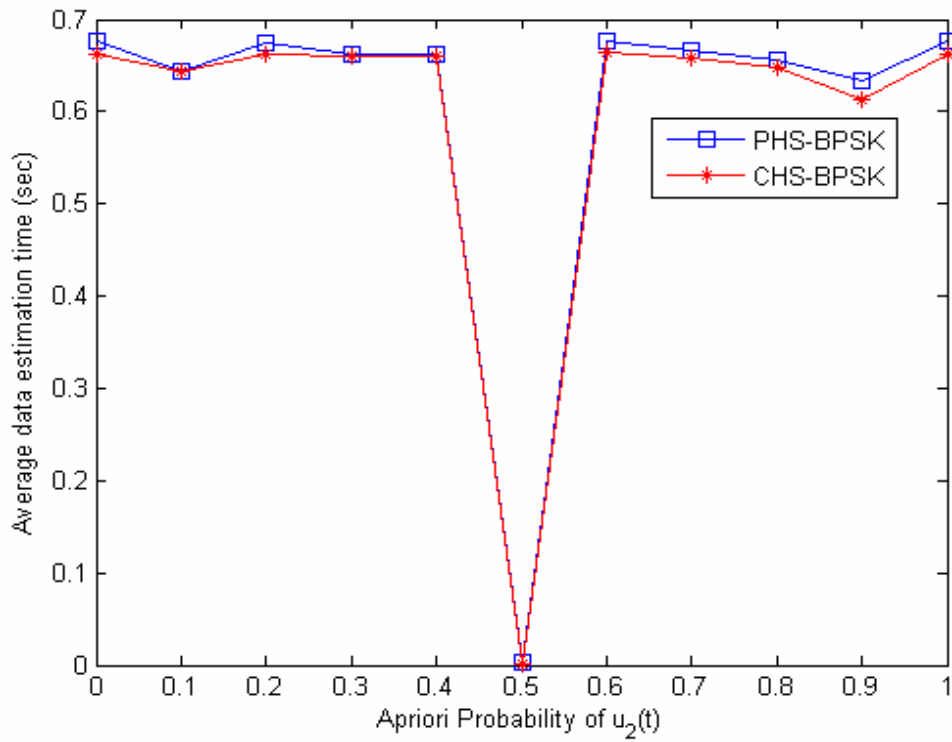


Figure 32: Computational time v.s. Apriori Probability of $u_2(t)$ for HS-BPSK

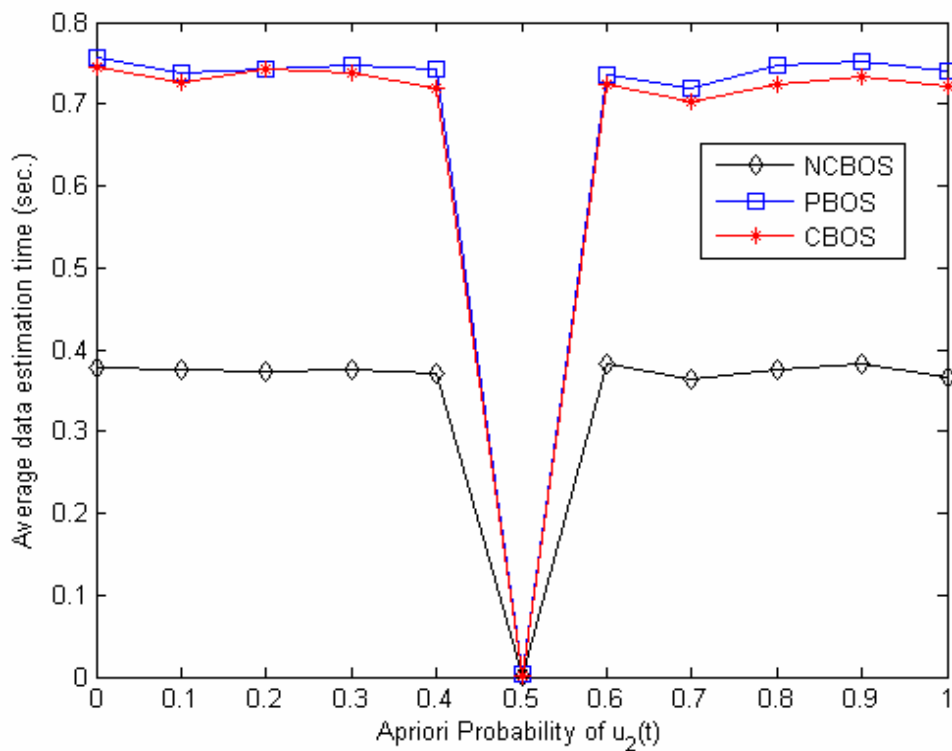


Figure 33: Computational time v.s. Apriori Probability of $u_2(t)$ for BOS

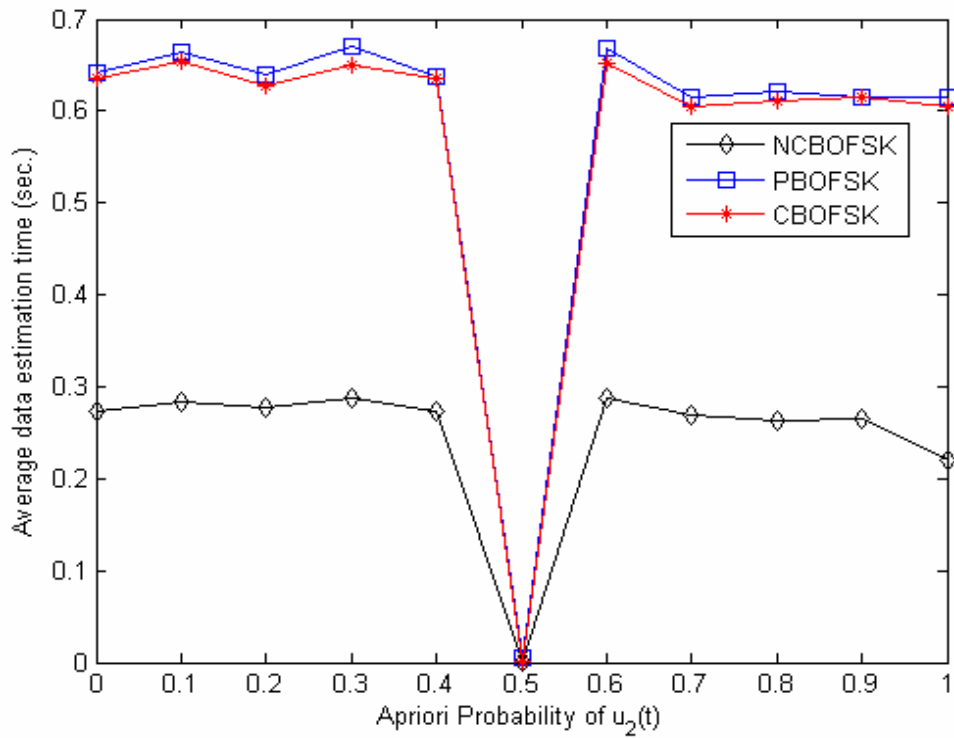


Figure 34: Computational time v.s. Apriori Probability of $u_2(t)$ for BOFSK

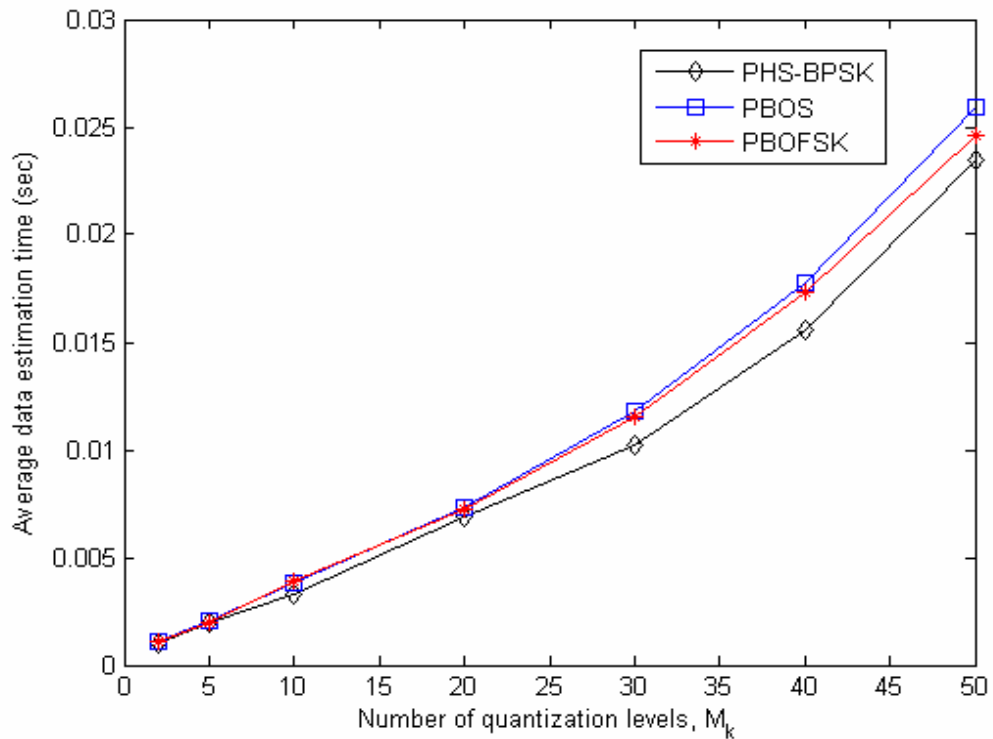


Figure 35: Computational time v.s. Number of quantization levels M_k

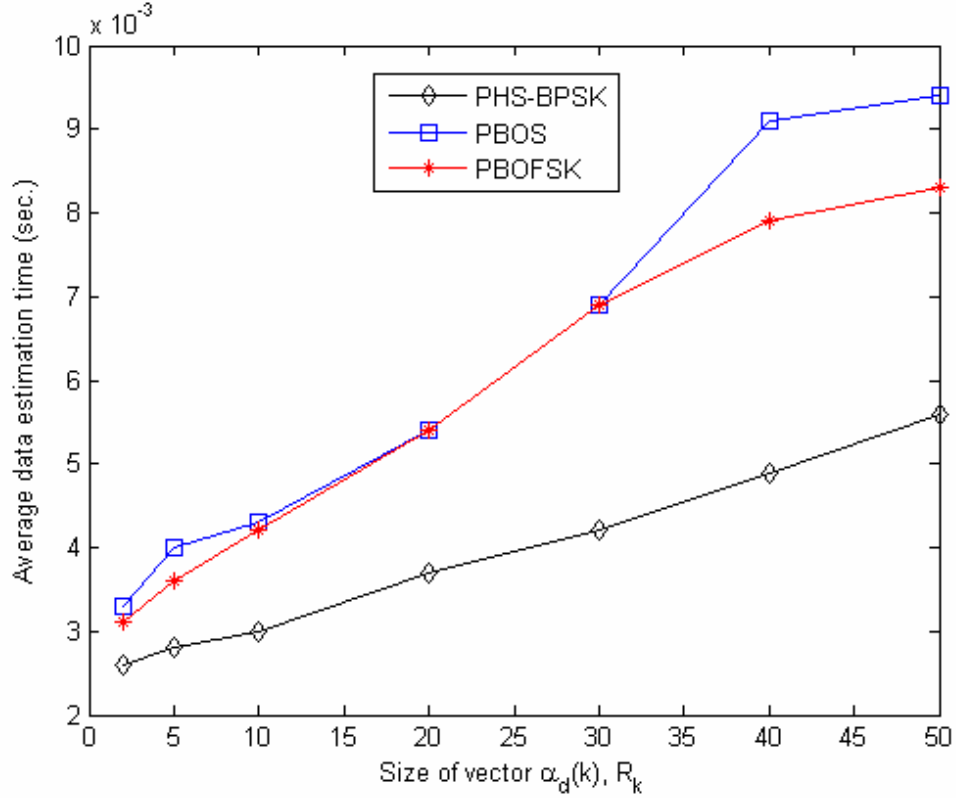


Figure 36: Computational time v.s. Size of $\alpha_d(k), R_k$

Comment: Increasing the number of quantization levels, M_k , increases the computational time exponentially. Increasing the size of the vector $\alpha_d(k), R_k$ increases the computational time of the proposed (channel phase and data estimation) detector linearly.

5.7 Performance comparisons of ODSA with optimum noncoherent and coherent detectors using the Gaussian random walk phase transition model in Gaussian Channels

We use the phase transition and observation models in Eq. (4.60), Eq. (4.61) and Eq. (4.66), Eq. (4.67) to investigate the performance of proposed receiver for Binary Orthogonal and BPSK signals respectively in Figure 37, Figure 38 and Figure 39 where SNR is defined as $2E/N_0$ and $A=1$.

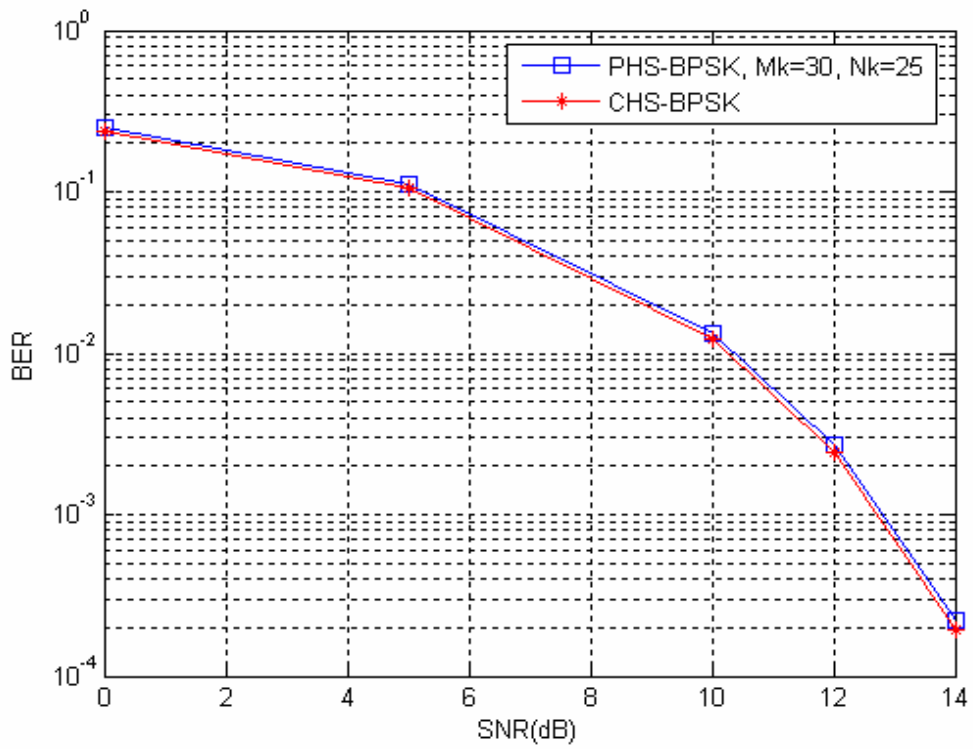


Figure 37: SNR v.s. BER for HS-BPSK signals

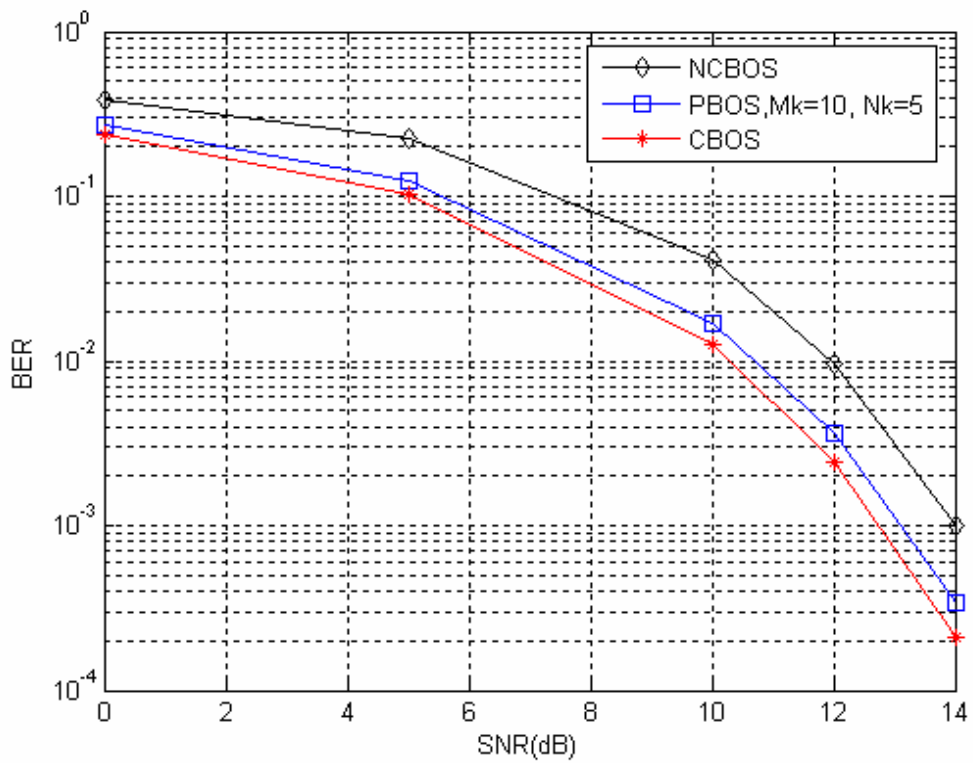


Figure 38: SNR v.s. BER for BOS signals

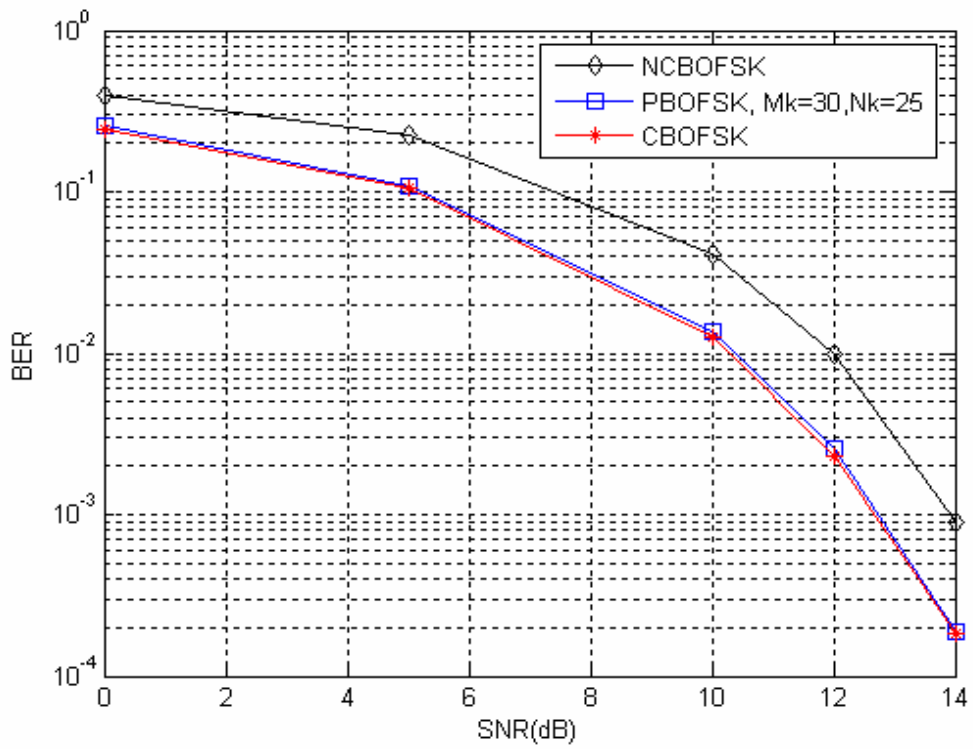


Figure 39: SNR v.s. BER for BOFSK signals

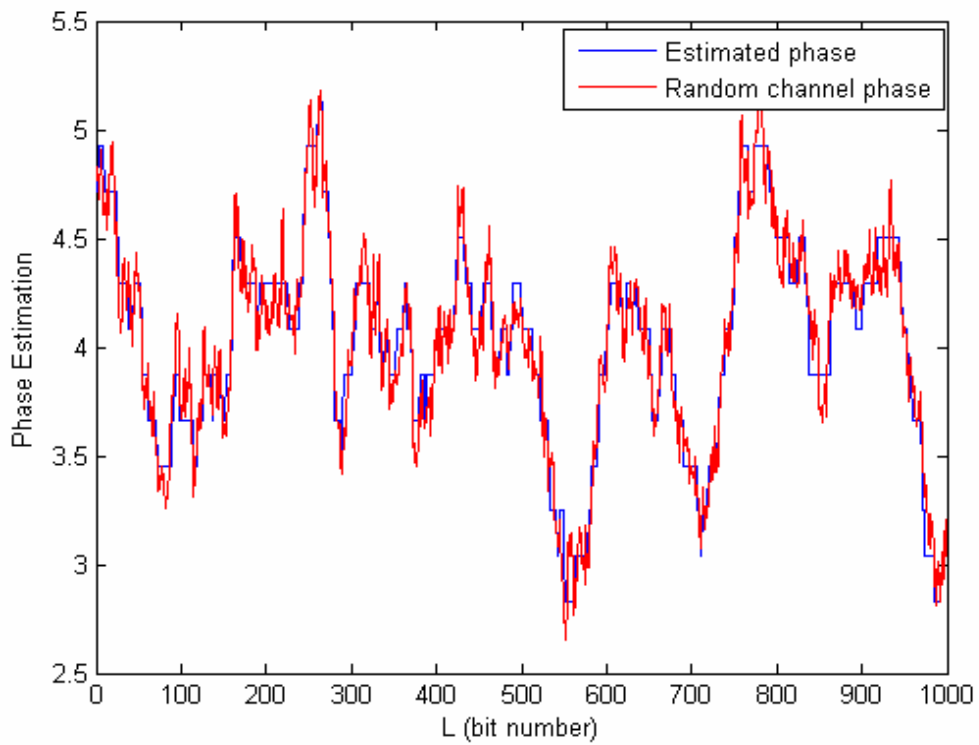


Figure 40: Channel Phase and Estimated Phase at SNR=14 dB

CHAPTER 6

CONCLUSIONS

Throughout this thesis, Channel phase estimation in a transmitted data sequence and data estimation in symbol by symbol MAP receiver with minimum symbol error probability criterion is investigated in frequency nonselective slowly fading channels. Optimum receivers for binary orthogonal and PSK signals have been derived in these channels.

ODSA that is explained in Chapter 3 reduces the phase transition and observation models into a finite state model and uses the quantized channel phase in a trellis diagram. Channel phase estimation in a sequence is obtained by using the Viterbi Decoding Algorithm (VDA) that uses the observation and phase transition models in order to obtain the most probable path in the trellis diagram. The detector observes the observation and estimated channel phase and decides on the transmitted signal in a symbol-by-symbol MAP receiver. The performance of the proposed detector is compared with optimum coherent and noncoherent detectors.

In Chapter 5, we have investigated the performance of proposed channel phase estimation algorithm when the parameters of the ODSA are changed. The results of the simulation results can be summarized as below:

- Increasing the quantization levels or number of nodes, M_k increases the performance of the proposed receiver since better channel phase estimates are obtained. Increasing M_k is useful especially at high SNR.

- Increasing the size of the discrete vector $\alpha_d(k)$ R_k , increases the performance of the proposed receiver, because more accurate metric calculations are obtained in ODSA. Increasing R_k is needed at high SNR for good performance of proposed receiver.
- Increasing the channel correlation coefficient of the first order Markov fading process λ , increases the performance of proposed receiver, because VDA performs well, however at every symbol Rayleigh distributed envelopes become more correlated which makes the ODSA more suboptimum algorithm for channel phase estimation.
- BER v.s. SNR plots are obtained comparing the performance of ODSA with noncoherent and coherent detectors in SFFNC. In addition, Phase estimation with ODSA using the constant gain observation model and Gaussian random walk phase transition model which can be used in Gaussian channels is simulated. Proposed receiver's performance is between the performances of optimum coherent and noncoherent detectors.
- When the apriori probabilities of the transmitted signals are not equally likely, the optimum detectors are more complex. The performance of proposed receiver is simulated at different apriori probabilities, comparing it with the performances of optimum coherent and noncoherent detectors.
- The computational time of one symbol data estimation with proposed receiver is plotted for proposed receiver, optimum noncoherent and coherent detectors.
- The optimum numbers for the parameters of the ODSA can be obtained from simulation results by conveniently selecting N_k , R_k and M_k .
- Although the proposed channel phase estimation algorithm with ODSA is suboptimum (since the Rayleigh amplitude gains $\alpha(k)$ are correlated at every transmitted symbol), it performs well.

Therefore, the parameters of the ODSA can be selected properly taking into account the trade-off between the computational complexity or time and the performance of the proposed receiver.

Channel phase estimation with ODSA in a transmitted sequence and data estimation in symbol by symbol MAP receiver using the estimated channel phase sequence can

be useful for applications requiring robust coherent receivers and better performance results. One drawback may be that the statistical property of the channel phase transition model of the channel has to be known a priori.

As a future work, the performance of ODSA with data estimation can be investigated for M-ary Orthogonal FSK and M-ary PSK signals. Complex Gaussian channel coefficient can also be estimated with Kalman filtering and ODSA by appropriate selection of Channel coefficient and observation model in SFFNC. In addition, performance results of phase estimation with ODSA can be compared with performance of the phase tracking loops like Costas loop in SFFNC.

REFERENCES

- [1] O. Macchi and L.L. Scharf, "A dynamic programming algorithm for phase estimation and data decoding on random phase channels," *IEEE Trans. Inform. Theory*, pp. 581–595, September 1981
- [2] R. Haeb and H. Meyr, "A systematic approach to carrier recovery and detection of digitally phase modulated signals on fading channels," *IEEE Trans. Commun.*, vol. COM-37, no. 7, pp. 748-754, July 1989
- [3] J. K. Cavers, "An analysis of pilot symbol assisted modulation for Rayleigh fading channels," *IEEE Trans. Veh. Technol.*, vol. 40, pp. 686–693, Nov. 1991
- [4] J. X. Tang, M.-S. Alouini, and A. J. Goldsmith, "Effect of channel estimation error on M-QAM BER performance in Rayleigh fading," *IEEE Trans. Commun.*, vol. 47, pp. 1856–1864, Dec. 1999
- [5] Demirbaş, K., "Information Theoretic Smoothing Algorithms for Dynamic Systems with or without Interference", *Advances in Control and Dynamic Systems*, Vol XXI, Academic Press, pp. 175-295, 1984.
- [6] Proakis John .G.,*Digital Communications*,McGraw Hill,NY,4th edition, 2001
- [7] Stark H. , Woods W. John, *Probability and Random Processes with applications to Signal Processing*, Prentice Hall, NJ, 3rd edition,2002.
- [8] C. N. Georghiades and J. C. Han, "Sequence estimation in the presence of random parameters via the EM algorithm," *IEEE Trans. Communications*, vol. 45, no. 3, pp. 300–308, Mar. 1997.
- [9] Demirbas, K., "Manoeuvring-Target Tracking with the Viterbi Algorithm in the Presence of Interference", *IEEE Proceedings. Part F*, December 1989; 136 (6) : pp. 262 - 268
- [10] S. Stein, "Fading Channel Issues in System Engineering," *IEEE J. Select. Areas. Commun.*, Vol. 5, No. 2, Feb. 1987, pp. 68 - 69.

- [11] B. Sklar, "Rayleigh Fading Channels in Mobile Digital Communication Systems, Part 1: Characterization," *IEEE Commun. Mag.*, Vol. 35, No. 7, July 1997, pp. 90 – 100
- [12] M. Shayesteh, A. Aghamohammadi, "On the Error Probability of Linearly Modulated Signals on Frequency-Flat Ricean, Rayleigh, and AWGN channels," *IEEE Transactions on Communications*, vol. 43, no. 2/3/4, Feb/Mar/Apr 1995.
- [13] W. J. Weber, III, "Performance of phase-locked loops in the presence of fading communication channels" *IEEE Transactions on Communication.*, vol. COM-24, pp. 487-499, May 1976.
- [14] P.Y. Kam. "Optimal Detection of Digital Data over the Nonselective Rayleigh Fading Channel with Diversity Reception." *IEEE Transactions on Communication.*, COM-39(2):pp.214-219, Feb. 1991
- [15] J. H. Lodge and M. L. Moher, "Maximum likelihood sequence estimation of CPM signals transmitted over Rayleigh Flat-fading channels," *IEEE Trans. on Communications*, vol. 38, pp. 787-794, June 1990.
- [16] R. Raheli, A. Polydoros, and C.-K. Tzou, "Per-survivor processing: A general approach to MLSE in uncertain environments," *IEEE Trans. Communications*, vol. 43, no. 2/3/4, pp. 354–364, Feb/Mar/Apr. 1995
- [17] Vitetta, G. M. and Taylor, D. P.. "Maximum likelihood decoding of uncoded and coded PSK signal sequences transmitted over Rayleigh flat-fading channels." *IEEE Transactions on Communications*, vol. 43, pp. 2750-2758, Nov 1995.
- [18] D'Andrea, A. N., Diglio, A., and Mengali, U. "Symbol-aided channel estimation with nonselective Rayleigh fading channels" *IEEE Transactions on Communications*, vol. 44, pp. 41-48, Jan 1995.
- [19] J. Gertsman and J.H. Lodge, "Symbol-by-symbol MAP demodulation of CPM and PSK signals on Rayleigh flat-fading channels," *IEEE Transactions on Communications.*, vol. COM-45, no. 7, pp. 788-799, July 1997
- [20] Haykin S. *Adaptive Filter Theory*. Prentice-Hall, Inc, 4th edition, 2002.
- [21] Haykin S., *Communication Systems*, Second Edition, John Wiley & Sons Inc., 1983

- [22] C. Komninakis and R.D. Wesel, "Joint iterative channel estimation and decoding in flat correlated Rayleigh fading", *IEEE Journal on Selected area on Communications*, 19(9):1697-1705, Sep 2001.
- [23] H. Zamiri-Jafarian and S. Pasupathy, "Adaptive MLSD receiver with identification of flat fading channels," in *Proc. IEEE Vehicular Technology Conference*, vol. 2, pp. 695–699, 1997
- [24] Y. Liu and S. D. Blostein, "Identification of frequency non-selective fading channels using decision feedback and adaptive linear prediction," *IEEE Trans. Communications*, vol. 43, no. 2/3/4, pp. 1484–1492, 2–4 1995
- [25] D. Warrier and U. Madhow, "Spectrally efficient noncoherent communication," *IEEE Trans. Inform. Theory*, vol. 48, no. 3, pp. 651–668, March 2002.
- [26] R.-R. Chen, R. Koetter, U. Madhow, and D. Agrawal. "Joint Noncoherent Demodulation and Decoding for the Block Fading Channel: A Practical Framework for Approaching Shannon Capacity". *IEEE Trans. Com.*, 51(10): 1626-1689, October 2003.
- [27] P. Y. Kam, K. H. Chua, and X. Yu. "Adaptive Symbol-by-Symbol Reception of MPSK on the Gaussian Channel with Unknown Carrier Phase Characteristics" *IEEE Trans. on Commun.*, COM-46:1275-1279, October 1998
- [28] P. Y. Kam., "Bit error probabilities of MDPSK over the nonselective Rayleigh fading channel with diversity reception," *IEEE Trans. Commun.*, vol. 39, pp. 220-224, Feb. 1991.
- [29] P.Y. Kam and C.H. Teh, "Reception of PSK Signals Over Fading Channels Via Quadrature Amplitude Estimation," *IEEE Trans. Com.*, vol. 31, pp. 1024–1027, Aug. 1983
- [30] J.C. Han and C.N. Georghiades, "Maximum Likelihood Sequence Estimation for Fading Channels via the EM Algorithm", *Proc. GLOBECOM'93*, vol. 4, (Houston), pp. 133–137, 1993

APPENDIX A

MODIFIED BESSEL FUNCTION OF ORDER ZERO

$I_0(x) = \frac{1}{2\pi} \int_0^{2\pi} \exp(x \cos(\theta)) d\theta$ is the definition of Modified Bessel function in [6],

[7]. We want to show that,

$$I_0(K\sqrt{a^2 + b^2}) = \frac{1}{2\pi} \int_0^{2\pi} \exp(K[a \cos(\theta) - b \sin(\theta)]) d\theta \quad (\text{A.1})$$

If we make some calculations on Eq. (A.1),

$$\begin{aligned} \Rightarrow \frac{1}{2\pi} \int_0^{2\pi} \exp(K[a \cos(\theta) - b \sin(\theta)]) d\theta \\ = \frac{1}{2\pi} \int_0^{2\pi} \exp\left(K\sqrt{a^2 + b^2} \left[\frac{a}{\sqrt{a^2 + b^2}} \cos(\theta) - \frac{b}{\sqrt{a^2 + b^2}} \sin(\theta) \right]\right) d\theta \end{aligned} \quad (\text{A.2})$$

Where by definition,

$$\frac{a}{\sqrt{a^2 + b^2}} = \cos(\psi) , \quad \frac{b}{\sqrt{a^2 + b^2}} = \sin(\psi) \text{ and } K \text{ is some constant.}$$

Therefore,

$$\begin{aligned} \Rightarrow \frac{1}{2\pi} \int_0^{2\pi} \exp\left(K\sqrt{a^2 + b^2} [\cos(\psi) \cos(\theta) - \sin(\psi) \sin(\theta)]\right) d\theta \\ = \frac{1}{2\pi} \int_0^{2\pi} \exp\left(K\sqrt{a^2 + b^2} \cos(\theta + \psi)\right) d\theta \end{aligned} \quad (\text{A.3})$$

where , by change of variables, $\theta + \psi = \phi$, $d\theta = d\phi$,

$$\begin{aligned} I_0(K\sqrt{a^2+b^2}) &= \frac{1}{2\pi} \int_{\psi}^{2\pi+\psi} \exp\left(K\sqrt{a^2+b^2} \cos(\phi)\right) d\phi \\ &= \frac{1}{2\pi} \int_0^{2\pi} \exp\left(K[a \cos(\theta) - b \sin(\theta)]\right) d\theta \end{aligned} \tag{A.4}$$

APPENDIX B

APPROXIMATION OF AN ABSOLUTELY CONTINUOUS RANDOM VECTOR BY A DISCRETE RANDOM VECTOR [5]

We want to find the optimum discrete random variable with n possible values that approximates an absolutely continuous random variable X with distribution $F_{y0}(\cdot)$ which minimizes the objective function $J(\cdot)$:

$$\begin{aligned} J(F_{y0}(\cdot)) &= \min_{F_y(\cdot)} J(F_y(\cdot)) \\ &= \min_{g(\cdot)} J(g(\cdot)) \end{aligned} \tag{B.1}$$

where

$$J(F_y(\cdot)) = \int_{-\infty}^{\infty} [F_x(a) - F_y(a)]^2 da \tag{B.2}$$

Therefore, our aim is to find a step-function $g_0(\cdot)$ which minimizes the objective function $J(\cdot)$. That is, we would like to minimize the following function over $y_i \in (-\infty, \infty)$ and $p_j \in (-\infty, \infty)$ (where $i=1,2,\dots,n$; $j=1,2,\dots,n-1$):

$$\begin{aligned}
J(g(\cdot)) = & \int_{-\infty}^{y_1} F_x^2(a) da + \int_{y_1}^{y_2} [F_x(a) - p_1]^2 da \\
& + \int_{y_2}^{y_3} [F_x(a) - (p_1 + p_2)]^2 da + \dots + \int_{y_{n-1}}^{y_n} [F_x(a) - (p_1 + p_2 + \dots + p_{n-1})]^2 da \\
& + \int_{y_n}^{\infty} [F_x(a) - 1]^2 da
\end{aligned}
\tag{B.3}$$

It follows from [5, Theorem B.1] that if $g_0(x)$, which is defined by

$$g_0(x) = \begin{cases} 0, & x < y_{1,0}, \\ p_{1,0}, & \text{if } y_{1,0} < x < y_{2,0}, \\ p_{1,0} + p_{2,0}, & \text{if } y_{2,0} < x < y_{3,0}, \\ p_{1,0} + p_{2,0} + p_{3,0}, & \text{if } y_{3,0} < x < y_{4,0}, \\ \cdot & \cdot \\ \cdot & \cdot \\ \cdot & \cdot \\ 1, & x > y_{n,0} \end{cases}
\tag{B.4}$$

is a step-function which minimizes Eq. (B.3), this must satisfy the following set of equations:

$$\begin{aligned}
\frac{p_{1,0}}{2} &= F_x(y_{1,0}); \\
p_{1,0} + \frac{p_{2,0}}{2} &= F_x(y_{2,0}); \\
p_{1,0} + p_{2,0} + \frac{p_{3,0}}{2} &= F_x(y_{3,0}); \\
&\cdot \qquad \qquad \qquad \cdot \\
&\cdot \qquad \qquad \qquad \cdot \\
&\cdot \qquad \qquad \qquad \cdot \\
p_{1,0} + p_{2,0} + p_{3,0} + \dots + \frac{p_{n,0}}{2} &= F_x(y_{n,0})
\end{aligned}
\tag{B.5}$$

and

$$\begin{aligned}
(p_{1,0}) (y_{2,0} - y_{1,0}) &= \int_{y_{1,0}}^{y_{2,0}} F_x(a) da, \\
(p_{1,0} + p_{2,0}) (y_{3,0} - y_{2,0}) &= \int_{y_{2,0}}^{y_{3,0}} F_x(a) da, \\
(p_{1,0} + p_{2,0} + p_{3,0}) (y_{4,0} - y_{3,0}) &= \int_{y_{3,0}}^{y_{4,0}} F_x(a) da, \\
&\cdot \qquad \qquad \qquad \cdot \\
&\cdot \qquad \qquad \qquad \cdot \\
&\cdot \qquad \qquad \qquad \cdot \\
(p_{1,0} + p_{2,0} + p_{3,0} + \dots + p_{n-1,0}) (y_{n,0} - y_{n-1,0}) &= \int_{y_{n-1,0}}^{y_{n,0}} F_x(a) da, \qquad (B.6)
\end{aligned}$$

Using Eq. (B.5), Eq. (B.6) and [5, Theorem B.2], the discrete random variables (with n possible values where n=1,2,.....,50) which approximate the normal random variable with zero-mean and unit variance have been numerically obtained in Appendix B.3. The discrete random variables which approximate the Rayleigh distributed random variable with mean $\sqrt{\frac{\pi}{2}} = 1.2533$ and variance $2(1 - \frac{\pi}{4}) = 0.4292$ have also been numerically obtained in Appendix B.2 up to 50 possible values.

Let y_0 is the discrete random variable with n possible values $y_{1,0}, y_{2,0}, y_{3,0}, \dots, y_{n,0}$ with corresponding probabilities $p_{1,0}, p_{2,0}, p_{3,0}, \dots, p_{n,0}$ that approximates a random variable with zero mean and unit variance Then the optimum discrete random variables z_0 with n possible values $z_{1,0}, z_{2,0}, z_{3,0}, \dots, z_{n,0}$ that approximate the random variable with mean μ and variance σ^2 is;

$$z_{i,0} = \sigma y_{i,0} + \mu, \qquad p'_{i,0} = p_{i,0}, \quad i=1,2,3,\dots,n \qquad (B.7)$$

B.1 Rayleigh and Gaussian cumulative distribution functions

Rayleigh Cumulative Distribution function:

Probability Density function of Rayleigh distribution is:

$$p(\alpha) = \frac{\alpha}{\sigma_1^2} \exp\left\{-\frac{\alpha^2}{2\sigma_1^2}\right\} \quad \alpha \geq 0 \quad (\text{B.8})$$

where

$$\text{Mean} = E\{\alpha\} = \sigma_1 \sqrt{\frac{\pi}{2}} \quad \text{Variance} = 2\sigma_1^2 \left(1 - \frac{\pi}{4}\right) \quad (\text{B.9})$$

The cumulative distribution function $F_\alpha(x)$, which gives the probability that a variate will assume a value $\leq x$, is then the integral of the probability density function:

$$F_\alpha(x) = \int_0^x p(\alpha) d\alpha = \begin{cases} 1 - \exp\left(-\frac{x^2}{2\sigma_1^2}\right) & , x \geq 0 \\ 0 & , x < 0 \end{cases} \quad (\text{B.10})$$

Gaussian Cumulative Distribution function:

Probability Density function of Gaussian distribution is:

$$p(x) = \frac{1}{\sigma\sqrt{2\pi}} \exp\left\{-\frac{(x-\mu)^2}{2\sigma^2}\right\} \quad -\infty < x < \infty \quad (\text{B.11})$$

where

$$\text{Mean} = E\{x\} = \mu \quad \text{Variance} = \sigma^2 \quad (\text{B.12})$$

Therefore, the cumulative distribution function $F_g(x)$ is:

$$\begin{aligned} F_g(x) &= \int_0^x p(x') dx' = \frac{1}{\sigma\sqrt{2\pi}} \int_{-\infty}^x \exp\left(-\frac{(x'-\mu)^2}{2\sigma^2}\right) \\ &= \frac{1}{2} \left[1 + \text{erf}\left(\frac{x-\mu}{\sigma\sqrt{2}}\right) \right] \end{aligned} \quad (\text{B.13})$$

where erf(.) is the so-called error function.

B.2 Approximation of a Rayleigh random variable with discrete random variables up to 50 possible values

Possible values of the discrete random variable approximating the Rayleigh random variable with parameter $\sigma_1^2 = 1$, i.e. mean $\sqrt{\frac{\pi}{2}} = 1.2533$ and Variance $2\left(1 - \frac{\pi}{4}\right) = 0.4292$.

<u>R_k</u>	<u>p&y</u>						
1	p = 1 y = 1.1774						
2	p = 0.5303 y = 0.7850	0.4697 1.7022					
3	p = 0.3499 y = 0.6202	0.3625 1.2308	0.2876 1.9695				
4	p = 0.2570 y = 0.5244	0.2810 1.0066	0.2621 1.4870	0.1999 2.1461			
5	p = 0.2011 y = 0.4603	0.2258 0.8681	0.2229 1.2433	0.2005 1.6652	0.1498 2.2768		
6	p = 0.1640 y = 0.4137	0.1872 0.7718	0.1902 1.0872	0.1812 1.4138	0.1597 1.8007	0.1178 2.3799	
7	p = 0.1378 y = 0.3779	0.1589 0.6999	0.1643 0.9759	0.1612 1.2489	0.1507 1.5463	0.1313 1.9094	0.0959 2.4648
8	p = 0.1176 0.0799 y = 0.3481 2.5379	0.1372 0.6419	0.1441 0.8897	0.1442 1.1286	0.1389 1.3772	0.1280 1.6558	0.1100 2.0017
9	p = 0.1027 0.0942 y = 0.3248 2.7890	0.1204 0.0681 0.5964 2.5999	0.1275 0.8223	0.1292 1.0359	0.1268 1.2520	0.1207 1.4831	0.1103 1.7469
10	p = 0.0910 0.0963 y = 0.3052 1.8251	0.1070 0.0819 0.5587 2.1460	0.1140 0.0590 0.7673 2.6543	0.1165 0.9617	0.1158 1.1544	0.1124 1.3547	0.1060 1.5729
11	p = 0.0815 0.0941 y = 0.2885 1.6506	0.0961 0.0851 0.5268 1.8936	0.1028 0.0721 0.7212 2.2052	0.1058 0.0519 0.9004 2.7027	0.1061 1.0756	0.1043 1.2539	0.1003 1.4426
12	p = 0.0737 0.0902 y = 0.2741 1.5191	0.0870 0.0842 0.4994 1.7191	0.0935 0.0759 0.6819 1.9544	0.0966 0.0641 0.8488 2.2582	0.0976 0.0461 1.0101 2.7463	0.0968 1.1719	0.0943 1.3396

13	p =	0.0672	0.0794	0.0855	0.0888	0.0901	0.0900	0.0885
		0.0858	0.0817	0.0760	0.0683	0.0575	0.0413	
	y =	0.2615	0.4755	0.6480	0.8045	0.9546	1.1034	1.2553
		1.4147	1.5869	1.7801	2.0089	2.3059	2.7859	
14	p =	0.0617	0.0729	0.0787	0.0820	0.0835	0.0839	0.0831
		0.0813	0.0784	0.0744	0.0690	0.0619	0.0520	0.0373
	y =	0.2503	0.4545	0.6182	0.7660	0.9067	1.0450	1.1846
		1.3288	1.4814	1.6475	1.8351	2.0583	2.3494	2.8221
15	p =	0.0569	0.0674	0.0728	0.0760	0.0778	0.0784	0.0781
		0.0769	0.0749	0.0720	0.0681	0.0631	0.0564	0.0474
		0.0339						
	y =	0.2403	0.4358	0.5919	0.7322	0.8649	0.9944	1.1240
	1.2563	1.3943	1.5413	1.7024	1.8850	2.1033	2.3892	
	2.8555							
16	p =	0.0528	0.0625	0.0677	0.0708	0.0726	0.0735	0.0735
		0.0728	0.0714	0.0693	0.0664	0.0627	0.0579	0.0517
		0.0434	0.0310					
	y =	0.2314	0.4191	0.5684	0.7021	0.8279	0.9501	1.0714
	1.1941	1.3206	1.4534	1.5958	1.7524	1.9307	2.1448	
	2.4260	2.8864						
17	p =	0.0492	0.0583	0.0632	0.0662	0.0681	0.0690	0.0693
		0.0689	0.0680	0.0665	0.0643	0.0615	0.0580	0.0534
		0.0476	0.0399	0.0285				
	y =	0.2232	0.4040	0.5473	0.6751	0.7950	0.9108	1.0251
	1.1399	1.2572	1.3788	1.5072	1.6456	1.7984	1.9730	
	2.1832	2.4603	2.9154					
18	p =	0.0461	0.0545	0.0592	0.0621	0.0640	0.0651	0.0655
		0.0654	0.0648	0.0636	0.0620	0.0599	0.0572	0.0538
		0.0495	0.0441	0.0369	0.0264			
	y =	0.2158	0.3902	0.5282	0.6508	0.7654	0.8757	0.9839
	1.0921	1.2017	1.3144	1.4319	1.5566	1.6914	1.8408	
	2.0121	2.2189	2.4922	2.9425				
19	p =	0.0432	0.0512	0.0556	0.0585	0.0603	0.0615	0.0620
		0.0621	0.0617	0.0609	0.0597	0.0581	0.0560	0.0533
		0.0501	0.0461	0.0410	0.0342	0.0245		
	y =	0.2091	0.3777	0.5107	0.6287	0.7386	0.8440	0.9470
	1.0494	1.1526	1.2578	1.3666	1.4807	1.6021	1.7338	
	1.8802	2.0485	2.2522	2.5221	2.9679			
20	p =	0.0407	0.0482	0.0525	0.0552	0.0570	0.0582	0.0588
		0.0590	0.0589	0.0583	0.0574	0.0562	0.0545	0.0524

		0.0499	0.0468	0.0430	0.0382	0.0319	0.0228	
	y =	0.2029	0.3662	0.4948	0.6086	0.7143	0.8153	0.9137
		1.0111	1.1087	1.2077	1.3093	1.4148	1.5257	1.6443
		1.7732	1.9169	2.0825	2.2834	2.5501	2.9918	
21	p =	0.0385	0.0456	0.0496	0.0522	0.0540	0.0552	0.0559
		0.0562	0.0562	0.0559	0.0552	0.0542	0.0529	0.0513
		0.0493	0.0468	0.0439	0.0403	0.0357	0.0298	0.0213
	y =	0.1971	0.3556	0.4801	0.5901	0.6920	0.7891	0.8834
		0.9764	1.0692	1.1629	1.2584	1.3568	1.4593	1.5676
		1.6835	1.8100	1.9513	2.1144	2.3126	2.5764	3.0143
22	p =	0.0365	0.0432	0.0470	0.0495	0.0513	0.0525	0.0532
		0.0537	0.0537	0.0535	0.0531	0.0523	0.0513	0.0500
		0.0484	0.0464	0.0441	0.0412	0.0378	0.0335	0.0280
		0.0200						
	y =	0.1918	0.3458	0.4666	0.5730	0.6714	0.7650	0.8557
		0.9448	1.0334	1.1224	1.2127	1.3051	1.4008	1.5008
		1.6066	1.7202	1.8445	1.9835	2.1444	2.3402	2.6013
		3.0356						
23	p =	0.0346	0.0410	0.0446	0.0471	0.0488	0.0500	0.0508
		0.0513	0.0514	0.0513	0.0510	0.0504	0.0496	0.0486
		0.0473	0.0457	0.0438	0.0415	0.0388	0.0356	0.0315
		0.0263	0.0188					
	y =	0.1869	0.3367	0.4540	0.5572	0.6525	0.7429	0.8302
		0.9158	1.0007	1.0856	1.1714	1.2588	1.3486	1.4418
		1.5395	1.6432	1.7547	1.8769	2.0139	2.1726	2.3663
		2.6248	3.0558					
24	p =	0.0330	0.0390	0.0425	0.0448	0.0465	0.0477	0.0485
		0.0490	0.0493	0.0493	0.0491	0.0487	0.0480	0.0472
		0.0461	0.0448	0.0433	0.0414	0.0393	0.0367	0.0336
		0.0298	0.0248	0.0177				
	y =	0.1823	0.3283	0.4424	0.5426	0.6349	0.7224	0.8068
		0.8892	0.9707	1.0520	1.1338	1.2168	1.3016	1.3891
		1.4802	1.5758	1.6775	1.7871	1.9074	2.0426	2.1994
		2.3909	2.6471	3.0749				
25	p =	0.0314	0.0372	0.0405	0.0428	0.0444	0.0456	0.0464
		0.0470	0.0473	0.0474	0.0472	0.0469	0.0464	0.0458
		0.0449	0.0438	0.0426	0.0411	0.0393	0.0372	0.0347
		0.0318	0.0281	0.0234	0.0167			
	y =	0.1780	0.3204	0.4315	0.5289	0.6186	0.7034	0.7850
		0.8646	0.9431	1.0211	1.0994	1.1785	1.2591	1.3417
		1.4271	1.5162	1.6100	1.7099	1.8178	1.9363	2.0697
		2.2247	2.4143	2.6682	3.0931			

26	p =	0.0300	0.0355	0.0387	0.0409	0.0425	0.0436	0.0445
		0.0450	0.0454	0.0455	0.0455	0.0453	0.0449	0.0444
		0.0437	0.0428	0.0417	0.0405	0.0390	0.0373	0.0353
		0.0329	0.0301	0.0267	0.0222	0.0159		
	y =	0.1739	0.3129	0.4213	0.5162	0.6034	0.6857	0.7648
		0.8417	0.9175	0.9926	1.0678	1.1435	1.2203	1.2986
		1.3793	1.4628	1.5501	1.6422	1.7405	1.8467	1.9637
		2.0955	2.2488	2.4366	2.6884	3.1105		
27	p =	0.0287	0.0340	0.0371	0.0392	0.0407	0.0418	0.0427
		0.0433	0.0436	0.0438	0.0439	0.0437	0.0435	0.0430
		0.0425	0.0417	0.0409	0.0398	0.0386	0.0372	0.0355
		0.0336	0.0313	0.0286	0.0253	0.0211	0.0151	
	y =	0.1701	0.3060	0.4117	0.5042	0.5891	0.6691	0.7459
		0.8205	0.8937	0.9662	1.0386	1.1112	1.1846	1.2593
		1.3358	1.4146	1.4964	1.5821	1.6727	1.7694	1.8742
		1.9897	2.1200	2.2717	2.4578	2.7076	3.1271	
28	p =	0.0276	0.0326	0.0355	0.0376	0.0390	0.0402	0.0410
		0.0416	0.0420	0.0422	0.0423	0.0423	0.0421	0.0417
		0.0413	0.0407	0.0399	0.0390	0.0380	0.0368	0.0354
		0.0338	0.0320	0.0298	0.0272	0.0241	0.0200	0.0143
	y =	0.1666	0.2994	0.4027	0.4930	0.5057	0.6536	0.7282
		0.8006	0.8716	0.9417	1.0114	1.0813	1.1518	1.2232
		1.2960	1.3708	1.4480	1.5283	1.6125	1.7016	1.7969
		1.9004	2.0145	2.1433	2.2936	2.4780	2.7259	3.1429
29	p =	0.0265	0.0313	0.0341	0.0361	0.0375	0.0386	0.0394
		0.0400	0.0405	0.0407	0.0409	0.0408	0.0407	0.0405
		0.0401	0.0396	0.0390	0.0382	0.0374	0.0363	0.0352
		0.0338	0.0323	0.0305	0.0284	0.0260	0.0229	0.0191
		0.0137						
	y =	0.1632	0.2933	0.3942	0.4824	0.5632	0.6391	0.7117
		0.7820	0.8509	0.9188	0.9862	1.0536	1.1214	1.1899
		1.2595	1.3307	1.4038	1.4796	1.5584	1.6413	1.7291
	1.8231	1.9253	2.0381	2.1656	2.3145	2.4974	2.7435	
	3.1581							
30	p =	0.0254	0.0300	0.0328	0.0347	0.0361	0.0372	0.0380
		0.0386	0.0390	0.0393	0.0395	0.0395	0.0394	0.0392
		0.0389	0.0385	0.0380	0.0374	0.0367	0.0358	0.0348
		0.0337	0.0324	0.0309	0.0291	0.0271	0.0248	0.0219
		0.0182	0.0130					
	y =	0.1600	0.2874	0.3862	0.4724	0.5513	0.6253	0.6961
		0.7646	0.8315	0.8973	0.9626	1.0278	1.0931	1.1590
		1.2258	1.2938	1.3635	1.4352	1.5096	1.5872	1.6688
	1.7554	1.8482	1.9492	2.0608	2.1870	2.3346	2.5161	

2.7606 3.1729

31 p = 0.0245 0.0289 0.0315 0.0334 0.0348 0.0358 0.0366
 0.0372 0.0377 0.0380 0.0382 0.0383 0.0382 0.0381
 0.0378 0.0375 0.0371 0.0366 0.0359 0.0352 0.0343
 0.0334 0.0323 0.0310 0.0295 0.0279 0.0260 0.0237
 0.0209 0.0174 0.0125
 y = 0.1570 0.2819 0.3786 0.4630 0.5401 0.6124 0.6814
 0.7481 0.8132 0.8772 0.9406 1.0036 1.0668 1.1303
 1.1945 1.2597 1.3263 1.3946 1.4650 1.5382 1.6146
 1.6950 1.7805 1.8722 1.9720 2.0825 2.2076 2.3540
 2.5341 2.7770 3.1872

32 p = 0.0236 0.0279 0.0304 0.0322 0.0335 0.0345 0.0353
 0.0359 0.0364 0.0367 0.0369 0.0371 0.0371 0.0370
 0.0368 0.0365 0.0362 0.0357 0.0352 0.0345 0.0338
 0.0330 0.0320 0.0309 0.0297 0.0283 0.0267 0.0249
 0.0227 0.0200 0.0167 0.0119
 y = 0.1541 0.2766 0.3714 0.4540 0.5294 0.6001 0.6675
 0.7326 0.7960 0.8583 0.9198 0.9810 1.0421 1.1035
 1.1654 1.2281 1.2919 1.3571 1.4242 1.4934 1.5654
 1.6407 1.7201 1.8045 1.8952 1.9939 2.1034 2.2274
 2.3726 2.5514 2.7928 3.2010

33 p = 0.0228 0.0269 0.0293 0.0310 0.0323 0.0333 0.0341
 0.0347 0.0352 0.0356 0.0358 0.0359 0.0360 0.0359
 0.0358 0.0356 0.0353 0.0349 0.0344 0.0339 0.0332
 0.0325 0.0317 0.0308 0.0297 0.0285 0.0272 0.0256
 0.0238 0.0217 0.0192 0.0160 0.0114
 y = 0.1513 0.2716 0.3646 0.4455 0.5194 0.5885 0.6544
 0.7179 0.7798 0.8404 0.9003 0.9597 1.0190 1.0784
 1.1382 1.1986 1.2599 1.3224 1.3865 1.4524 1.5205
 1.5914 1.6657 1.7441 1.8275 1.9172 2.0150 2.1234
 2.2464 2.3904 2.5681 2.8080 3.2142

34 p = 0.0220 0.0259 0.0283 0.0300 0.0312 0.0322 0.0330
 0.0336 0.0341 0.0344 0.0347 0.0348 0.0349 0.0349
 0.0348 0.0346 0.0344 0.0341 0.0337 0.0332 0.0327
 0.0320 0.0313 0.0305 0.0296 0.0286 0.0274 0.0261
 0.0246 0.0229 0.0209 0.0184 0.0153 0.0110
 y = 0.1487 0.2668 0.3581 0.4375 0.5098 0.5775 0.6420
 0.7040 0.7644 0.8236 0.8819 0.9397 0.9972 1.0548
 1.1127 1.1710 1.2301 1.2902 1.3515 1.4144 1.4793
 1.5464 1.6164 1.6897 1.7671 1.8496 1.9384 2.0352
 2.1427 2.2646 2.4077 2.5842 2.8228 3.2271

35 p = 0.0213 0.0251 0.0274 0.0290 0.0302 0.0312 0.0319
 0.0325 0.0330 0.0334 0.0336 0.0338 0.0339 0.0339
 0.0338 0.0337 0.0335 0.0333 0.0329 0.0325 0.0320

		0.0315	0.0309	0.0302	0.0294	0.0285	0.0275	0.0264
		0.0251	0.0236	0.0220	0.0200	0.0177	0.0147	0.0105
	y =	0.1462	0.2623	0.3519	0.4298	0.5007	0.5670	0.6301
		0.6909	0.7499	0.8076	0.8645	0.9207	0.9767	1.0326
		1.0887	1.1451	1.2022	1.2601	1.3190	1.3793	1.4412
		1.5050	1.5712	1.6402	1.7127	1.7892	1.8708	1.9587
		2.0547	2.1612	2.2823	2.4243	2.5997	2.8370	3.2395
36	p =	0.0206	0.0243	0.0265	0.0281	0.0292	0.0302	0.0309
		0.0315	0.0320	0.0324	0.0326	0.0328	0.0329	0.0330
		0.0329	0.0329	0.0327	0.0325	0.0322	0.0318	0.0314
		0.0310	0.0304	0.0298	0.0291	0.0283	0.0275	0.0265
		0.0254	0.0242	0.0228	0.0212	0.0193	0.0170	0.0141
		0.0101						
	y =	0.1438	0.2579	0.3460	0.4224	0.4920	0.5571	0.6189
		0.6783	0.7360	0.7924	0.8479	0.9028	0.9573	1.0117
		1.0661	1.1208	1.1760	1.2319	1.2887	1.3466	1.4058
		1.4668	1.5297	1.5950	1.6632	1.7347	1.8104	1.8912
		1.9783	2.0734	2.1791	2.2993	2.4404	2.6147	2.8507
		3.2515						
37	p =	0.0199	0.0235	0.0256	0.0272	0.0283	0.0293	0.0300
		0.0306	0.0310	0.0314	0.0317	0.0319	0.0320	0.0321
		0.0321	0.0320	0.0319	0.0317	0.0315	0.0312	0.0308
		0.0304	0.0299	0.0294	0.0288	0.0281	0.0273	0.0265
		0.0255	0.0245	0.0233	0.0219	0.0204	0.0186	0.0164
		0.0136	0.0097					
	y =	0.1416	0.2538	0.3403	0.4154	0.4837	0.5476	0.6081
		0.6664	0.7229	0.7780	0.8322	0.8858	0.9389	0.9918
		1.0448	1.0979	1.1514	1.2054	1.2602	1.3160	1.3729
		1.4313	1.4913	1.5534	1.6179	1.6852	1.7560	1.8309
		1.9109	1.9972	2.0915	2.1964	2.3157	2.4559	2.6292
		2.8640	3.2631					
38	p =	0.0193	0.0228	0.0249	0.0263	0.0275	0.0284	0.0291
		0.0297	0.0301	0.0305	0.0308	0.0310	0.0312	0.0312
		0.0313	0.0312	0.0311	0.0310	0.0308	0.0305	0.0302
		0.0298	0.0294	0.0290	0.0284	0.0278	0.0271	0.0264
		0.0256	0.0246	0.0236	0.0225	0.0211	0.0196	0.0179
		0.0158	0.0131	0.0094				
	y =	0.1394	0.2498	0.3349	0.4087	0.4758	0.5385	0.5979
		0.6550	0.7103	0.7643	0.8173	0.8696	0.9215	0.9731
		1.0246	1.0762	1.1281	1.1805	1.2335	1.2873	1.3421
		1.3981	1.4556	1.5149	1.5761	1.6398	1.7064	1.7764
		1.8506	1.9299	2.0154	2.1090	2.2131	2.3316	2.4709
		2.6432	2.8769	3.2744				
39	p =	0.0188	0.0221	0.0241	0.0255	0.0267	0.0275	0.0282

	0.0288	0.0293	0.0297	0.0299	0.0302	0.0303	0.0304
	0.0305	0.0304	0.0304	0.0303	0.0301	0.0299	0.0296
	0.0293	0.0289	0.0285	0.0280	0.0275	0.0269	0.0262
	0.0255	0.0247	0.0238	0.0228	0.0217	0.0204	0.0189
	0.0173	0.0152	0.0126	0.0091			
y =	0.1373	0.2460	0.3297	0.4023	0.4683	0.5298	0.5881
	0.6441	0.6984	0.7512	0.8031	0.8543	0.9049	0.9552
	1.0055	1.0557	1.1062	1.1570	1.2083	1.2604	1.3132
	1.3672	1.4224	1.4791	1.5375	1.5980	1.6610	1.7269
	1.7962	1.8696	1.9482	2.0331	2.1259	2.2293	2.3470
	2.4855	2.6569	2.8894	3.2854			

40

p =	0.0182	0.0214	0.0234	0.0248	0.0259	0.0267	0.0274
	0.0280	0.0285	0.0288	0.0291	0.0294	0.0295	0.0296
	0.0297	0.0297	0.0296	0.0296	0.0294	0.0292	0.0290
	0.0287	0.0284	0.0280	0.0276	0.0271	0.0266	0.0260
	0.0254	0.0247	0.0239	0.0230	0.0220	0.0209	0.0197
	0.0183	0.0167	0.0147	0.0122	0.0087		
y =	0.1353	0.2424	0.3248	0.3962	0.4610	0.5215	0.5788
	0.6337	0.6869	0.7388	0.7896	0.8396	0.8891	0.9383
	0.9873	1.0362	1.0853	1.1347	1.1846	1.2350	1.2861
	1.3381	1.3912	1.4457	1.5016	1.5593	1.6191	1.6814
	1.7466	1.8152	1.8880	1.9659	2.0501	2.1423	2.2449
	2.3619	2.4996	2.6701	2.9015	3.2960		

41

p =	0.0177	0.0208	0.0227	0.0241	0.0251	0.0260	0.0267
	0.0272	0.0277	0.0281	0.0284	0.0286	0.0288	0.0289
	0.0290	0.0290	0.0290	0.0289	0.0288	0.0286	0.0284
	0.0282	0.0279	0.0276	0.0272	0.0268	0.0263	0.0258
	0.0252	0.0246	0.0239	0.0231	0.0223	0.0213	0.0202
	0.0191	0.0177	0.0161	0.0142	0.0118	0.0085	
y =	0.1333	0.2388	0.3200	0.3903	0.4541	0.5135	0.5698
	0.6238	0.6760	0.7268	0.7766	0.8256	0.8741	0.9221
	0.9700	1.0177	1.0656	1.1136	1.1621	1.2109	1.2605
	1.3108	1.3620	1.4144	1.4681	1.5233	1.5803	1.6395
	1.7011	1.7656	1.8336	1.9058	1.9831	2.0666	2.1581
	2.2601	2.3764	2.5132	2.6829	2.9133	3.3064	

42

p =	0.0172	0.0203	0.0221	0.0234	0.0245	0.0253	0.0259
	0.0265	0.0269	0.0273	0.0276	0.0279	0.0280	0.0282
	0.0283	0.0283	0.0283	0.0282	0.0281	0.0280	0.0278
	0.0276	0.0274	0.0271	0.0268	0.0264	0.0260	0.0255
	0.0250	0.0244	0.0238	0.0231	0.0224	0.0216	0.0206
	0.0196	0.0184	0.0171	0.0156	0.0137	0.0114	0.0082
y =	0.1315	0.2355	0.3154	0.3846	0.4474	0.5058	0.5612
	0.6142	0.6655	0.7154	0.7642	0.8123	0.8597	0.9067
	0.9535	1.0001	1.0468	1.0936	1.1407	1.1882	1.2363
	1.2850	1.3345	1.3850	1.4367	1.4897	1.5442	1.6006

		1.6591	1.7201	1.7841	1.8515	1.9230	1.9997	2.0826
		2.1735	2.2748	2.3904	2.5265	2.6953	2.9247	3.3164
43	p =	0.0168	0.0197	0.0215	0.0228	0.0238	0.0246	0.0253
		0.0258	0.0262	0.0266	0.0269	0.0272	0.0273	0.0275
		0.0276	0.0276	0.0276	0.0276	0.0275	0.0274	0.0273
		0.0271	0.0269	0.0266	0.0263	0.0260	0.0256	0.0252
		0.0248	0.0243	0.0237	0.0231	0.0224	0.0217	0.0209
		0.0200	0.0190	0.0178	0.0166	0.0151	0.0133	0.0110
		0.0079						
	y =	0.1297	0.2322	0.3110	0.3791	0.4410	0.4985	0.5529
		0.6051	0.6555	0.7045	0.7524	0.7995	0.8460	0.8920
		0.9377	0.9833	1.0289	1.0746	1.1204	1.1667	1.2133
		1.2606	1.3085	1.3574	1.4072	1.4582	1.5105	1.5644
		1.6202	1.6781	1.7385	1.8019	1.8687	1.9397	2.0158
		2.0981	2.1884	2.2891	2.4040	2.5394	2.7074	2.9359
		3.3262						
44	p =	0.0163	0.0192	0.0209	0.0222	0.0232	0.0239	0.0246
		0.0251	0.0256	0.0259	0.0262	0.0265	0.0267	0.0268
		0.0269	0.0270	0.0270	0.0270	0.0269	0.0269	0.0267
		0.0266	0.0264	0.0262	0.0259	0.0256	0.0253	0.0249
		0.0245	0.0240	0.0236	0.0230	0.0224	0.0218	0.0210
		0.0202	0.0194	0.0184	0.0173	0.0160	0.0146	0.0129
		0.0107	0.0077					
	y =	0.1280	0.2291	0.3067	0.3739	0.4348	0.4914	0.5450
		0.5963	0.6458	0.6939	0.7410	0.7872	0.8328	0.8779
		0.9227	0.9673	1.0118	1.0564	1.1011	1.1462	1.1916
		1.2375	1.2840	1.3312	1.3794	1.4285	1.4789	1.5306
		1.5840	1.6392	1.6965	1.7564	1.8192	1.8854	1.9559
		2.0314	2.1132	2.2029	2.3030	2.4172	2.5520	2.7192
		2.9467	3.3358					
45	p =	0.0159	0.0187	0.0204	0.0216	0.0226	0.0233	0.0240
		0.0245	0.0249	0.0253	0.0256	0.0258	0.0260	0.0262
		0.0263	0.0264	0.0264	0.0264	0.0264	0.0263	0.0262
		0.0261	0.0259	0.0257	0.0255	0.0252	0.0249	0.0246
		0.0242	0.0238	0.0234	0.0229	0.0223	0.0218	0.0211
		0.0204	0.0196	0.0188	0.0178	0.0168	0.0156	0.0141
		0.0125	0.0104	0.0074				
	y =	0.1263	0.2261	0.3027	0.3688	0.4288	0.4846	0.5374
		0.5878	0.6365	0.6839	0.7301	0.7755	0.8202	0.8644
		0.9083	0.9519	0.9955	1.0391	1.0827	1.1266	1.1709
		1.2155	1.2607	1.3065	1.3531	1.4006	1.4492	1.4989
		1.5501	1.6029	1.6575	1.7143	1.7736	1.8359	1.9017
		1.9716	2.0465	2.1278	2.2169	2.3165	2.4301	2.5642
		2.7307	2.9573	3.3451				

46	p =	0.0155	0.0182	0.0199	0.0211	0.0220	0.0227	0.0234
		0.0239	0.0243	0.0247	0.0250	0.0252	0.0254	0.0256
		0.0257	0.0258	0.0258	0.0258	0.0258	0.0258	0.0257
		0.0256	0.0254	0.0253	0.0250	0.0248	0.0245	0.0243
		0.0239	0.0236	0.0232	0.0227	0.0222	0.0217	0.0211
		0.0205	0.0198	0.0191	0.0182	0.0173	0.0163	0.0151
		0.0137	0.0121	0.0101	0.0072			
	y =	0.1247	0.2232	0.2987	0.3640	0.4231	0.4781	0.5300
		0.5797	0.6276	0.6742	0.7196	0.7642	0.8081	0.8515
		0.8945	0.9373	0.9799	1.0225	1.0652	1.1080	1.1511
		1.1946	1.2386	1.2831	1.3282	1.3742	1.4211	1.4691
		1.5183	1.5689	1.6212	1.6753	1.7316	1.7904	1.8522
		1.9174	1.9868	2.0613	2.1420	2.2306	2.3296	2.4426
		2.5761	2.7418	2.9676	3.3542			
47	p =	0.0151	0.0178	0.0194	0.0205	0.0214	0.0222	0.0228
		0.0233	0.0237	0.0241	0.0244	0.0246	0.0248	0.0250
		0.0251	0.0252	0.0253	0.0253	0.0253	0.0252	0.0252
		0.0251	0.0250	0.0248	0.0246	0.0244	0.0242	0.0239
		0.0236	0.0233	0.0229	0.0225	0.0221	0.0216	0.0211
		0.0205	0.0199	0.0193	0.0185	0.0177	0.0168	0.0158
		0.0146	0.0133	0.0117	0.0098	0.0070		
	y =	0.1232	0.2204	0.2949	0.3593	0.4176	0.4718	0.5229
		0.5719	0.6190	0.6648	0.7095	0.7533	0.7964	0.8390
		0.8812	0.9232	0.9649	1.0066	1.0484	1.0902	1.1323
		1.1747	1.2175	1.2608	1.3046	1.3492	1.3946	1.4410
		1.4884	1.5371	1.5872	1.6389	1.6925	1.7483	1.8067
		1.8679	1.9327	2.0016	2.0756	2.1558	2.2439	2.3424
		2.4548	2.5877	2.7527	2.9776	3.3630		
48	p =	0.0148	0.0173	0.0189	0.0200	0.0209	0.0216	0.0222
		0.0227	0.0232	0.0235	0.0238	0.0241	0.0243	0.0245
		0.0246	0.0247	0.0247	0.0248	0.0248	0.0247	0.0247
		0.0246	0.0245	0.0244	0.0242	0.0240	0.0238	0.0236
		0.0233	0.0230	0.0227	0.0223	0.0219	0.0215	0.0210
		0.0205	0.0200	0.0194	0.0187	0.0180	0.0172	0.0163
		0.0153	0.0142	0.0129	0.0114	0.0095	0.0068	
	y =	0.1217	0.2177	0.2912	0.3547	0.4122	0.4657	0.5161
		0.5643	0.6108	0.6558	0.6998	0.7429	0.7853	0.8271
		0.8685	0.9097	0.9506	0.9915	1.0323	1.0732	1.1143
		1.1557	1.1974	1.2396	1.2822	1.3255	1.3695	1.4144
		1.4602	1.5071	1.5552	1.6049	1.6561	1.7093	1.7646
		1.8225	1.8833	1.9476	2.0160	2.0895	2.1693	2.2569
		2.3548	2.4667	2.5990	2.7633	2.9874	3.3716	
49	p =	0.0144	0.0169	0.0184	0.0196	0.0204	0.0211	0.0217
		0.0222	0.0226	0.0230	0.0233	0.0235	0.0237	0.0239
		0.0240	0.0241	0.0242	0.0243	0.0243	0.0243	0.0242

	0.0241	0.0241	0.0239	0.0238	0.0236	0.0234	0.0232
	0.0230	0.0227	0.0224	0.0221	0.0217	0.0213	0.0209
	0.0205	0.0200	0.0194	0.0188	0.0182	0.0175	0.0167
	0.0159	0.0149	0.0138	0.0126	0.0111	0.0092	0.0066
y = 0.1202	0.2150	0.2877	0.3504	0.4071	0.4598	0.5095	
	0.5570	0.6028	0.6472	0.6904	0.7328	0.7745	0.8156
	0.8563	0.8967	0.9368	0.9769	1.0169	1.0570	1.0971
	1.1376	1.1783	1.2193	1.2609	1.3029	1.3457	1.3891
	1.4335	1.4788	1.5252	1.5729	1.6220	1.6728	1.7255
	1.7804	1.8378	1.8982	1.9620	2.0300	2.1031	2.1824
	2.2695	2.3669	2.4783	2.6100	2.7737	2.9970	3.3801

50	p = 0.0141	0.0165	0.0180	0.0191	0.0199	0.0206	0.0212
	0.0217	0.0221	0.0225	0.0228	0.0230	0.0232	0.0234
	0.0235	0.0236	0.0237	0.0238	0.0238	0.0238	0.0238
	0.0237	0.0236	0.0235	0.0234	0.0232	0.0231	0.0229
	0.0227	0.0224	0.0222	0.0219	0.0215	0.0212	0.0208
	0.0204	0.0199	0.0194	0.0189	0.0183	0.0177	0.0170
	0.0163	0.0154	0.0145	0.0134	0.0122	0.0108	0.0089
	0.0064						
y = 0.1188	0.2125	0.2842	0.3461	0.4021	0.4541	0.5031	
	0.5500	0.5951	0.6388	0.6814	0.7231	0.7641	0.8045
	0.8445	0.8842	0.9236	0.9629	1.0021	1.0413	1.0807
	1.1202	1.1599	1.2000	1.2405	1.2814	1.3230	1.3652
	1.4081	1.4520	1.4968	1.5427	1.5900	1.6387	1.6890
	1.7413	1.7958	1.8527	1.9127	1.9761	2.0437	2.1163
	2.1951	2.2818	2.3787	2.4896	2.6207	2.7838	3.0063
	3.3883						

B.3 Approximation of a Gaussian random variable with discrete random variables up to 50 possible values

Possible values of the discrete random variable approximating the Gaussian random variable with mean 0 and Variance 1.

<u>N_k</u>	<u>$p&y$</u>
1	p = 1 y = 0
2	p = 0.5000 0.5000 y = -0.6745 0.6745
3	p = 0.3148 0.3704 0.3148 y = -1.0051 -0.0000 1.0051

4 p = 0.2225 0.2775 0.2775 0.2225
 y = -1.2198 -0.3551 0.3551 1.2198

5 p = 0.1685 0.2167 0.2296 0.2167 0.1685
 y = -1.3769 -0.5921 -0.0000 0.5921 1.3769

6 p = 0.1337 0.1752 0.1913 0.1911 0.1751 0.1336
 y = -1.4996 -0.7677 -0.2415 0.2424 0.7684 1.5001

7 p = 0.1095 0.1454 0.1617 0.1666 0.1617 0.1454 0.1095
 y = -1.6004 -0.9069 -0.4239 -0.0000 0.4239 0.9069 1.6004

8 p = 0.0920 0.1233 0.1389 0.1458 0.1458 0.1389 0.1233
 0.0920
 y = -1.6850 -1.0209 -0.5687 -0.1837 0.1837 0.5687 1.0209
 1.6850

9 p = 0.0787 0.1064 0.1209 0.1285 0.1308 0.1285 0.1209
 0.1064 0.0787
 y = -1.7580 -1.1173 -0.6883 -0.3310 -0.0000 0.3310 0.6883
 1.1173 1.7580

10 p = 0.0683 0.0929 0.1064 0.1141 0.1176 0.1177 0.1143
 0.1069 0.0931 0.0687
 y = -1.8228 -1.2014 -0.7911 -0.4547 -0.1497 0.1463 0.4514
 0.7883 1.1992 1.8206

11 p = 0.0599 0.0818 0.0947 0.1026 0.1069 0.1083 0.1069
 0.1026 0.0947 0.0818 0.0599
 y = -1.8815 -1.2771 -0.8815 -0.5603 -0.2731 -0.0000 0.2731
 0.5603 0.8815 1.2771 1.8815

12 p = 0.0536 0.0736 0.0851 0.0923 0.0967 0.0988 0.0988
 0.0967 0.0923 0.0851 0.0735 0.0536
 y = -1.9299 -1.3383 -0.9552 -0.6482 -0.3774 -0.1240 0.1242
 0.3777 0.6485 0.9556 1.3386 1.9302

13 p = 0.0479 0.0657 0.0767 0.0839 0.0886 0.0912 0.0921
 0.0912 0.0886 0.0839 0.0767 0.0657 0.0479
 y = -1.9785 -1.4002 -1.0282 -0.7316 -0.4720 -0.2318 -0.0000
 0.2318 0.4720 0.7316 1.0282 1.4002 1.9785

14	p =	0.0435	0.0601	0.0700	0.0766	0.0810	0.0837	0.0851
		0.0851	0.0837	0.0810	0.0766	0.0700	0.0601	0.0435
	y =	-2.0189	-1.4499	-1.0866	-0.7998	-0.5513	-0.3238	-0.1069
		0.1069	0.3238	0.5513	0.7998	1.0866	1.4499	2.0189
15	p =	0.0395	0.0544	0.0638	0.0703	0.0748	0.0778	0.0795
		0.0801	0.0795	0.0778	0.0748	0.0703	0.0638	0.0544
		0.0395						
	y =	-2.0593	-1.5013	-1.1469	-0.8678	-0.6271	-0.4082	-0.2013
		-0.0000	0.2013	0.4082	0.6271	0.8678	1.1469	1.5013
		2.0593						
16	p =	0.0363	0.0504	0.0590	0.0649	0.0691	0.0720	0.0738
		0.0747	0.0747	0.0738	0.0720	0.0691	0.0649	0.0590
		0.0504	0.0363					
	y =	-2.0939	-1.5427	-1.1946	-0.9228	-0.6902	-0.4801	-0.2834
		-0.0937	0.0937	0.2834	0.4801	0.6902	0.9228	1.1946
		1.5427	2.0939					
17	p =	0.0333	0.0460	0.0542	0.0600	0.0642	0.0672	0.0693
		0.0705	0.0708	0.0705	0.0693	0.0672	0.0642	0.0600
		0.0542	0.0460	0.0333				
	y =	-2.1288	-1.5869	-1.2462	-0.9804	-0.7536	-0.5497	-0.3598
		-0.1780	0.0000	0.1780	0.3598	0.5497	0.7536	0.9804
		1.2462	1.5869	2.1288				
18	p =	0.0310	0.0431	0.0507	0.0560	0.0598	0.0626	0.0646
		0.0658	0.0664	0.0664	0.0658	0.0646	0.0626	0.0598
		0.0560	0.0507	0.0431	0.0310			
	y =	-2.1571	-1.6206	-1.2847	-1.0245	-0.8040	-0.6071	-0.4248
		-0.2515	-0.0833	0.0833	0.2515	0.4248	0.6071	0.8040
		1.0245	1.2847	1.6206	2.1571			
19	p =	0.0286	0.0396	0.0468	0.0520	0.0559	0.0588	0.0609
		0.0624	0.0633	0.0635	0.0633	0.0624	0.0609	0.0588
		0.0559	0.0520	0.0468	0.0396	0.0286		
	y =	-2.1896	-1.6612	-1.3315	-1.0762	-0.8601	-0.6675	-0.4899
		-0.3219	-0.1596	-0.0000	0.1596	0.3219	0.4899	0.6675
		0.8601	1.0762	1.3315	1.6612	2.1896		
20	p =	0.0267	0.0373	0.0441	0.0489	0.0525	0.0552	0.0572

		0.0586	0.0596	0.0600	0.0600	0.0596	0.0586	0.0572
		0.0552	0.0525	0.0489	0.0441	0.0373	0.0267	
	y =	-2.2160	-1.6915	-1.3653	-1.1145	-0.9033	-0.7160	-0.5441
		-0.3824	-0.2271	-0.0753	0.0753	0.2270	0.3824	0.5441
		0.7160	0.9033	1.1145	1.3653	1.6915	2.2159	
21	p =	0.0249	0.0345	0.0410	0.0457	0.0492	0.0520	0.0541
		0.0557	0.0568	0.0574	0.0576	0.0574	0.0568	0.0557
		0.0541	0.0520	0.0492	0.0457	0.0410	0.0345	0.0249
	y =	-2.2434	-1.7263	-1.4058	-1.1591	-0.9516	-0.7679	-0.5998
		-0.4420	-0.2912	-0.1446	0.0000	0.1446	0.2912	0.4420
		0.5998	0.7679	0.9516	1.1591	1.4058	1.7263	2.2434
22	p =	0.0234	0.0328	0.0388	0.0432	0.0465	0.0491	0.0510
		0.0525	0.0536	0.0543	0.0547	0.0547	0.0543	0.0536
		0.0525	0.0510	0.0491	0.0465	0.0432	0.0388	0.0328
		0.0234						
	y =	-2.2669	-1.7529	-1.4350	-1.1919	-0.9883	-0.8090	-0.6454
		-0.4927	-0.3473	-0.2066	-0.0686	0.0685	0.2065	0.3472
		0.4926	0.6453	0.8088	0.9882	1.1917	1.4348	1.7526
		2.2666						
23	p =	0.0219	0.0305	0.0363	0.0405	0.0438	0.0464	0.0484
		0.0500	0.0512	0.0520	0.0525	0.0527	0.0525	0.0520
		0.0512	0.0500	0.0484	0.0464	0.0438	0.0405	0.0363
		0.0305	0.0219					
	y =	-2.2915	-1.7843	-1.4715	-1.2320	-1.0316	-0.8551	-0.6945
		-0.5449	-0.4029	-0.2659	-0.1322	-0.0000	0.1322	0.2659
		0.4029	0.5449	0.6945	0.8551	1.0316	1.2320	1.4715
		1.7843	2.2915					
24	p =	0.0207	0.0292	0.0346	0.0385	0.0416	0.0440	0.0459
		0.0474	0.0485	0.0494	0.0499	0.0502	0.0502	0.0499
		0.0494	0.0485	0.0474	0.0459	0.0440	0.0416	0.0386
		0.0346	0.0292	0.0208				
	y =	-2.3127	-1.8078	-1.4970	-1.2604	-1.0633	-0.8904	-0.7336
		-0.5881	-0.4504	-0.3182	-0.1896	-0.0630	0.0628	0.1894
		0.3180	0.4502	0.5879	0.7334	0.8901	1.0630	1.2601
		1.4966	1.8073	2.3122				
25	p =	0.0195	0.0272	0.0324	0.0363	0.0393	0.0417	0.0437
		0.0452	0.0465	0.0474	0.0480	0.0484	0.0485	0.0484
		0.0480	0.0474	0.0465	0.0452	0.0437	0.0417	0.0393

		0.0363	0.0324	0.0272	0.0195			
	y =	-2.3350	-1.8363	-1.5303	-1.2970	-1.1025	-0.9320	-0.7777
		-0.6346	-0.4995	-0.3702	-0.2447	-0.1218	-0.0000	0.1218
		0.2447	0.3702	0.4995	0.6346	0.7777	0.9320	1.1025
		1.2970	1.5303	1.8363	2.3350			
26	p =	0.0186	0.0262	0.0311	0.0347	0.0375	0.0398	0.0416
		0.0430	0.0442	0.0451	0.0457	0.0462	0.0464	0.0464
		0.0462	0.0457	0.0451	0.0442	0.0430	0.0416	0.0398
		0.0375	0.0347	0.0311	0.0262	0.0186		
	y =	-2.3544	-1.8574	-1.5527	-1.3218	-1.1300	-0.9626	-0.8114
		-0.6718	-0.5403	-0.4148	-0.2935	-0.1750	-0.0582	0.0582
		0.1750	0.2935	0.4148	0.5403	0.6717	0.8114	0.9626
		1.1300	1.3217	1.5527	1.8573	2.3543		
27	p =	0.0176	0.0245	0.0292	0.0328	0.0356	0.0378	0.0397
		0.0412	0.0424	0.0433	0.0441	0.0446	0.0449	0.0450
		0.0449	0.0446	0.0441	0.0433	0.0424	0.0412	0.0397
		0.0378	0.0356	0.0328	0.0292	0.0245	0.0176	
	y =	-2.3746	-1.8835	-1.5834	-1.3554	-1.1660	-1.0007	-0.8515
		-0.7139	-0.5845	-0.4613	-0.3424	-0.2267	-0.1129	0.0000
		0.1129	0.2267	0.3424	0.4613	0.5845	0.7139	0.8515
		1.0007	1.1660	1.3554	1.5834	1.8835	2.3746	
28	p =	0.0167	0.0236	0.0281	0.0315	0.0341	0.0362	0.0379
		0.0393	0.0405	0.0414	0.0421	0.0426	0.0429	0.0431
		0.0431	0.0429	0.0426	0.0421	0.0414	0.0405	0.0393
		0.0379	0.0362	0.0341	0.0315	0.0281	0.0236	0.0167
	y =	-2.3925	-1.9026	-1.6034	-1.3773	-1.1903	-1.0275	-0.8811
		-0.7463	-0.6200	-0.5000	-0.3846	-0.2725	-0.1626	-0.0541
		0.0540	0.1626	0.2724	0.3845	0.4999	0.6199	0.7462
		0.8810	1.0274	1.1902	1.3772	1.6033	1.9024	2.3923
29	p =	0.0159	0.0222	0.0265	0.0298	0.0324	0.0345	0.0362
		0.0377	0.0389	0.0398	0.0406	0.0412	0.0416	0.0418
		0.0419	0.0418	0.0416	0.0412	0.0406	0.0398	0.0389
		0.0377	0.0362	0.0345	0.0324	0.0298	0.0265	0.0222
		0.0159						
	y =	-2.4109	-1.9266	-1.6317	-1.4084	-1.2235	-1.0626	-0.9179
		-0.7848	-0.6602	-0.5420	-0.4285	-0.3186	-0.2111	-0.1052
		-0.0000	0.1052	0.2111	0.3186	0.4285	0.5420	0.6602
		0.7848	0.9179	1.0626	1.2235	1.4084	1.6317	1.9266
		2.4109						

30	p =	0.0152	0.0215	0.0256	0.0287	0.0311	0.0331	0.0347
		0.0361	0.0372	0.0381	0.0389	0.0394	0.0399	0.0401
		0.0403	0.0403	0.0401	0.0399	0.0394	0.0389	0.0381
		0.0372	0.0361	0.0347	0.0331	0.0311	0.0287	0.0256
		0.0215	0.0153					
	y =	-2.4278	-1.9442	-1.6498	-1.4281	-1.2451	-1.0864	-0.9441
		-0.8135	-0.6915	-0.5761	-0.4655	-0.3586	-0.2544	-0.1520
		-0.0507	0.0503	0.1516	0.2540	0.3582	0.4651	0.5756
		0.6910	0.8129	0.9435	1.0858	1.2444	1.4273	1.6489
		1.9429	2.4262					
31	p =	0.0145	0.0203	0.0242	0.0272	0.0296	0.0316	0.0333
		0.0346	0.0358	0.0368	0.0375	0.0382	0.0386	0.0390
		0.0392	0.0392	0.0392	0.0390	0.0386	0.0382	0.0375
		0.0368	0.0358	0.0346	0.0333	0.0316	0.0296	0.0272
		0.0242	0.0203	0.0145				
	y =	-2.4444	-1.9662	-1.6760	-1.4569	-1.2759	-1.1188	-0.9780
		-0.8488	-0.7283	-0.6144	-0.5054	-0.4002	-0.2979	-0.1975
		-0.0984	-0.0000	0.0984	0.1975	0.2979	0.4002	0.5054
		0.6144	0.7283	0.8488	0.9780	1.1188	1.2759	1.4569
		1.6760	1.9662	2.4444				
32	p =	0.0139	0.0197	0.0235	0.0263	0.0286	0.0304	0.0320
		0.0333	0.0344	0.0353	0.0360	0.0366	0.0371	0.0374
		0.0377	0.0378	0.0378	0.0377	0.0374	0.0371	0.0366
		0.0360	0.0353	0.0344	0.0333	0.0320	0.0304	0.0286
		0.0263	0.0235	0.0197	0.0139			
	y =	-2.4603	-1.9825	-1.6924	-1.4745	-1.2952	-1.1400	-1.0012
		-0.8742	-0.7560	-0.6444	-0.5379	-0.4354	-0.3358	-0.2384
		-0.1425	-0.0475	0.0473	0.1423	0.2382	0.3356	0.4352
		0.5377	0.6442	0.7558	0.8740	1.0009	1.1397	1.2949
		1.4741	1.6920	1.9818	2.4596			
33	p =	0.0133	0.0186	0.0222	0.0250	0.0273	0.0291	0.0307
		0.0320	0.0331	0.0341	0.0348	0.0355	0.0360	0.0364
		0.0367	0.0368	0.0369	0.0368	0.0367	0.0364	0.0360
		0.0355	0.0348	0.0341	0.0331	0.0320	0.0307	0.0291
		0.0273	0.0250	0.0222	0.0186	0.0133		
	y =	-2.4755	-2.0028	-1.7169	-1.5014	-1.3239	-1.1703	-1.0328
		-0.9071	-0.7901	-0.6798	-0.5747	-0.4735	-0.3755	-0.2797
		-0.1856	-0.0925	-0.0000	0.0925	0.1856	0.2797	0.3755
		0.4735	0.5747	0.6798	0.7901	0.9071	1.0328	1.1703
		1.3239	1.5014	1.7169	2.0028	2.4755		

34	p =	0.0128	0.0181	0.0216	0.0243	0.0264	0.0281	0.0296
		0.0308	0.0319	0.0328	0.0335	0.0341	0.0346	0.0350
		0.0353	0.0355	0.0356	0.0356	0.0355	0.0353	0.0350
		0.0346	0.0341	0.0335	0.0328	0.0319	0.0308	0.0296
		0.0281	0.0264	0.0243	0.0216	0.0181	0.0128	
	y =	-2.4907	-2.0180	-1.7319	-1.5174	-1.3413	-1.1893	-1.0536
		-0.9298	-0.8148	-0.7066	-0.6036	-0.5048	-0.4091	-0.3158
		-0.2244	-0.1342	-0.0447	0.0446	0.1341	0.2243	0.3157
		0.4089	0.5046	0.6035	0.7064	0.8146	0.9296	1.0534
		1.1891	1.3411	1.5172	1.7316	2.0176	2.4901	
35	p =	0.0123	0.0171	0.0205	0.0231	0.0252	0.0269	0.0284
		0.0297	0.0307	0.0317	0.0324	0.0331	0.0336	0.0341
		0.0344	0.0346	0.0348	0.0348	0.0348	0.0346	0.0344
		0.0341	0.0336	0.0331	0.0324	0.0317	0.0307	0.0297
		0.0284	0.0269	0.0252	0.0231	0.0205	0.0171	0.0123
	y =	-2.5043	-2.0368	-1.7547	-1.5426	-1.3683	-1.2176	-1.0832
		-0.9605	-0.8466	-0.7395	-0.6376	-0.5400	-0.4455	-0.3536
		-0.2636	-0.1750	-0.0873	0.0000	0.0873	0.1750	0.2636
		0.3536	0.4455	0.5400	0.6376	0.7395	0.8466	0.9605
		1.0832	1.2176	1.3683	1.5426	1.7547	2.0368	2.5043
36	p =	0.0119	0.0169	0.0202	0.0227	0.0247	0.0263	0.0276
		0.0288	0.0297	0.0306	0.0312	0.0318	0.0323	0.0327
		0.0329	0.0331	0.0333	0.0333	0.0333	0.0333	0.0331
		0.0329	0.0327	0.0323	0.0318	0.0312	0.0306	0.0297
		0.0288	0.0276	0.0263	0.0247	0.0227	0.0202	0.0169
		0.0119						
	y =	-2.5151	-2.0466	-1.7636	-1.5518	-1.3783	-1.2289	-1.0962
		-0.9753	-0.8634	-0.7584	-0.6588	-0.5636	-0.4718	-0.3825
		-0.2954	-0.2100	-0.1255	-0.0417	0.0417	0.1255	0.2100
		0.2954	0.3825	0.4718	0.5636	0.6588	0.7584	0.8634
	0.9753	1.0962	1.2289	1.3783	1.5518	1.7636	2.0466	
	2.5151							
37	p =	0.0114	0.0159	0.0190	0.0214	0.0234	0.0250	0.0264
		0.0276	0.0286	0.0295	0.0303	0.0309	0.0315	0.0319
		0.0323	0.0326	0.0328	0.0329	0.0329	0.0329	0.0328
		0.0326	0.0323	0.0319	0.0315	0.0309	0.0303	0.0295
		0.0286	0.0276	0.0264	0.0250	0.0234	0.0214	0.0190
		0.0159	0.0114					
	y =	-2.5313	-2.0684	-1.7898	-1.5809	-1.4094	-1.2615	-1.1297
		-1.0097	-0.8986	-0.7942	-0.6953	-0.6006	-0.5093	-0.4207

-0.3342	-0.2493	-0.1656	-0.0826	0.0000	0.0826	0.1656
0.2493	0.3342	0.4207	0.5093	0.6006	0.6953	0.7942
0.8986	1.0097	1.1297	1.2615	1.4094	1.5809	1.7898
2.0684	2.5313					

38 p = 0.0109 0.0155 0.0186 0.0209 0.0228 0.0243 0.0256
0.0267 0.0277 0.0285 0.0293 0.0299 0.0304 0.0308
0.0312 0.0315 0.0317 0.0318 0.0319 0.0319 0.0318
0.0317 0.0315 0.0312 0.0308 0.0304 0.0299 0.0293
0.0285 0.0277 0.0267 0.0256 0.0243 0.0228 0.0209
0.0186 0.0155 0.0109

y = -2.5457 -2.0823 -1.8030 -1.5944 -1.4239 -1.2772 -1.1468
-1.0283 -0.9186 -0.8159 -0.7187 -0.6257 -0.5363 -0.4496
-0.3651 -0.2823 -0.2008 -0.1201 -0.0400 0.0400 0.1201
0.2007 0.2822 0.3650 0.4495 0.5362 0.6257 0.7186
0.8159 0.9186 1.0282 1.1467 1.2771 1.4238 1.5943
1.8029 2.0821 2.5455

39 p = 0.0106 0.0148 0.0177 0.0199 0.0218 0.0233 0.0247
0.0258 0.0268 0.0276 0.0284 0.0290 0.0296 0.0300
0.0304 0.0307 0.0310 0.0311 0.0312 0.0313 0.0312
0.0311 0.0310 0.0307 0.0304 0.0300 0.0296 0.0290
0.0284 0.0276 0.0268 0.0258 0.0247 0.0233 0.0218
0.0199 0.0177 0.0148 0.0106

y = -2.5566 -2.0980 -1.8227 -1.6165 -1.4476 -1.3022 -1.1729
-1.0553 -0.9466 -0.8448 -0.7484 -0.6563 -0.5677 -0.4820
-0.3985 -0.3168 -0.2365 -0.1571 -0.0784 0.0000 0.0784
0.1571 0.2365 0.3168 0.3985 0.4820 0.5677 0.6563
0.7484 0.8448 0.9466 1.0553 1.1729 1.3022 1.4476
1.6165 1.8227 2.0980 2.5566

40 p = 0.0101 0.0144 0.0173 0.0195 0.0212 0.0227 0.0240
0.0250 0.0260 0.0268 0.0275 0.0281 0.0286 0.0290
0.0294 0.0297 0.0300 0.0301 0.0302 0.0303 0.0303
0.0302 0.0301 0.0300 0.0297 0.0294 0.0290 0.0286
0.0281 0.0275 0.0268 0.0260 0.0250 0.0240 0.0227
0.0212 0.0195 0.0173 0.0145 0.0102

y = -2.5709 -2.1115 -1.8353 -1.6293 -1.4612 -1.3168 -1.1887
-1.0724 -0.9650 -0.8646 -0.7697 -0.6792 -0.5923 -0.5082
-0.4265 -0.3467 -0.2682 -0.1909 -0.1143 -0.0382 0.0378
0.1139 0.1905 0.2678 0.3462 0.4261 0.5078 0.5918
0.6787 0.7692 0.8641 0.9644 1.0717 1.1880 1.3160
1.4603 1.6283 1.8340 2.1098 2.5688

41 p = 0.0099 0.0138 0.0165 0.0186 0.0204 0.0218 0.0231

0.0242	0.0251	0.0259	0.0266	0.0273	0.0278	0.0283
0.0287	0.0290	0.0293	0.0295	0.0296	0.0297	0.0297
0.0297	0.0296	0.0295	0.0293	0.0290	0.0287	0.0283
0.0278	0.0273	0.0266	0.0259	0.0251	0.0242	0.0231
0.0218	0.0204	0.0186	0.0165	0.0138	0.0099	

y =	-2.5803	-2.1258	-1.8535	-1.6499	-1.4834	-1.3403	-1.2132
	-1.0978	-0.9913	-0.8916	-0.7975	-0.7078	-0.6216	-0.5384
	-0.4575	-0.3786	-0.3012	-0.2249	-0.1495	-0.0746	-0.0000
	0.0746	0.1495	0.2249	0.3012	0.3786	0.4575	0.5384
	0.6216	0.7078	0.7975	0.8916	0.9913	1.0978	1.2132
	1.3403	1.4834	1.6499	1.8535	2.1258	2.5803	

42 p =

0.0095	0.0135	0.0162	0.0182	0.0199	0.0213	0.0225
0.0235	0.0244	0.0252	0.0258	0.0264	0.0270	0.0274
0.0278	0.0281	0.0284	0.0286	0.0287	0.0288	0.0289
0.0289	0.0288	0.0287	0.0286	0.0284	0.0281	0.0278
0.0274	0.0270	0.0264	0.0258	0.0252	0.0244	0.0235
0.0225	0.0213	0.0199	0.0182	0.0162	0.0135	0.0095

y =	-2.5946	-2.1390	-1.8655	-1.6619	-1.4960	-1.3537	-1.2276
	-1.1133	-1.0080	-0.9097	-0.8169	-0.7285	-0.6438	-0.5621
	-0.4828	-0.4055	-0.3297	-0.2552	-0.1817	-0.1088	-0.0362
	0.0362	0.1087	0.1816	0.2552	0.3297	0.4054	0.4828
	0.5620	0.6438	0.7285	0.8168	0.9096	1.0080	1.1133
	1.2275	1.3536	1.4959	1.6618	1.8654	2.1388	2.5944

43 p =

0.0092	0.0129	0.0155	0.0175	0.0191	0.0205	0.0217
0.0227	0.0236	0.0244	0.0251	0.0257	0.0262	0.0267
0.0271	0.0275	0.0277	0.0280	0.0281	0.0283	0.0283
0.0284	0.0283	0.0283	0.0281	0.0280	0.0277	0.0275
0.0271	0.0267	0.0262	0.0257	0.0251	0.0244	0.0236
0.0227	0.0217	0.0205	0.0191	0.0175	0.0155	0.0129
0.0092						

y =	-2.6027	-2.1519	-1.8824	-1.6812	-1.5169	-1.3759	-1.2508
	-1.1374	-1.0329	-0.9353	-0.8432	-0.7555	-0.6715	-0.5905
	-0.5120	-0.4355	-0.3606	-0.2870	-0.2144	-0.1425	-0.0711
	-0.0000	0.0711	0.1425	0.2144	0.2870	0.3606	0.4355
	0.5120	0.5905	0.6715	0.7555	0.8432	0.9353	1.0329
	1.1374	1.2508	1.3759	1.5169	1.6812	1.8824	2.1519
	2.6027						

44 p =

0.0089	0.0126	0.0152	0.0171	0.0187	0.0200	0.0211
0.0221	0.0230	0.0237	0.0244	0.0250	0.0255	0.0259
0.0263	0.0266	0.0269	0.0271	0.0273	0.0274	0.0275
0.0276	0.0276	0.0275	0.0274	0.0273	0.0271	0.0269
0.0266	0.0263	0.0259	0.0255	0.0250	0.0244	0.0237

		0.0230	0.0221	0.0211	0.0200	0.0187	0.0171	0.0152
		0.0127	0.0089					
	y =	-2.6171	-2.1651	-1.8942	-1.6928	-1.5289	-1.3885	-1.2643
		-1.1519	-1.0485	-0.9520	-0.8611	-0.7747	-0.6920	-0.6123
		-0.5352	-0.4601	-0.3867	-0.3147	-0.2437	-0.1736	-0.1040
		-0.0347	0.0344	0.1037	0.1733	0.2434	0.3144	0.3864
		0.4598	0.5348	0.6120	0.6916	0.7743	0.8607	0.9516
		1.0480	1.1515	1.2638	1.3880	1.5283	1.6921	1.8932
		2.1638	2.6156					
45	p =	0.0087	0.0121	0.0145	0.0164	0.0180	0.0193	0.0204
		0.0214	0.0222	0.0230	0.0237	0.0243	0.0248	0.0253
		0.0257	0.0260	0.0263	0.0266	0.0268	0.0269	0.0270
		0.0271	0.0271	0.0271	0.0270	0.0269	0.0268	0.0266
		0.0263	0.0260	0.0257	0.0253	0.0248	0.0243	0.0237
		0.0230	0.0222	0.0214	0.0204	0.0193	0.0180	0.0164
		0.0145	0.0121	0.0087				
	y =	-2.6238	-2.1765	-1.9096	-1.7107	-1.5485	-1.4093	-1.2861
		-1.1746	-1.0718	-0.9761	-0.8858	-0.8001	-0.7180	-0.6390
		-0.5625	-0.4881	-0.4155	-0.3442	-0.2741	-0.2048	-0.1362
		-0.0680	-0.0000	0.0680	0.1362	0.2048	0.2741	0.3442
		0.4155	0.4881	0.5625	0.6390	0.7180	0.8001	0.8858
		0.9761	1.0718	1.1746	1.2861	1.4093	1.5485	1.7107
		1.9096	2.1765	2.6238				
46	p =	0.0083	0.0119	0.0143	0.0161	0.0176	0.0188	0.0199
		0.0209	0.0217	0.0224	0.0230	0.0236	0.0241	0.0245
		0.0249	0.0253	0.0256	0.0258	0.0260	0.0262	0.0263
		0.0263	0.0264	0.0264	0.0264	0.0263	0.0262	0.0260
		0.0258	0.0256	0.0253	0.0249	0.0246	0.0241	0.0236
		0.0230	0.0224	0.0217	0.0209	0.0199	0.0189	0.0176
		0.0161	0.0143	0.0119	0.0084			
	y =	-2.6385	-2.1898	-1.9212	-1.7219	-1.5599	-1.4213	-1.2988
		-1.1881	-1.0864	-0.9916	-0.9024	-0.8177	-0.7368	-0.6590
		-0.5838	-0.5107	-0.4394	-0.3695	-0.3008	-0.2331	-0.1660
		-0.0995	-0.0332	0.0329	0.0992	0.1657	0.2328	0.3005
		0.3692	0.4390	0.5104	0.5834	0.6587	0.7365	0.8174
		0.9020	0.9911	1.0859	1.1876	1.2983	1.4207	1.5592
		1.7211	1.9202	2.1884	2.6368			
47	p =	0.0082	0.0114	0.0137	0.0155	0.0169	0.0182	0.0192
		0.0202	0.0210	0.0217	0.0224	0.0230	0.0235	0.0239
		0.0244	0.0247	0.0250	0.0253	0.0255	0.0257	0.0258
		0.0259	0.0259	0.0260	0.0259	0.0259	0.0258	0.0257
		0.0255	0.0253	0.0250	0.0247	0.0244	0.0239	0.0235

		0.0230	0.0224	0.0217	0.0210	0.0202	0.0192	0.0182
		0.0169	0.0155	0.0137	0.0114	0.0082		
	y =	-2.6437	-2.1997	-1.9353	-1.7385	-1.5782	-1.4408	-1.3193
		-1.2095	-1.1084	-1.0143	-0.9258	-0.8417	-0.7614	-0.6842
		-0.6095	-0.5371	-0.4664	-0.3972	-0.3293	-0.2623	-0.1961
		-0.1304	-0.0651	0.0000	0.0651	0.1304	0.1961	0.2623
		0.3293	0.3972	0.4664	0.5371	0.6095	0.6842	0.7614
		0.8417	0.9258	1.0143	1.1084	1.2095	1.3193	1.4408
		1.5782	1.7385	1.9353	2.1997	2.6437		
48	p =	0.0078	0.0112	0.0135	0.0152	0.0166	0.0178	0.0188
		0.0197	0.0205	0.0212	0.0218	0.0224	0.0229	0.0233
		0.0237	0.0240	0.0243	0.0246	0.0248	0.0250	0.0251
		0.0252	0.0253	0.0253	0.0253	0.0253	0.0252	0.0251
		0.0250	0.0248	0.0246	0.0243	0.0240	0.0237	0.0233
		0.0229	0.0224	0.0218	0.0212	0.0205	0.0197	0.0188
		0.0178	0.0166	0.0152	0.0135	0.0112	0.0079	
	y =	-2.6587	-2.2131	-1.9469	-1.7495	-1.5892	-1.4522	-1.3313
		-1.2222	-1.1220	-1.0287	-0.9411	-0.8581	-0.7788	-0.7026
		-0.6291	-0.5578	-0.4883	-0.4204	-0.3537	-0.2881	-0.2232
		-0.1590	-0.0953	-0.0317	0.0317	0.0952	0.1590	0.2232
		0.2880	0.3536	0.4203	0.4882	0.5577	0.6290	0.7026
		0.7787	0.8580	0.9410	1.0287	1.1219	1.2221	1.3312
		1.4521	1.5891	1.7493	1.9467	2.2129	2.6584	
49	p =	0.0078	0.0108	0.0129	0.0146	0.0160	0.0172	0.0182
		0.0191	0.0199	0.0206	0.0212	0.0218	0.0223	0.0227
		0.0231	0.0235	0.0238	0.0241	0.0243	0.0245	0.0246
		0.0248	0.0248	0.0249	0.0249	0.0249	0.0248	0.0248
		0.0246	0.0245	0.0243	0.0241	0.0238	0.0235	0.0231
		0.0227	0.0223	0.0218	0.0212	0.0206	0.0199	0.0191
		0.0182	0.0172	0.0160	0.0146	0.0129	0.0108	0.0078
	y =	-2.6626	-2.2217	-1.9597	-1.7648	-1.6062	-1.4706	-1.3507
		-1.2424	-1.1429	-1.0503	-0.9633	-0.8808	-0.8021	-0.7265
		-0.6535	-0.5828	-0.5139	-0.4466	-0.3805	-0.3156	-0.2515
		-0.1880	-0.1251	-0.0625	0.0000	0.0625	0.1251	0.1880
		0.2515	0.3156	0.3805	0.4466	0.5139	0.5828	0.6535
		0.7265	0.8021	0.8808	0.9633	1.0503	1.1429	1.2424
		1.3507	1.4706	1.6062	1.7648	1.9597	2.2217	2.6626
50	p =	0.0076	0.0108	0.0129	0.0146	0.0159	0.0171	0.0181
		0.0189	0.0197	0.0203	0.0209	0.0214	0.0218	0.0222
		0.0225	0.0228	0.0231	0.0232	0.0235	0.0236	0.0238
		0.0238	0.0238	0.0238	0.0239	0.0239	0.0238	0.0238
		0.0238	0.0238	0.0236	0.0235	0.0232	0.0231	0.0228

	0.0225	0.0222	0.0218	0.0214	0.0209	0.0203	0.0197
	0.0189	0.0181	0.0171	0.0159	0.0146	0.0129	0.0108
	0.0076						
y =	-2.6693	-2.2262	-1.9625	-1.7672	-1.6086	-1.4732	-1.3535
	-1.2456	-1.1467	-1.0548	-0.9687	-0.8871	-0.8095	-0.7352
	-0.6637	-0.5945	-0.5271	-0.4616	-0.3974	-0.3342	-0.2720
	-0.2106	-0.1500	-0.0899	-0.0300	0.0300	0.0899	0.1500
	0.2106	0.2720	0.3342	0.3974	0.4616	0.5271	0.5945
	0.6637	0.7352	0.8095	0.8871	0.9687	1.0548	1.1467
	1.2456	1.3535	1.4732	1.6086	1.7672	1.9625	2.2262
	2.6693						

APPENDIX C

NUMERICAL CALCULATION OF CHANNEL PHASE TRANSITION PROBABILITIES BY SIMULATING FIRST ORDER MARKOV FADING PROCESS IN MATLAB

The transition probability $\pi_{JM}(k)$ between the gates R_J^n and R_M^n is defined in Eq. (3.3). It is not usually easy to evaluate the transition probability $\pi_{JM}(k)$ analytically. Calculation difficulties of the conditional probability density function $p(\phi(k+1) | \phi(k))$ in first order Markov fading process makes it difficult to approximate the channel phase transition probabilities between the gates with FSM. Therefore, the transition probabilities between the quantized channel phases are obtained from the simulation results in MATLAB by running the Rayleigh fading channel model which is first order Markov fading process in Eq. 3.30 for L (# of bits)=1000 with R_u (# of runs) = 2000. We quantize the channel phase for $k=1, \dots, L$ as explained in Figure 3,

$$\begin{aligned} \phi_q(k+1) &= Q \left\{ \tan^{-1} \left(\frac{\lambda Y(k) + n_1(k)}{\lambda X(k) + n_2(k)} \right) \right\} \\ &= Q \left\{ \tan^{-1} \left(\frac{-\lambda \alpha(k) \sin(\phi_q(k)) + n_1(k)}{\lambda \alpha(k) \cos(\phi_q(k)) + n_2(k)} \right) \right\} \end{aligned} \quad (C.1)$$

where $\phi_q(k) = \{\phi_{q1}(k), \phi_{q2}(k), \phi_{q3}(k), \dots, \phi_{qMk}(k)\}$. The transition probability from $\phi_{qi}(k-1)$ to $\phi_{qj}(k)$ is denoted by π_{ij} for $k=1, \dots, L$. π_{ij} is obtained by

counting the number of transitions from $\phi_{qi}(k-1)$ to $\phi_{qj}(k)$ in the $1 \times L$ quantized channel phase vector ϕ_q^L (where ϕ_q^L is calculated by quantizing $1 \times L$ channel phase vector ϕ^L by Eq. (3.4)) and running the simulation with $R_u = 2000$ runs. Possible values of the transition probabilities of the channel phase are shown below for different quantization levels, M_k and channel correlation coefficient, λ values.

$\lambda=1.00, \gamma=0.25$

$M_k=10$

$\pi_{ij} =$							
$i=1 \rightarrow j=1, \dots, 10$	1.0000	0.0000	0.0000	0.0000	0.0000	0.0000	0.0000
	0.0000	0.0000					
$i=2 \rightarrow j=1, \dots, 10$	0.0000	1.0000	0.0000	0.0000	0.0000	0.0000	0.0000
	0.0000	0.0000	0.0000				
$i=3 \rightarrow j=1, \dots, 10$	0.0000	0.0000	1.0000	0.0000	0.0000	0.0000	0.0000
	0.0000	0.0000	0.0000				
$i=4 \rightarrow j=1, \dots, 10$	0.0000	0.0000	0.0000	1.0000	0.0000	0.0000	0.0000
	0.0000	0.0000	0.0000				
$i=5 \rightarrow j=1, \dots, 10$	0.0000	0.0000	0.0000	0.0000	1.0000	0.0000	0.0000
	0.0000	0.0000	0.0000				
$i=6 \rightarrow j=1, \dots, 10$	0.0000	0.0000	0.0000	0.0000	0.0000	1.0000	0.0000
	0.0000	0.0000	0.0000				
$i=7 \rightarrow j=1, \dots, 10$	0.0000	0.0000	0.0000	0.0000	0.0000	0.0000	1.0000
	0.0000	0.0000	0.0000				
$i=8 \rightarrow j=1, \dots, 10$	0.0000	0.0000	0.0000	0.0000	0.0000	0.0000	0.0000
	1.0000	0.0000	0.0000				
$i=9 \rightarrow j=1, \dots, 10$	0.0000	0.0000	0.0000	0.0000	0.0000	0.0000	0.0000
	0.0000	1.0000	0.0000				
$i=10 \rightarrow j=1, \dots, 10$	0.0000	0.0000	0.0000	0.0000	0.0000	0.0000	0.0000
	0.0000	0.0000	1.0000				

$\lambda=0.9995, \gamma=0.25$

$M_k=10$

$\pi_{ij} =$							
$i=1 \rightarrow j=1, \dots, 10$	0.8347	0.0779	0.0046	0.0015	0.0004	0.0004	0.0008
	0.0009	0.0023	0.0765				

$i=2 \rightarrow j=1, \dots, 10$	0.0772	0.8317	0.0747	0.0040	0.0023	0.0002	0.0024
	0.0007	0.0020	0.0048				
$i=3 \rightarrow j=1, \dots, 10$	0.0044	0.0721	0.8394	0.0757	0.0047	0.0003	0.0003
	0.0004	0.0005	0.0021				
$i=4 \rightarrow j=1, \dots, 10$	0.0039	0.0035	0.0656	0.8489	0.0680	0.0036	0.0015
	0.0024	0.0015	0.0010				
$i=5 \rightarrow j=1, \dots, 10$	0.0001	0.0025	0.0041	0.0741	0.8368	0.0730	0.0053
	0.0035	0.0003	0.0004				
$i=6 \rightarrow j=1, \dots, 10$	0.0002	0.0003	0.0013	0.0026	0.0764	0.8356	0.0737
	0.0081	0.0003	0.0016				
$i=7 \rightarrow j=1, \dots, 10$	0.0000	0.0048	0.0010	0.0018	0.0039	0.0735	0.8367
	0.0733	0.0041	0.0009				
$i=8 \rightarrow j=1, \dots, 10$	0.0021	0.0000	0.0009	0.0014	0.0007	0.0048	0.0718
	0.8436	0.0721	0.0027				
$i=9 \rightarrow j=1, \dots, 10$	0.0016	0.0006	0.0009	0.0014	0.0013	0.0005	0.0025
	0.0729	0.8415	0.0768				
$i=10 \rightarrow j=1, \dots, 10$	0.0710	0.0038	0.0016	0.0003	0.0005	0.0006	0.0026
	0.0034	0.0690	0.8472				

$M_k=20$

$\pi_{ij} =$

$i=1 \rightarrow j=1, \dots, 20$	0.7721	0.1047	0.0110	0.0027	0.0015	0.0018	0.0001
	0.0000	0.0000	0.0000	0.0005	0.0000	0.0001	0.0002
	0.0000	0.0007	0.0006	0.0023	0.0063	0.0956	
$i=2 \rightarrow j=1, \dots, 20$	0.1089	0.7519	0.1076	0.0059	0.0014	0.0032	0.0001
	0.0014	0.0000	0.0000	0.0000	0.0001	0.0000	0.0007
	0.0007	0.0013	0.0000	0.0002	0.0032	0.0133	
$i=3 \rightarrow j=1, \dots, 20$	0.0104	0.0993	0.7607	0.1088	0.0089	0.0017	0.0001
	0.0004	0.0014	0.0010	0.0013	0.0003	0.0001	0.0001
	0.0001	0.0000	0.0013	0.0002	0.0011	0.0027	
$i=4 \rightarrow j=1, \dots, 20$	0.0029	0.0070	0.1104	0.7699	0.0929	0.0065	0.0024
	0.0002	0.0016	0.0004	0.0003	0.0000	0.0000	0.0000
	0.0000	0.0002	0.0005	0.0014	0.0013	0.0021	

i=5→j=1,....20	0.0016	0.0022	0.0121	0.1108	0.7536	0.1037	0.0091
	0.0024	0.0016	0.0003	0.0000	0.0003	0.0000	0.0002
	0.0001	0.0000	0.0007	0.0002	0.0006	0.0006	
i=6→j=1,....20	0.0009	0.0007	0.0018	0.0068	0.1065	0.7496	0.1063
	0.0150	0.0052	0.0010	0.0006	0.0004	0.0001	0.0001
	0.0034	0.0000	0.0027	0.0000	0.0022	0.0000	
i=7→j=1,....20	0.0002	0.0004	0.0002	0.0047	0.0061	0.1035	0.7625
	0.1019	0.0101	0.0008	0.0023	0.0009	0.0011	0.0001
	0.0003	0.0013	0.0014	0.0002	0.0000	0.0021	
i=8→j=1,....20	0.0003	0.0004	0.0001	0.0012	0.0028	0.0114	0.1052
	0.7580	0.1050	0.0108	0.0032	0.0005	0.0001	0.0001
	0.0000	0.0006	0.0000	0.0001	0.0000	0.0000	
i=9→j=1,....20	0.0000	0.0000	0.0022	0.0005	0.0012	0.0009	0.0095
	0.1024	0.7659	0.1048	0.0055	0.0038	0.0006	0.0015
	0.0004	0.0000	0.0002	0.0001	0.0005	0.0000	
i=10→j=1,....20	0.0002	0.0007	0.0001	0.0025	0.0000	0.0003	0.0026
	0.0113	0.1002	0.7586	0.1091	0.0057	0.0032	0.0027
	0.0000	0.0000	0.0004	0.0026	0.0000	0.0000	
i=11→j=1,....20	0.0000	0.0005	0.0015	0.0000	0.0001	0.0012	0.0009
	0.0037	0.0103	0.1054	0.7704	0.0958	0.0068	0.0018
	0.0003	0.0008	0.0001	0.0001	0.0003	0.0000	
i=12→j=1,....20	0.0000	0.0013	0.0006	0.0000	0.0001	0.0003	0.0015
	0.0015	0.0033	0.0085	0.0975	0.7641	0.1073	0.0082
	0.0031	0.0014	0.0012	0.0001	0.0001	0.0000	
i=13→j=1,....20	0.0000	0.0001	0.0002	0.0002	0.0000	0.0000	0.0002
	0.0001	0.0001	0.0020	0.0112	0.1103	0.7632	0.0956
	0.0109	0.0020	0.0010	0.0016	0.0005	0.0009	
i=14→j=1,....20	0.0013	0.0001	0.0002	0.0000	0.0000	0.0000	0.0001
	0.0001	0.0006	0.0023	0.0082	0.0053	0.1053	0.7610
	0.1038	0.0078	0.0017	0.0002	0.0009	0.0013	
i=15→j=1,....20	0.0020	0.0000	0.0001	0.0000	0.0002	0.0001	0.0028
	0.0006	0.0016	0.0001	0.0004	0.0042	0.0078	0.1152
	0.7537	0.0993	0.0082	0.0032	0.0005	0.0000	

i=16→j=1,....20	0.0004	0.0004	0.0002	0.0001	0.0004	0.0000	0.0004
	0.0015	0.0006	0.0000	0.0008	0.0036	0.0023	0.0099
	0.1008	0.7564	0.1111	0.0881	0.0021	0.0008	
i=17→j=1,....20	0.0021	0.0002	0.0018	0.0000	0.0003	0.0000	0.0002
	0.0002	0.0000	0.0006	0.0001	0.0008	0.0007	0.0024
	0.0068	0.0975	0.7744	0.1038	0.0066	0.0015	
i=18→j=1,....20	0.0035	0.0006	0.0014	0.0002	0.0021	0.0000	0.0000
	0.0000	0.0000	0.0000	0.0013	0.0004	0.0017	0.0014
	0.0036	0.0101	0.1089	0.7603	0.0963	0.0081	
i=19→j=1,....20	0.0073	0.0013	0.0030	0.0001	0.0005	0.0000	0.0000
	0.0000	0.0000	0.0000	0.0000	0.0015	0.0002	0.0014
	0.0012	0.0011	0.0094	0.1051	0.7710	0.0968	
i=20→j=1,....20	0.1091	0.0092	0.0027	0.0006	0.0002	0.0000	0.0001
	0.0016	0.0009	0.0007	0.0000	0.0000	0.0000	0.0000
	0.0006	0.0038	0.0030	0.0080	0.1023	0.7570	

$\lambda=0.95, \gamma=0.25$

$M_k=10$

$\pi_{ij} =$							
i=1→j=1,....10	0.5896	0.1681	0.0222	0.0081	0.0045	0.0039	0.0044
	0.0073	0.0227	0.1691				
i=2→j=1,....10	0.1677	0.5903	0.1692	0.0220	0.0077	0.0049	0.0042
	0.0043	0.0078	0.0220				
i=3→j=1,....10	0.0230	0.1699	0.5871	0.1696	0.0218	0.0077	0.0045
	0.0039	0.0048	0.0078				
i=4→j=1,....10	0.0077	0.0228	0.1702	0.5862	0.1701	0.0227	0.0075
	0.0044	0.0038	0.0046				
i=5→j=1,....10	0.0044	0.0081	0.0224	0.1698	0.5874	0.1698	0.0228
	0.0073	0.0043	0.0038				
i=6→j=1,....10	0.0036	0.0046	0.0076	0.0226	0.1689	0.5891	0.1682
	0.0228	0.0080	0.0046				
i=7→j=1,....10	0.0044	0.0041	0.0045	0.0076	0.0231	0.1698	0.5857
	0.1705	0.0223	0.0079				

$i=8 \rightarrow j=1, \dots, 10$	0.0074	0.0044	0.0040	0.0042	0.0077	0.0227	0.1685
	0.5894	0.1697	0.0219				
$i=9 \rightarrow j=1, \dots, 10$	0.0228	0.0077	0.0048	0.0039	0.0045	0.0075	0.0229
	0.1701	0.5854	0.1704				
$i=10 \rightarrow j=1, \dots, 10$	0.1695	0.0225	0.0077	0.0047	0.0040	0.0045	0.0079
	0.0224	0.1690	0.5901				

$\lambda=0.90, \gamma=0.25$

$M_k=10$

$\pi_{ij} =$							
$i=1 \rightarrow j=1, \dots, 10$	0.4829	0.1918	0.0390	0.0144	0.0087	0.0065	0.0087
	0.0147	0.0383	0.1950				
$i=2 \rightarrow j=1, \dots, 10$	0.1913	0.4857	0.1927	0.0384	0.0139	0.0086	0.0074
	0.0087	0.0145	0.0389				
$i=3 \rightarrow j=1, \dots, 10$	0.0385	0.1921	0.4836	0.1929	0.0390	0.0144	0.0087
	0.0071	0.0088	0.0150				
$i=4 \rightarrow j=1, \dots, 10$	0.0150	0.0390	0.1958	0.4805	0.1917	0.0396	0.0142
	0.0086	0.0074	0.0081				
$i=5 \rightarrow j=1, \dots, 10$	0.0083	0.0149	0.0388	0.1925	0.4818	0.1937	0.0387
	0.0150	0.0086	0.0077				
$i=6 \rightarrow j=1, \dots, 10$	0.0069	0.0087	0.0144	0.0390	0.1938	0.4813	0.1937
	0.0391	0.0146	0.0085				
$i=7 \rightarrow j=1, \dots, 10$	0.0086	0.0075	0.0087	0.0146	0.0393	0.1951	0.4804
	0.1927	0.0388	0.0144				
$i=8 \rightarrow j=1, \dots, 10$	0.0147	0.0092	0.0077	0.0088	0.0143	0.0395	0.1923
	0.4816	0.1932	0.0386				
$i=9 \rightarrow j=1, \dots, 10$	0.0397	0.0146	0.0089	0.0075	0.0088	0.0141	0.0392
	0.1912	0.4828	0.1932				
$i=10 \rightarrow j=1, \dots, 10$	0.1934	0.0391	0.0142	0.0087	0.0074	0.0088	0.0142
	0.0385	0.1930	0.4828				

$\lambda=0.50, \gamma=0.25$

$M_k=10$

$\pi_{ij} =$

$i=1 \rightarrow j=1, \dots, 10$	0.2083 0.0622	0.1681 0.1003	0.1010 0.1676	0.0617	0.0446	0.0405	0.0458
$i=2 \rightarrow j=1, \dots, 10$	0.1680 0.0445	0.2084 0.0623	0.1680 0.1000	0.1017	0.0618	0.0449	0.0403
$i=3 \rightarrow j=1, \dots, 10$	0.1004 0.0401	0.1682 0.0446	0.2079 0.0618	0.1688	0.1023	0.0610	0.0449
$i=4 \rightarrow j=1, \dots, 10$	0.0613 0.0451	0.1012 0.0402	0.1672 0.0449	0.2111	0.1667	0.1004	0.0618
$i=5 \rightarrow j=1, \dots, 10$	0.0445 0.0618	0.0616 0.0459	0.1021 0.0407	0.1680	0.2080	0.1665	0.1008
$i=6 \rightarrow j=1, \dots, 10$	0.0400 0.1013	0.0452 0.0613	0.0614 0.0459	0.1004	0.1684	0.2073	0.1688
$i=7 \rightarrow j=1, \dots, 10$	0.0447 0.1675	0.0394 0.1010	0.0454 0.0623	0.0612	0.1015	0.1681	0.2089
$i=8 \rightarrow j=1, \dots, 10$	0.0614 0.2081	0.0445 0.1691	0.0410 0.1004	0.0454	0.0621	0.0997	0.1684
$i=9 \rightarrow j=1, \dots, 10$	0.1008 0.1662	0.0614 0.2121	0.0444 0.1678	0.0404	0.0445	0.0603	0.1021
$i=10 \rightarrow j=1, \dots, 10$	0.1684 0.1003	0.1016 0.1681	0.0618 0.2077	0.0446	0.0406	0.0444	0.0624

$\lambda=0.00, \gamma=0.25$

$M_k=10$

$\pi_{ij} =$ $i=1 \rightarrow j=1, \dots, 10$	0.0997 0.1010	0.1005 0.1006	0.0991 0.0990	0.1002	0.1008	0.0985	0.1006
$i=2 \rightarrow j=1, \dots, 10$	0.0998 0.0999	0.1000 0.1015	0.1001 0.1004	0.1000	0.1000	0.0987	0.0996
$i=3 \rightarrow j=1, \dots, 10$	0.1006 0.0988	0.1002 0.0998	0.1003 0.0987	0.1003	0.1011	0.1003	0.0999
$i=4 \rightarrow j=1, \dots, 10$	0.0995 0.0994	0.1000 0.1010	0.1006 0.1010	0.0989	0.1006	0.0994	0.0996

$i=5 \rightarrow j=1, \dots, 10$	0.0999	0.1003	0.1000	0.0987	0.1004	0.1006	0.1005
	0.0997	0.1004	0.0995				
$i=6 \rightarrow j=1, \dots, 10$	0.0994	0.0997	0.1005	0.1005	0.1001	0.0978	0.1005
	0.1007	0.0993	0.1016				
$i=7 \rightarrow j=1, \dots, 10$	0.0993	0.1004	0.1000	0.0996	0.0999	0.0997	0.0995
	0.1003	0.1006	0.1007				
$i=8 \rightarrow j=1, \dots, 10$	0.1001	0.1002	0.1008	0.0993	0.1001	0.1011	0.0997
	0.0991	0.1001	0.0995				
$i=9 \rightarrow j=1, \dots, 10$	0.0994	0.0998	0.1012	0.1002	0.0999	0.1005	0.1002
	0.1003	0.0984	0.1000				
$i=10 \rightarrow j=1, \dots, 10$	0.0990	0.1011	0.0994	0.1008	0.1007	0.0999	0.1011
	0.0993	0.1005	0.0982				